2003

Organogermanium chemistry: germacyclobutanes and digermane additions to acetylenes

Andrew Michael Chubb
Iowa State University

Organogermanium chemistry:

Germacyclobutanes and digermane additions to acetylenes

by

Andrew Michael Chubb

A dissertation submitted to the graduate faculty

in partial fulfillment of the requirements for the degree of

DOCTOR OF PHILOSOPHY

Major: Organic Chemistry

Program of Study Committee:
Thomas J. Barton, Major Professor
William S. Jenks
Valerie V. Sheares Ashby
Mark S. Gordon
Constance P. Hargrave

Iowa State University

Ames, Iowa

2003

Graduate College

Iowa State University

This is to certify that the doctoral dissertation of

Andrew Michael Chubb

has met the dissertation requirements of Iowa State University

Signature was redacted for privacy.

Major Professor

Signature was redacted for privacy.

For the Major Program

DEDICATION

For Elmie.

TABLE OF CONTENTS

ABSTRACT

This dissertation comprises two main research projects. The first project, presented in Chapter 1, involves the synthesis and thermochemistry of germacyclobutanes (germetanes). Four new germetanes (spirodigermetane, diallylgermetane, dichlorogermetane, and germacyclobutane) have been synthesized using a modified di-Grignard synthesis. Diallylgermetane is shown to be a useful starting material for obtaining other germetanes, particularly the parent germetane, germacyclobutane. The gas-phase thermochemistries of spirodigermetane, diallylgermetane and germacyclobutane have been explored *via* pulsed stirred-flow reactor (SFR) studies, showing remarkable differences in decomposition, depending on the substitution at the germanium atom.

The second project investigates the thermochemical, photochemical, and catalytic additions of several digermanes to acetylenes. The first examples of thermo- and photochemical additions of Ge–Ge bonds to C≡C are demonstrated. Mechanistic investigations are described and comparisons are made to analogous disilane addition reactions, previously studied in our group.

GENERAL INTRODUCTION

This dissertation is divided into two chapters, each dealing with a separate project in the area of organogermanium chemistry. Each chapter is self-contained, with its own introduction, results and discussion, conclusions, experimental, and references sections. Four appendices are included and contain ancillary data that is important for reference purposes, but was deemed unnecessarily bulky to include in the main body of the dissertation.

The first chapter describes the synthesis and thermochemistry of germacyclobutanes (germetanes). Four new germetanes (spirodigermetane, diallylgermetane, germacyclobutane, and dichlorogermetane) have been synthesized using a modified di-Grignard synthesis. The gas-phase thermal rearrangements of the first three germetanes were investigated *via* pulsed stirred-flow reactor (SFR) studies and possible mechanisms were proposed and explored.

The second chapter involves the thermochemical, photochemical, and catalytic additions of several digermanes to acetylenes. This work is based on analogous disilane addition reactions, previously studied in our group. The first examples of thermo- and photochemical additions of Ge–Ge bonds to C≡C are demonstrated and mechanistic investigations are described with comparisons being made to the aforementioned disilane addition reactions.

I. SYNTHESIS AND THERMOCHEMISTRY OF GERMACYCLOBUTANES

A. Introduction

1. Cyclobutane. Since the first report[1] of its synthesis from cyclobutene in 1907, cyclobutane (**1**) has been the subject of considerable interest over the years.[2-9] In particular, the thermochemistry of this deceptively simple molecule has engendered a rather vigorous debate.[2,3,10-18] As a result, the attempted elucidation of the mechanism of thermal decomposition of cyclobutane has produced some very excellent examples of physical and mechanistic organic chemistry for nearly a century.

The first reported thermolysis of cyclobutane is a 1951 communication by Genaux and Walters (Scheme 1).[2] The authors monitored the change in pressure in the thermal decomposition of cyclobutane from 430 to 480 °C. In each of the thermolyses, the pressure increase was a first order process and the final pressures were twice the initial pressures, consistent with a fragmentation of cyclobutane into two molecules. Infrared spectroscopy confirmed that the thermolysis of cyclobutane is quite clean, with ethylene being formed almost exclusively.

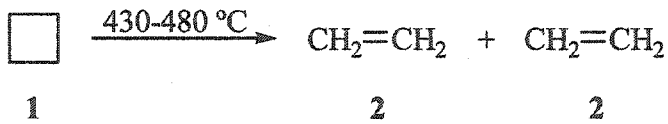

Scheme 1. Thermolysis of cyclobutane.

Further investigations by the Walters group confirmed the first order nature of the decomposition and Arrhenius treatment of their data yielded an activation energy (E_a) of 62.5 kcal/mol and log *A* of 15.6.[19,20] A free radical chain mechanism was ruled out by the results of several experiments. First, no decrease in reaction rate was observed upon addition of the free radical inhibitors nitric oxide, propene, and toluene. Second, dimethyl ether, which reacts with free radicals, did not undergo decomposition when added to the thermolysis mixture. Third, two reactions whose rates increase in the presence of free radicals,

formaldehyde decomposition and ethylene polymerization, did not have an appreciable difference in rate upon thermolysis in the presence of cyclobutane. Although attempts to trap a 1,4-diradical intermediate (3) with added hydrogen failed, the authors proposed that the decomposition occurred *via* initial homolytic cleavage of a carbon-carbon bond (Scheme 2). Such a mechanism is consistent with the calculated Arrhenius parameters and the failure to trap the proposed intermediate does not rule out its formation, particularly if it is short-lived.

1 3 2

Scheme 2. Decomposition of cyclobutane *via* sequential homolytic cleavages.

Likewise, the thermolysis of ethylcyclobutane (4) also was found to be clean, yielding ethylene and butene in a first order process (Scheme 3).[21] The Arrhenius parameters reported for ethylcyclobutane decomposition were nearly identical to those obtained for cyclobutane thermolysis: E_a = 62.0 kcal/mol and log A = 15.6. Again, as in the case of cyclobutane thermolysis, no inhibition was observed upon addition of propylene, toluene or nitric oxide, ruling out a free radical chain mechanism.

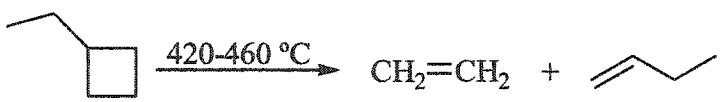

4 2 5

Scheme 3. Thermolysis of ethylcyclobutane.

Experiments by Trotman-Dickenson's group also showed a first order decomposition upon thermolysis of cyclobutane.[3] However, Trotman-Dickenson noted several similarities between the thermolyses of cyclobutane and cyclopropane. In particular, the plots of log k/k_∞ *vs.* log P for the two decompositions were quite similar in shape and magnitude, with the curve for cyclobutane being shifted to lower pressures. This shifting of the cyclobutane curve relative to that of cyclopropane was not unexpected due to the greater complexity of

the cyclobutane molecule. These similarities led the authors to propose a more concerted-type mechanism similar to that proposed[22] for the thermal isomerization of cyclopropane.

Using thermochemical arguments, Trotman-Dickenson's group estimated that cyclobutane has around 26 kcal/mol of ring strain.[3] This ring strain, assuming a typical C–C bond energy on the order of 85 kcal/mol, would lead to an E_a for homolytic bond cleavage in cyclobutane around 59 kcal/mol. Although this estimated E_a is close to the experimental value, the authors argued that, as in Slater's cyclopropane mechanism, the sequential homolytic cleavage mechanism does not occur in the thermolysis of cyclobutane. Instead, they proposed a concerted mechanism involving alternate stretching and contracting of opposite C–C bonds (Scheme 4). Since two concerted C–C homolyses would cost 144 kcal/mol in total (85 kcal/mol per C–C bond, less 26 kcal/mol ring strain), a fairly late transition state involving substantial double-bond character was assumed. The larger than expected log *A* value then could be explained by the increased entropy due to the formation of nearly free ethylene molecules.

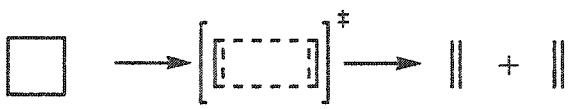

Scheme 4. Concerted mechanism for cyclobutane thermolysis.

Genaux, Kern and Walters argued, however, that the higher log *A* was more indicative of a homolytic ring cleavage.[20] Using the experimental *A* factor, they calculated an entropy of activation ($\Delta S^{\ddagger}$ at 449 °C) of +9 cal/mol·K. Further thermodynamic calculations using experimental and literature data yielded an overall entropy change (ΔS_{rxn}) of +43 cal/mol·K for the reaction. Since ΔS_{rxn} is considerably larger than $\Delta S^{\ddagger}$, the authors concluded that the structure of the transition state is much more reactantlike than productlike. Realizing that the diradical formed upon homolytic ring cleavage could be an intermediate, rather than a transition state, Walters and coworkers compared the calculated entropy change (ΔS_{rad}) upon diradical formation with the calculated entropy of activation. Calculations gave a value of $\Delta S_{rad} \geq 15$ cal/mol·K, which is larger than $\Delta S^{\ddagger}$. The transition state, therefore,

most likely lies somewhere between cyclobutane and the fully-formed diradical (Scheme 5). The authors point out that, although attempts at trapping a diradical intermediate have failed, estimates of the E_a for decomposition of the diradical to two molecules of ethylene are on the order of 15 kcal/mol, well within the experimental conditions for favoring unimolecular decomposition before bimolecular trapping.

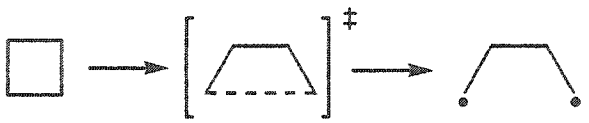

Scheme 5. Formation of the tetramethylene diradical from cyclobutane.

Further support for the diradical mechanism appeared to come in 1961 with studies of the thermolysis of *cis*- and *trans*-1,2-dimethylcyclobutane (*cis*-**6** and *trans*-**6**).[11,23] Two modes of cleavage, symmetrical (route A) and asymmetrical (route B), are possible for both dimethylcyclobutanes (Scheme 6). In fact, products corresponding to both cleavages were detected upon thermolysis of either the *cis* or *trans* stereoisomer, though symmetrical cleavage was favored in both cases (83% for *cis* and 78% for *trans*). These results are not surprising, considering that steric repulsion between the methyl groups would result in preferential cleavage of the C1–C2 bond and that these steric effects would be greater in *cis*-dimethylcyclobutane, leading to the observed greater preference for symmetrical cleavage in that stereoisomer.

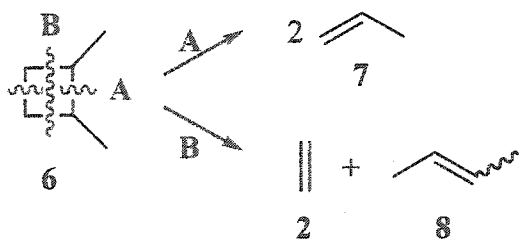

Scheme 6. Modes of decomposition of *cis*- and *trans*-1,2-dimethylcyclobutane.

However, it is the stereochemical outcomes of these thermolyses that strengthened the argument for the diradical mechanism. If the decompositions occur *via* a concerted

mechanism, as in Scheme 4, only the *cis*- or *trans*-2-butene (**8**) would be formed upon thermolysis of pure *cis*- or *trans*-dimethylcyclobutane, respectively. Instead, Gerberich and Walters found that *both* 2-butene isomers were formed in each of the thermolyses (each with ~15% decomposition of the starting material), suggesting that not only was the tetramethylene diradical formed, but also that it was long-lived enough to undergo bond rotation before cleavage of the second C–C bond (Scheme 7). In addition, isomerization of the initial cyclobutanes occurred in both cases, albeit in low yields (2-3%), presumably due to ring closure of the intermediate diradical after bond homolysis and rotation.

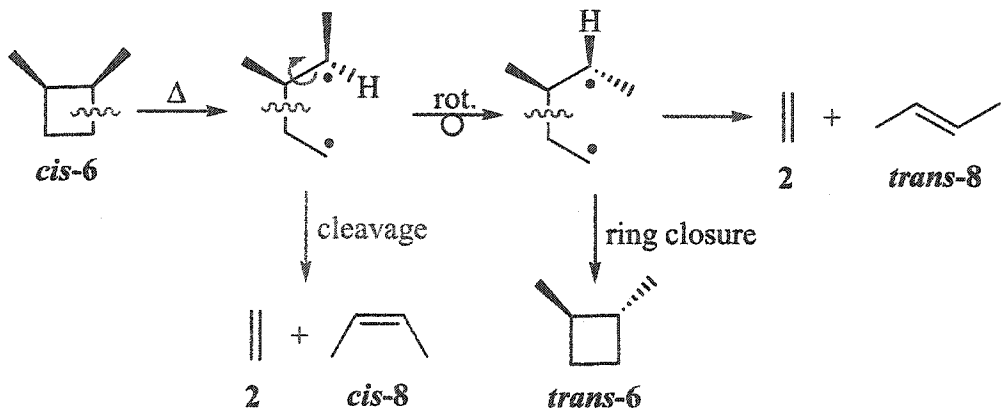

Scheme 7. Thermolytic isomerization of *cis*-dimethylcyclobutane.

At first glance, Woodward and Hoffmann's orbital symmetry theory also appeared to support the two-step hypothesis.[4,24] As a system with 4n (where n=1) π electrons, the *thermal* one-step cycloreversion of cyclobutane would be symmetry-forbidden. However, further elaboration of the rules governing such pericyclic reactions reveals that the situation is not quite so simple.[25-27] While the $[2_s+2_s]$ cycloreversion, leading to a single 2-butene isomer in the *cis*- and *trans*-1,2-dimethylcyclobutane thermolyses, is thermally forbidden, the $[2_s+2_a]$ cycloreversion is thermally *allowed*. This complicates the interpretation of the results of the dimethylcyclobutane thermolyses because in the $[2_s+2_a]$ cycloreversion, *both* 2-butene isomers should be formed. Salem and Wright, using an expanded set of orbitals which included contributions from the σ_{C-H} orbitals on cyclohexane, backed up Woodward and Hoffmann's orbital analysis in 1969.[28]

In order to shed some light on the nature of the proposed tetramethylene diradical intermediate, Hoffmann *et al.* used extended Hückel calculations to explore the potential energy surface (PES) for the stepwise cyclobutane decomposition.[15] Interestingly, the tetramethylene diradical was not found as a true minimum on the PES for the decomposition of cyclobutane. Instead, the calculations described a large, relatively flat area corresponding to the many possible conformations adoptable by the ring-opened cyclobutane. This large region allows the "twixtyl" species, as the authors named it, to have the longer lifetime expected for a true intermediate, rather than a transition state.

A more rigorous, *ab initio* study of the cyclobutane → diradical → ethylene PES was reported by Segal in 1974.[16] Segal's calculations found that the tetramethylene diradical was in fact an intermediate with a well depth of 3.6 kcal/mol, remarkably close to that found by Benson[29,30] (~4 kcal/mol), using thermochemical estimates. Since then, several groups have investigated, both theoretically and experimentally, the tetramethylene diradical in attempts to elucidate its nature, particularly with respect to its stability.[31-35]

A breakthrough for the proposed diradical mechanism came in 1994 with femtosecond investigations by Zewail's group.[18] The authors directly generated the tetramethylene diradical by photo-induced decarbonylation[36] of cyclopentanone (**9**) and then monitored its reaction along two paths, ring closure to cyclobutane and fragmentation to ethylene (Scheme 8). The lifetime for the tetramethylene diradical was measured to be around 700 fs, much longer than that expected for a transition state (~40 fs). A later study, including DFT calculations reinforced these results and showed that the measured lifetimes are sufficient to allow internal rotation around the C2–C3 bond of the tetramethylene diradical.[37] While the case for nonconcerted thermolytic decomposition of cyclobutane certainly is not closed, current thinking appears to be leaning in that direction.

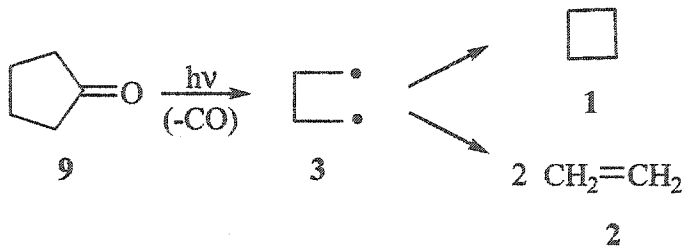

Scheme 8. Photochemical generation and subsequent reactions of tetramethylene diradical.

2. Silacyclobutanes (siletanes). The first reported isolation of a silacyclobutane (siletane) was the synthesis of 1,1-dimethyl-1-silacyclobutane (dimethylsiletane, **10**) in 1954 (Scheme 9).[38] Sommer and Baum reported an impressive yield of 66% for the siletane. This paper was followed shortly by the publication of West's synthesis of the 3,3-bisethyl ester substituted dimethylsiletane.[39]

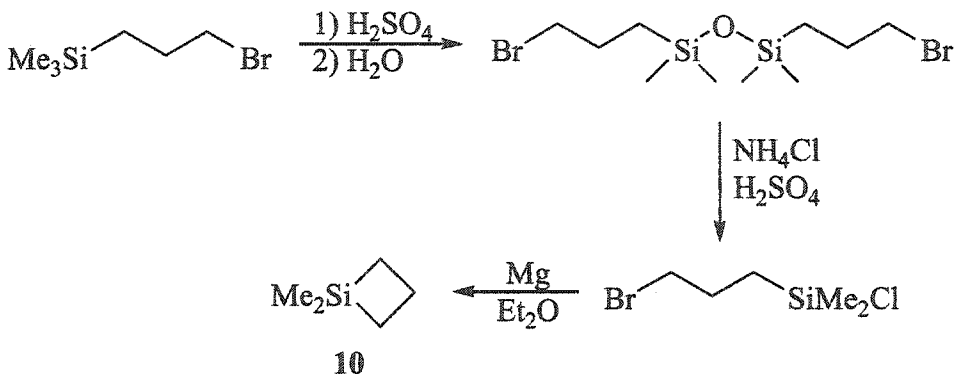

Scheme 9. The first synthesis of dimethylsiletane (**10**).

The thermochemistry of siletanes was to begin a little over a decade later. In 1968, Gusel'nikov and Flowers demonstrated that the gas-phase thermolysis of dimethylsiletane yields 1,1,3,3-tetramethyl-1,3-disilacyclobutane (**12**).[40] The decomposition was found to be first order with average Arrhenius parameters of E_a = 62.5 kcal/mol and log A = 15.64. Due to the similarity of these values to those obtained[10] in the thermolyses of cyclobutanes, the authors proposed that the reaction proceeded through the nonconcerted elimination of

ethylene to form 1,1-dimethylsilene (**11**). However, due to the kinetic instability of the C–Si double bond, the dimethylsilene the dimerizes in a head-to-tail fashion to form the observed disilacyclobutane (Scheme 10).

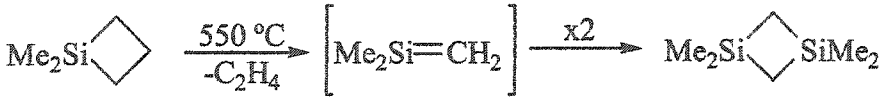

10 **11** **12**

Scheme 10. Thermolysis of dimethylsilacyclobutane.

Gusel'nikov and Flowers also noted that, unlike in the case of cyclobutanes, the decomposition of dimethylsiletane is inhibited by the presence of ethylene. To explain these observations, they proposed that the extrusion of ethylene is reversible. Experiments with added propene seemed to support their hypothesis, resulting in the appearance of an additional product whose mass and GC retention time were consistent with the formation of a trimethylsiletane. The authors also noted that this reversibility is not unprecedented; Butler describes just such a process (with an E_a for the back reaction of ~25 kcal/mol) in the octafluorocyclobutane thermolysis.[41]

It is important to note that, at that time, a stable Si–C doubly bonded species had not yet been identified and was a highly speculative entity.[42] Therefore, Gusel'nikov and Flowers did not propose the intermediacy of a silene casually. Scheme 11 summarizes some of the experimental evidence that led them to propose a silene intermediate. Cycloaddition

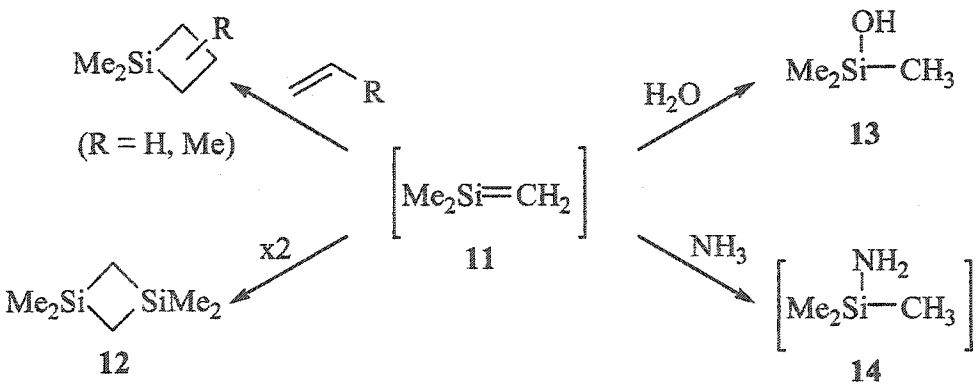

Scheme 11. Dimethylsilene reactions.

reactions, such as the silene dimerization and reaction with ethylene or propene, were well known in 1968.[43] Addition of water or ammonia across the Si–C double bond is easily visualized, owing to the polarity of the Si–C bond and the purported weakness of the π bond. Indeed, such nucleophilic additions are now characteristic reactions used to trap silenes.[44,45] The proposal of an intermediate silene proved to be quite sound as, for many years, thermolysis of silacyclobutanes became a standard method for cleanly generating silenes.[45]

As in the case of cyclobutane, the question of whether the decomposition of siletanes is concerted or stepwise (*i.e.*, involving a diradical intermediate) inevitably must arise. Gusel'nikov and Flowers ruled out a concerted mechanism because they deemed the *A* factor too large to accommodate such a constrained process.[40] It wasn't until 1997 that *ab initio* calculations were performed to address this issue.[46,47] In both papers, a cyclic transition state was found between the starting siletane and ethylene + silene products. However, this transition state is not one typical of a concerted 2+2 cycloaddition (or –reversion). Instead, the structure was quite unsymmetrical, indicating a "highly asynchronous route…along which there is considerable diradical character."[47] The mechanism appears to involve simultaneous lengthening of opposite bonds, but with one bond (C–C, *vide infra*) broken to a greater extent in the transition state.

Due to the lower symmetry of silacyclobutanes relative to cyclobutanes, two different initial bond cleavages are possible: Si–C and C–C (Scheme 12). In the case of dimethylsiletane (**10a**), both routes lead to the same products. Thus, Gusel'nikov and Flowers, recognizing that no definitive comparison of Si–C and C–C bond energies then were known, were unable to determine which bond scission was most likely.

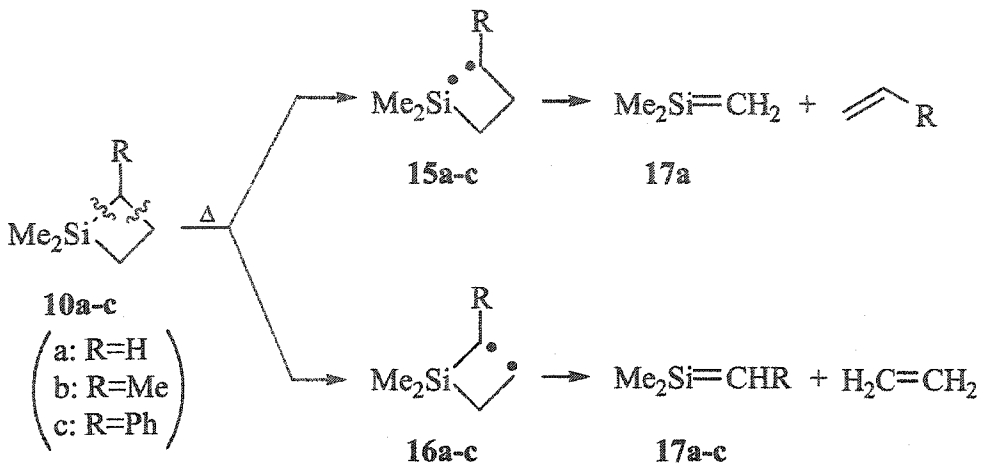

Scheme 12. Initial Si–C vs. C–C bond cleavage in dimethylsiletanes.

In 1975, two independent papers provided evidence for an initial C–C bond cleavage. Upon thermolysis of both 1,1,2-trimethyl-1-silacyclobutane[48,49] (**10b**) and 1,1-dimethyl-2-phenyl-1-silacyclobutane[49] (**10c**), the majority of cleavage produced the R-substituted silene (**17b-c**). The preference for C2–C3 cleavage vs. C3–C4 cleavage was assumed, due to the formation of a more stable 2° alkyl radical in the former.[48] In the case of **10c**, the preference for C–C scission was significantly more pronounced than with **10b**, presumably due to the better ability of a phenyl vs. a methyl group to stabilize an alpha radical. This conclusion is consistent with the finding of Golino *et al.* that, under their reaction conditions, **10b** required a higher temperature (611 °C, the same as for **10a**) than **10c** (530 °C) to effect complete decomposition of the initial siletane. *Ab initio* calculations, too, confirmed the preferential C–C bond cleavage (*vide supra*).[47]

Based on the thermolyses[9,20,50] of their all-carbon predecessors, little, if any, difference between the thermolyses of dimethylsiletane and the parent silacyclobutane was expected. In fact, when 1-silacyclobutane (**18**) was thermolyzed in 1975, eight years after its first synthesis,[51] very similar results were obtained (Scheme 13).[52] However, the expected dimerization product of the intermediate silene (**19**), was not formed. Instead, more reactive trapping agents, such as benzophenone and hexamethylcyclotrisiloxane (D3), had to be used.

In the absence of a trapping agent, the thermolysis gave a high molecular weight polymer, which the authors presumed to have come from condensation of **19**.

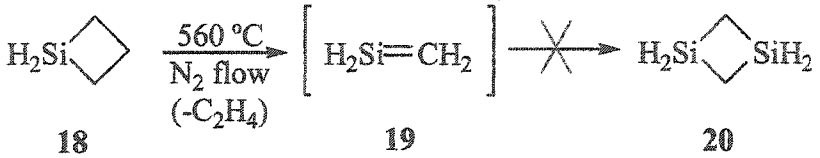

Scheme 13. Thermolysis of 1-silacyclobutane.

Eight years later, in his own study of the thermolysis of silacyclobutane, Conlin and Gill obtained some surprising results (Scheme 14).[53] In addition to the expected intermediate silene (**19**), they were able to trap two other reactive intermediates, the divalent carbene analogues silylene (**21**) and methylsilylene (**22**), using the known[54] silylene trap 1,3-butadiene (**24**). Also formed, in a 1:1 ratio with silylene (**21**), was cyclopropane (**23**), which isomerized to propene (**7**) at the higher temperature ranges. Conlin's group had observed very similar results in the vacuum pyrolysis of 1-methyl-1-silacyclobutane (methylsiletane) two years earlier.[55]

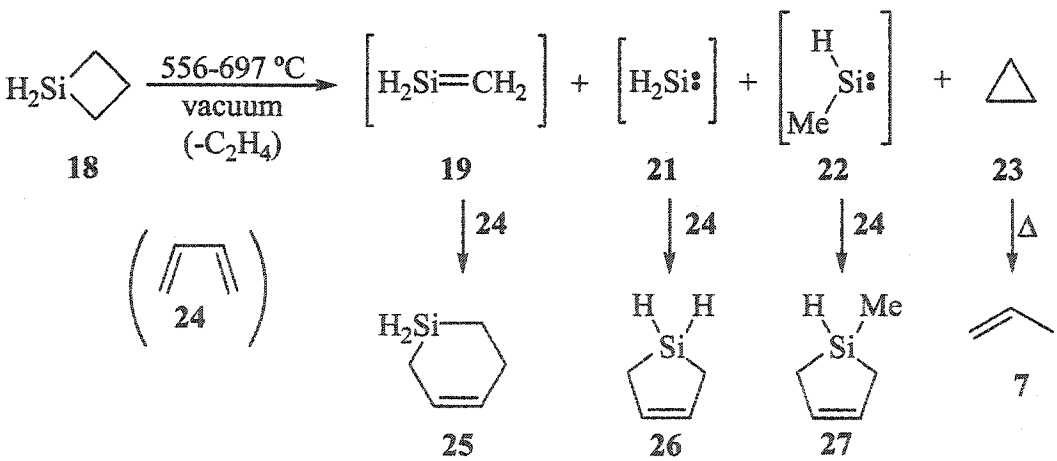

Scheme 14. Conlin & Gill's thermolysis of 1-silacyclobutane.

Conlin and Gill proposed that silylene and cyclopropane were formed in the same process (Scheme 15). Homolytic cleavage of a Si–C bond would yield diradical **28**, which then could undergo a C–C homolytic cleavage to silene and ethylene, much the same as in the cases of dimethylsiletane and cyclobutane. Alternatively, the diradical could decompose to silylene and cyclopropane through a second Si–C bond scission. Simultaneous formation of these two products would explain the observation that they are both formed in equal amounts.

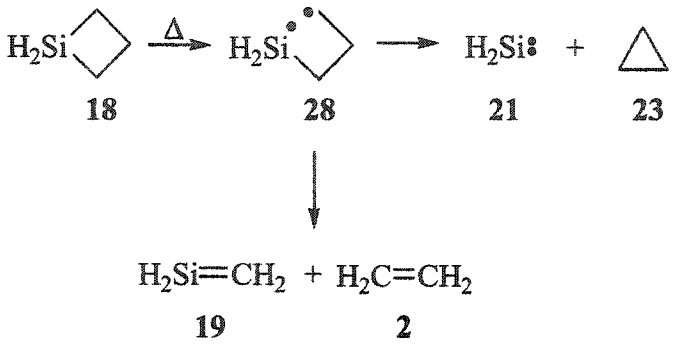

Scheme 15. Thermolytic formation of silene, silylene and cyclopropane.

The formation of methylsilylene was much less easily explained, considering that its components are not immediately available in the starting siletane. Also adding to the remarkable character of this intermediate was the fact that it is the major silicon-containing product at every temperature investigated. In fact, the ratio of **21** to **19** increased with temperature, up to a value of 5.1 at 697 °C. To explain these data, Conlin and Gill suggested that methylsilylene is formed from a 1,2-hydrogen migration of silene (Scheme 16).

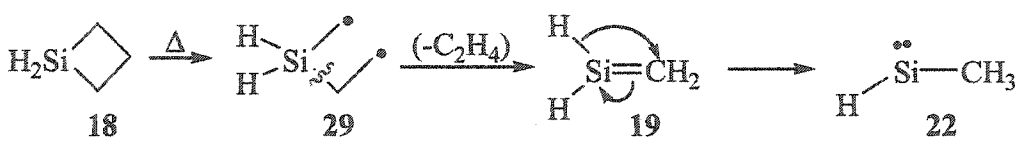

Scheme 16. Methylsilylene from a 1,2-hydrogen migration of silene.

This idea was not unprecedented; Conlin and Wood used the same 1,2-shift to explain the formation of dimethylsilylene (**30**) in the methylsiletane thermolysis.[55] They further predicted that silene would undergo this hydrogen migration more easily than methylsilene (**31**). In the article immediately following Conlin and Wood's paper, Drahnak, Michl and West provided evidence that this rearrangement is reversible.[56] Photochemically-generated dimethylsilylene[57] formed methylsilene and then disilacyclobutane **32** upon warming of the hydrocarbon matrix to 100 K (Scheme 17). The authors were careful to point out that disilacyclobutane **32** did not necessarily arise from dimerization of methylsilene. The same product had been observed by Gaspar and Conlin after dimerization of dimethylsilylene to form a disilene.[58] The mechanism for the formation of disilacyclobutanes from disilenes also had been the subject of considerable interest, but is outside the scope of the current discussion.[59-61]

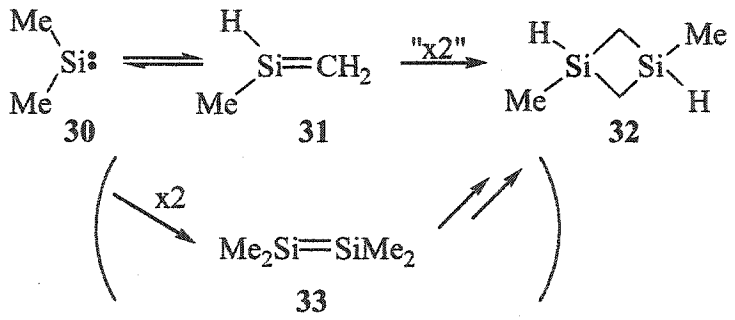

Scheme 17. Interconversion of dimethylsilylene and methylsilene.

Another possibility for the formation of methylsilylene is a 1,2-hydrogen shift of the diradical formed from initial C–C bond cleavage (Scheme 18, R=H). This mechanism initially was proposed by Barton for the formation of dimethylsilylene in the methylsiletane thermolysis (Scheme 18, R=Me).[62] In that study, independent retro-Diels-Alder generation of methylsilene in the presence of silylene traps *did not* result in the formation of dimethylsilylene-trapped products, suggesting that silenes may not be formed as thermal decomposition products of hydridosiletanes. Comparison of bond dissociation energies reveal that Barton's mechanism is thermochemically feasible; a silicon-centered radical is ~9

kcal/mol more stable than a carbon-centered radical.[63] Theoretical studies, too, cast a shadow on the silene → silylene mechanism, yielding an isomerization barrier of 41-45 kcal/mol.[64,65]

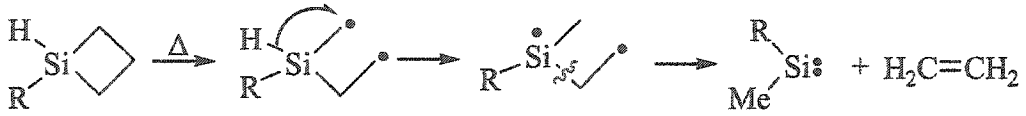

Scheme 18. Silylenes from 1,2-hydrogen migrations of diradicals.

Conlin and Gill[53] concluded that, both mechanisms are quite feasible, but that the entropic requirements of the key steps, namely homolysis or 1,2-H migration of the diradical, allow for a distinction. Since $\Delta S^{\ddagger}$ for the H migration should be lower than that for the bond homolysis to form silene, the silene route should be favored. Although it appears that this is not in fact the case, as lower silene yields were observed at higher temperatures, the high temperatures used in their study make a silene-silylene rearrangement accessible.

In 1984, the controversy surrounding the thermal decomposition of hydridosiletanes took another turn. While new experiments appeared to support the silylene-silene interconversion at higher temperatures,[66,67] other evidence called into question the mechanism of propene formation. Conlin and Gill proposed that the propene obtained in their thermolysis of silacyclobutane (**18**) came from thermal isomerization of cyclopropane, which they detected in the lower temperature range.[53] However, in the hands of Davidson *et al.*, no cyclopropane was detected upon thermolysis of **18**, even at lower temperatures and conversions; propene and ethylene were the only hydrocarbon products detected.[68] Particularly intriguing was the fact that no C_3 products had ever been detected in the thermolysis of dimethylsiletane. Thus it was clear to the authors that some mechanism other than direct elimination of cyclopropane from the initially formed diradical proposed by Conlin and Gill (Scheme 16) must be operating to form propene.

Based on stirred-flow reactor[69] (SFR) kinetic studies[68] coupled with deuterium labeling experiments,[70] Barton and coworkers were able to show that propene formation is

formed in a somewhat more complex manner (Scheme 19). Their data suggest that, in addition to homolytic C–C bond cleavage, hydridosiletanes (**34**) can undergo an alternative (essentially irreversible) 1,2-H/D shift to form silylene **35**. This silylene then can insert into a β-C–H bond to yield a silacyclopropane (silirane, **36**) which then eliminates a silylene and a deuterium-labeled propene (**38**). One remarkable aspect of this mechanism is that the silylene insertion into a C–H bond is *reversible*, leading to scrambling of the deuterium and, in some cases, more than one (and even zero) deuteria incorporated in the eventual propene. Independent generation of propylsilylene[68] (**35**, R=H) as well as subsequent investigations of alkylsilylenes[71,72] have confirmed that such an insertion does, in fact, occur.

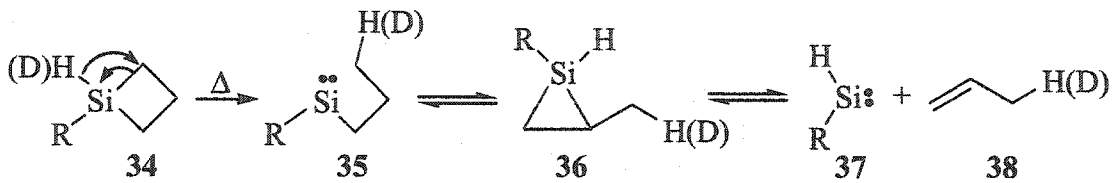

34 **35** **36** **37** **38**

(R=H/D or Me)

Scheme 19. Mechanism of propene formation.

Ab initio calculations[47,73,74] performed in 1997 also provided support for Barton's silirane mechanism and have served to help clarify the siletane decomposition mechanism. Skancke calculated[74] a barrier height of *ca.* 12 kcal/mol for **35** → **36** (R=H) and 23-26 kcal/mol for the reverse process. Any process involving diradicals (*e.g.*, ring opening) was ruled out as these species were calculated to lie significantly above the transition states for the **35** → **36** isomerization. The calculations of Gordon *et al.* confirmed Barton's hypothesis that the formation of the silylene is competitive with silene formation.

Though the history of silacyclobutane thermolysis has been short relative to that of cyclobutane, it has been no less fervid. At least for now, a consensus appears to have been reached regarding the mechanism of thermal silacyclobutane decomposition. Two characteristically different routes, summarized in Scheme 20, apparently are available to the siletanes. The first is the more "traditional" consecutive bond homolyses to yield two doubly bonded species, a silene and an alkene. The second, more exotic route is a 1,2-hydrogen

migration to form an intermediate silylene, which then reversibly inserts into a β-C–H bond until it finally decomposes to a silylene and an olefin.

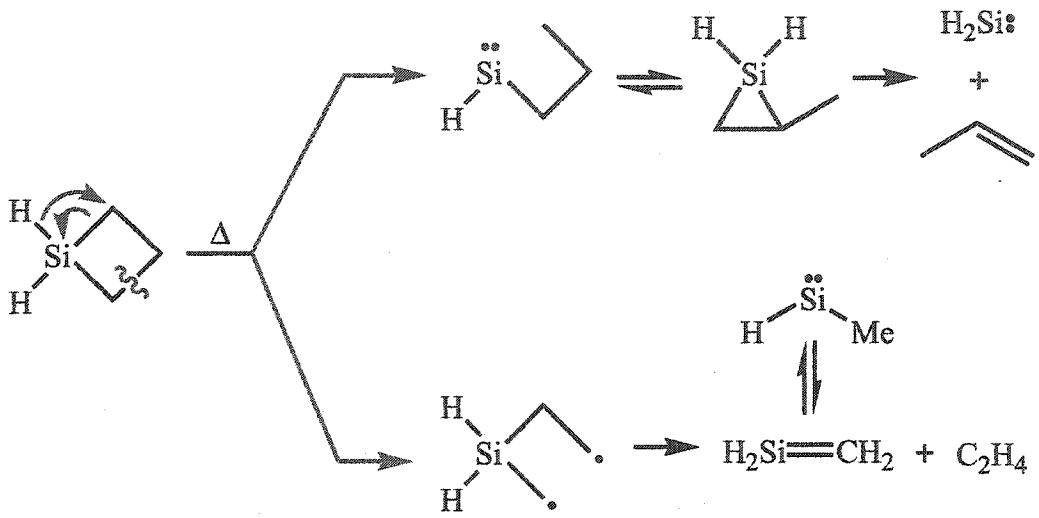

Scheme 20. Silacyclobutane decomposition.

3. Germacyclobutanes (germetanes). Only a few years after his initial silacyclobutane work, Gusel'nikov investigated the thermolysis of 1,1-dimethyl-1-germacyclobutane (dimethylgermetane, **39**) in 1970.[75] He discovered that the germanium analogue gave surprisingly different results from those of the silicon analogue. In addition to ethylene, the major products of thermolysis were cyclopropane, propene, and 1,1,2,2-tetramethyl-1,2-digermacyclopentane (**40**), the product of an apparent insertion of the silylene analogue, dimethylgermylene (**42**), into a Ge–C bond of the starting material (Scheme 21). No products, namely a 1,3-digermacyclobutane, indicating the formation of a Ge–C doubly bonded species (germene) were isolated.

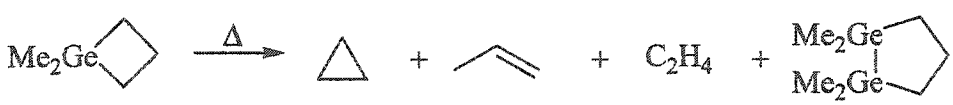

39 **23** **7** **2** **40**

Scheme 21. Gusel'nikov's dimethylgermetane thermolysis.

Gusel'nikov proposed that **39** was decomposing *via* two different routes (Scheme 22). The first route is analogous to the decomposition of dimethylsilacyclobutane and cyclobutane: formation of ethylene and 1,1-dimethyl-1-germene (dimethylgermene, **41**). All attempts at trapping the purported germene were unsuccessful, though a later report by Barton *et al.* showed that pyrolytically-generated diethylgermene does dimerize to form the expected digermacyclobutane.[76] The second route, comprising the majority of the decomposition, is homolytic cleavage of both Ge–C bonds, forming dimethylgermylene (**42**) and the trimethylene diradical (**43**), which undergoes a 1,2-H shift to propene or reversibly closes to cyclopropane. Independent synthesis and subsequent thermolysis of digermacyclopentane **40** indicated that it is more stable than **39** under the reaction conditions and thus is most likely not responsible for the observed products.

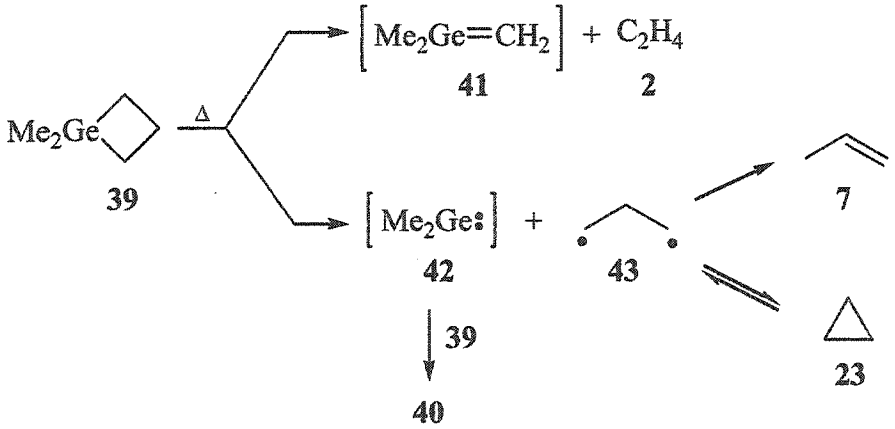

Scheme 22. Gusel'nikov's proposed mechanism for dimethylgermetane decomposition.

Conlin followed up Gusel'nikov's work in 1992 with some elegant trapping and kinetics experiments.[77] Conlin thermolyzed dimethylgermetane in the presence of 1,3-butadiene and isolated products corresponding to trapped dimethylgermylene (**42**) and 1,1-dimethylgermene (**41**). Based on his findings, Conlin proposed a mechanism (Scheme 23) which involves an initial homolytic germanium-carbon bond cleavage to yield a diradical intermediate (**41**). This intermediate then can decompose in one of three ways. First, simple homolysis of a C–C bond would eliminate ethylene and yield dimethylgermene. Second, an intramolecular elimination of cyclopropane would yield dimethylgermylene. The formation of propene is a bit more complicated. Intramolecular abstraction of a hydrogen atom from a

germanium methyl results in the formation of 1-methyl-1-propyl-1-germene (**45**). A retroene-type reaction then yields dimethylgermylene and propene.

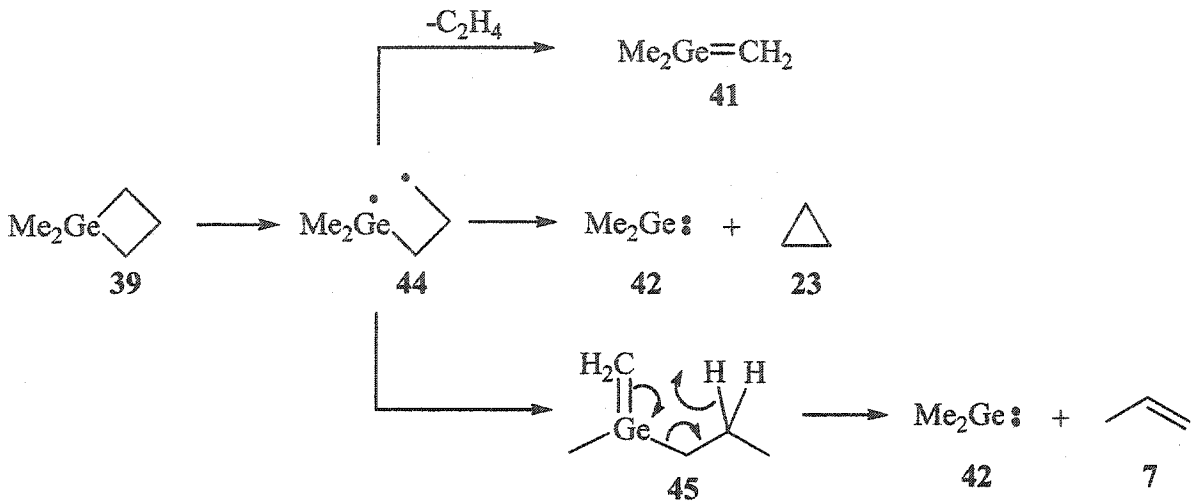

Scheme 23. Conlin's proposed mechanism for dimethylgermetane decomposition.

The only other germetane thermolysis reported in the literature is that of 1,1,3,3-tetramethylgermacyclobutane (tetramethylgermetane, **46**).[78] The vacuum pyrolysis of **46** was used to generate dimethylgermene (**41**) independently of dimethylgermetane (Scheme 24) in the hopes of providing evidence for its existence. Interestingly, the pyrolysis resulted in the formation of dimethylgermene and isobutylene (**48**), but not dimethylgermylene, dimethylcyclopropane or dimethylpropene, products expected based on the results of dimethylgermetane thermolysis. The authors concluded that tetramethylgermetane probably decomposes only by a homolytic cleavage process, as is the case with cyclobutane. This route is favored over one forming a germylene because of the relative stability of the 3° alkyl radical (**47**) formed in the initial homolysis.

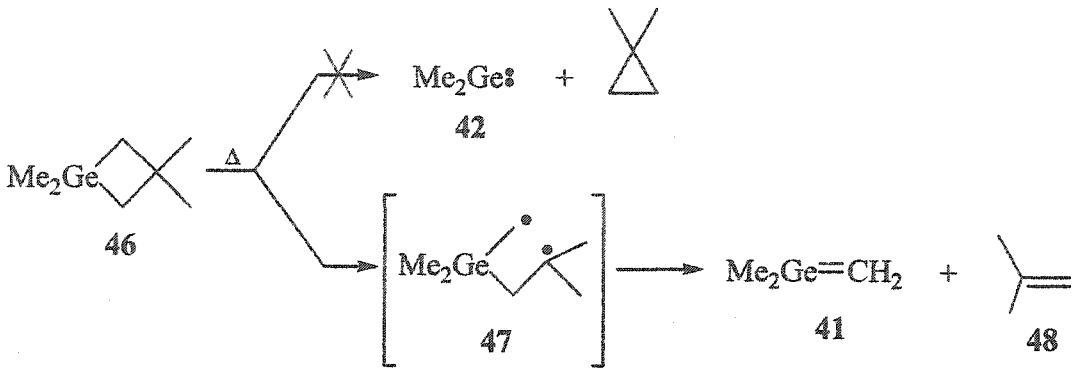

Scheme 24. Vacuum pyrolysis of tetramethylgermetane.

To date, no further investigations into the kinetics or mechanism of germetane thermolysis have been reported, though several studies on the photolysis of diphenylgermetane have been performed.[79,80] With the thermochemistries of dimethylsiletane and its parent system being so different, one must wonder if the chemistry of the parent germetane would differ as much from that of dimethylgermetane.

B. Results and discussion

1. The intramolecular cyclization strategy. Retrosynthetic analysis (Scheme 25) suggests that the most likely direct precursor of germacyclobutane would be dichlorogermacyclobutane (dichlorogermetane, **50**). As dichlorosiletane (**53**) is generally prepared *via* magnesium-induced intramolecular ring closure[81] of commercially-available 3-chloropropyltrichlorosilane (**52**), the analogous route to dichlorogermetane was envisioned. In fact, such reactions are known to give germacyclobutanes, using sodium/potassium alloy (NaK) or sodium metal in place of magnesium.[82] However, the synthesis of 3-chloropropyltrichlorogermane (**51**) would have to be undertaken due to the lack of a commercial source of this material.

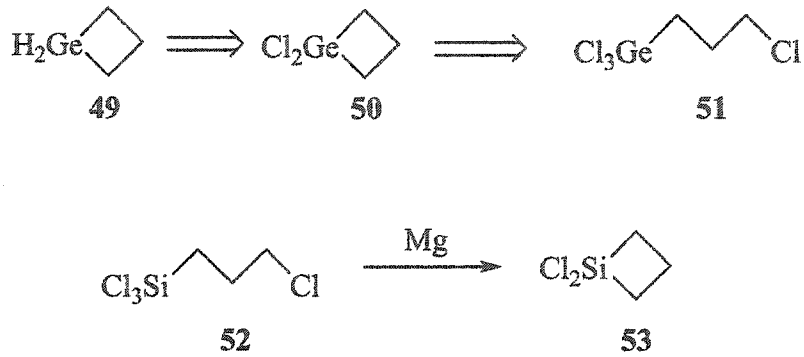

Scheme 25. Retrosynthetic analysis of germacyclobutane.

The first strategy employed (Scheme 26) utilized the ability of diiodogermylene (GeI_2, **54**) to insert into carbon-halogen bonds.[83] Thus, heating a mixture of GeI_2 and 1,3-diiodopropane (**55**) at 150 °C overnight yielded the intended 3-iodopropyltriiodogermane (**56**). Although attempts at isolating the product failed, its formation was demonstrated from the triphenyl derivative **57**, which was formed *in situ* in 10% yield by addition of phenylmagnesium bromide.

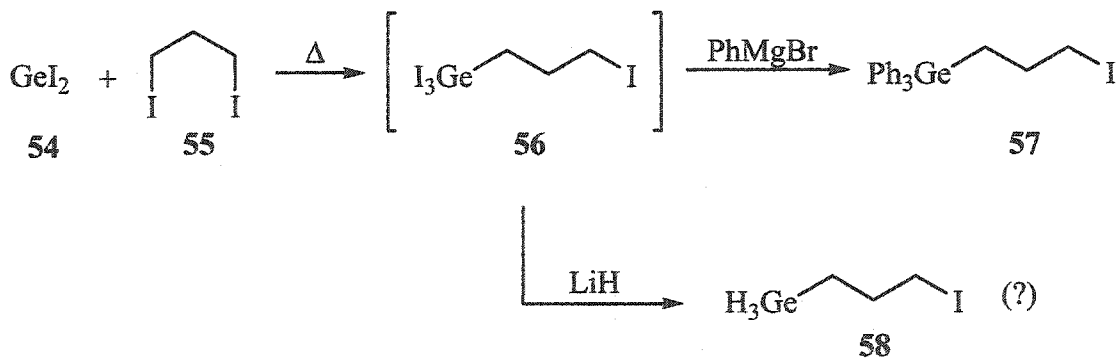

Scheme 26. Iodopropylgermane route.

Reduction of **56** with lithium hydride to form the trihydrido derivative **58**, which would offer an alternate route to germacyclobutane (Scheme 27), also was attempted. The reaction resulted in complete disappearance of the 1,3-diiodopropane and formation of a product whose GC-MS pattern is consistent with **58**. However, removal of the solvent from the reaction mixture resulted in complete loss of the product, possibly due to intermolecular

reduction of the carbon-iodine bond by germanium-hydride. Ge–H reductions of alkyl-halogen bonds are known to occur with reactivity decreasing as R–I > R–Br > R–Cl.[82]

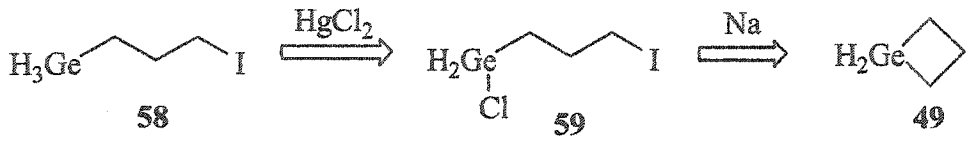

Scheme 27. Alternative intramolecular cyclization strategy.

The synthesis of 3-chloropropyltrichlorogermane was explored next. In 1996, Mazerolles and coworkers reported the hydrogermylation of an alkenylgermane with trichlorogermane generated *in situ* from tetrachlorogermane and triethylgermane (Scheme 28).[84] Preparation of trichlorogermane in this way is important because of its instability (it is in equilibrium with dichlorogermylene and hydrogen chloride). Hydrogermylation of 3-chloropropene (**65**) was thus envisioned as a useful route to intramolecular cyclization precursor **66**.

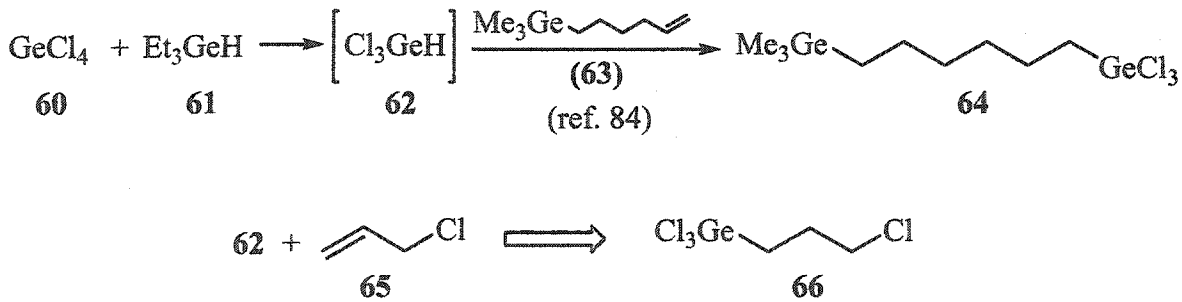

Scheme 28. Hydrogermylation with trichlorogermane prepared *in situ*.

Dichlorogermetane precursor **66** was prepared by first reacting tetrachlorogermane with ethylmagnesium bromide to form tetraethylgermane (**67**). Aluminum chloride-catalyzed chlorination of **67** gave chlorotriethylgermane (**68**), which then was reduced with lithium aluminum hydride to the desired **61** (Scheme 29). However, all attempts at forming **66** using Mazerolles' method failed (Scheme 28). The low boiling point (45 °C) of allyl

chloride relative to the reaction temperature (50 °C) probably hinders its chances of reacting before decomposition of trichlorogermane occurs.

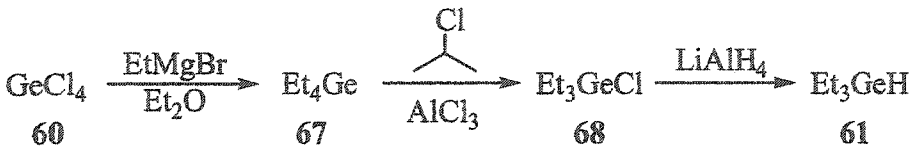

Scheme 29. Synthesis of triethylgermane.

2. Diaminogermetane. As formation of dialkylgermacyclobutanes is generally carried out through reaction of a dialkyldichlorogermane with the di-Grignard reagent **70** (Scheme 30),[85,86] this strategy next was considered.

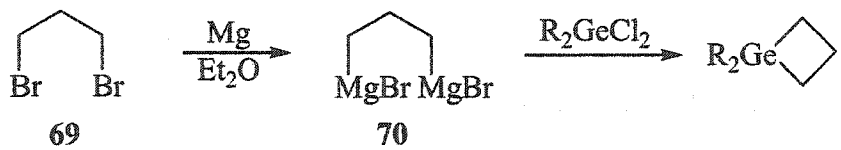

Scheme 30. Di-Grignard formation of dialkylgermacyclobutanes.

There is a problem with this route, however. Retrosynthetic analysis of dichlorogermacyclobutane (Scheme 31) suggests that the desired starting material would be dichlorogermane (H_2GeCl_2, **71**). However, the lack of commercial sources of and reliable synthetic routes to this material rendered this approach unfeasible. Instead, a strategy was envisioned that utilized the conversion of aminogermanes to chlorogermanes (Scheme 32).[87] In this method, the amino groups on germanium would serve as protecting groups on the germanium.

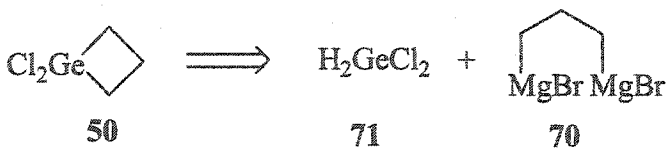

Scheme 31. Retrosynthesis of dichlorogermacyclobutane.

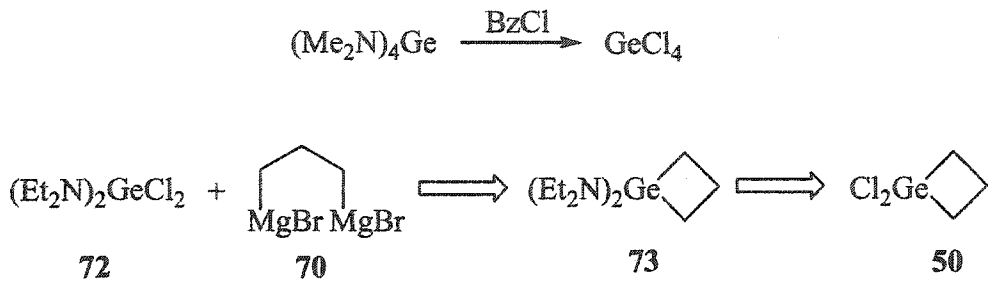

Scheme 32. Ge–N conversion to Ge–Cl.

Unfortunately, the preparation of bis(diethylamino)dichlorogermane (**72**) proved to be problematic. Reaction of tetrachlorogermane (**60**) with diethylamine (**74**) yielded a horrible mixture of aminochlorogermanes through apparent amine-catalyzed redistribution (Scheme 33).

Scheme 33. Attempted diamination of tetrachlorogermane.

3. Spirodigermetane. Direct synthesis of dichlorogermetane (**50**) by reacting di-Grignard **70** with tetrachlorogermane (**60**) was attempted next. The obvious problem with this strategy is that, once formed, dichlorogermetane can react with another equivalent of **70** to form 4-germaspiro[3.3]heptane (spirodigermetane, **75**). Therefore, careful control of reaction conditions, especially dilution, addition order and rate, and stoichiometry, must be maintained.

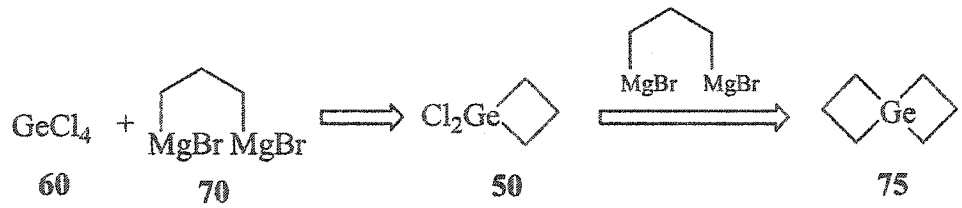

60 70 50 75

Scheme 34. Expected di-Grignard reaction with tetrachlorogermane.

In 1982, Bickelhaupt published a somewhat laborious procedure for the formation of 1,3-bis(bromomagnesio)propane (**70**) from 1,3-dibromopropane (**60**).[86] Two years later, he prepared dimethylgermetane (**39**) in 96% yield with the di-Grignard reagent prepared using this procedure. However, application of this method to the synthesis of dichlorogermetane **50** failed to yield the desired product (see Experimental section). Perturbations of Bickelhaupt's original procedure included increasing dilution, reversing reagent addition order, varying relative amounts of reagents, and using activated magnesium[88] (Mg*) in place of magnesium turnings. The only Ge-containing products (Scheme 35) isolated during these reactions were spirodigermetane **75**, 1,1-diallyl-1-germacyclobutane (diallylgermetane, **76**), and tetraallylgermane (**77**). Spectroscopically pure samples of germetanes **75** and **76** could be obtained only by preparative gas chromatography (prep-GC) as attempted distillation resulted in decomposition. The ^{1}H NMR spectra of both **75** and **76** contained ring proton resonances in the range 1.5-2.0 ppm, consistent with those reported for the corresponding dimethylgermetane.[85] Likewise, the ^{13}C resonances for the ring carbons corresponded well to those of dimethylgermetane, with values in the 20-25 ppm range.[85] The formation of the allylgermanium species can be rationalized by a $MgBr_2$-induced formation of allylmagnesium bromide (**78**) from di-Grignard **70** (Scheme 36).[86]

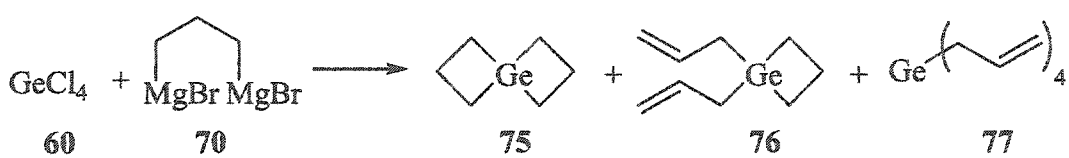

60 70 75 76 77

Scheme 35. Di-Grignard reaction with tetrachlorogermane.

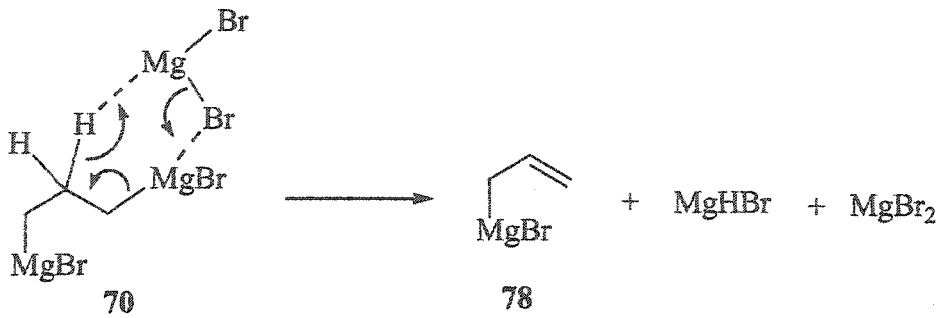

Scheme 36. Allymagnesium bromide formation from di-Grignard **70**.

These two new germetanes are interesting themselves. For instance, **75** contains two strained 4-membered rings instead of just one and has the potential for some interesting thermochemistry. Diallylgermetane **76**, which will be discussed in the next section, has allyl substituents on the germanium atom instead of the alkyl substituents seen in previously-synthesized germetanes and present the possibility of very interesting retroene processes. In order to carry out the thermochemical experiments, a better method for synthesizing **75** and **76** in higher yields would have to be designed. Thus, it was determined that "delayed coaddition" (see experimental section) of dibromopropane and tetrachlorogermane followed by simple column chromatography resulted in the isolation of spirodigermetane **75** in 45% yield. With a reliable synthesis in hand, the thermochemical studies of **75** were ready to begin.

Spirodigermetane is insufficiently volatile for neat introduction into the stirred-flow reactor (SFR, see experimental section), so it was used as a solution in benzene. SFR thermolysis (see Appendix A) from 430-500 °C resulted in the formation of cyclopropane, propene, and a small amount of ethylene in a 3:10:1 ratio (GC), respectively, at 490°C (Scheme 37). The hydrocarbons were identified by comparison of GC retention times (alumina column) and MS fragmentation with those of authentic samples. These results are consistent with those obtained from thermolysis of dimethylgermetane (which, for direct comparability, also was thermolyzed in the SFR; see Appendix A). However, the activation energy (E_a) for decomposition of spirodigermetane (51 kcal/mol) is 11 kcal/mol lower than the E_a for dimethylgermetane (62 kcal/mol)! Initially, it was believed that this significant lowering of E_a can be explained by the added ring strain inherent in spirodigermetane. The

driving force for ring cleavage in germacyclobutanes is the ring strain associated with forcing the sp^3-hybridized Ge to compress its bond angles from 109.5° to 90°. To accommodate this compression, the remaining C–Ge–C bond angle would expand to >109.5°. Addition of the second ring to this already strained system would introduce even more strain as the remaining bonds are compressed to approach the 90° angles of 4-membered rings.

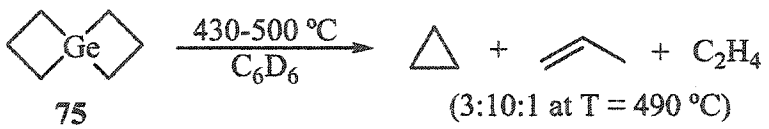

75

$E_a = 51.0 \pm 0.3$ kcal/mol
$\log A = 13.58 \pm 0.08$

Scheme 37. SFR thermolysis of spirodigermetane.

One common method used to estimate molecular ring strain is the use of isodesmic reactions.[89,90] Isodesmic calculations were carried out on a series of germetanes (see Appendix B); the results are summarized in Table 1. The results of the calculations confirm that, while each of the other germetanes investigated have ring strain energies around 20 kcal/mol, spirodigermetane does in fact have twice as much (*ca.* 40 kcal/mol). Therefore, **75** could have a lower E_a and faster rate of decomposition, as is observed, depending upon the mechanism of decomposition. However, this explanation could be true only if *both* rings were being cleaved simultaneously in the rate-determining step. As this is unlikely to occur, the lower E_a for spirodigermetane (compared to that for dimethylgermetane) still remains somewhat puzzling.

Table 1. Calculated ring strain energies (MP2//HF/6-31G*) of selected germetanes.

molecule	ring strain (kcal/mol)
germetane	-21.63
methylgermetane	-19.91
dimethylgermetane	-18.38
spirodigermetane	-39.79

In addition to simple ring cleavage, the formation of ethylene in the thermolysis can result from initial cleavage of one of the 4-membered rings in **75**, followed by ring expansion and subsequent decomposition to atomic germanium and two molecules of ethylene (Scheme 38). Visible germanium deposition on the inner walls of the SFR reactor after several thermolyses is consistent with such a process.

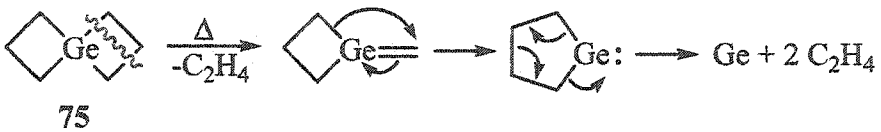

75

Scheme 38. A possible mechanism for thermolytic ethylene formation from **75**.

4. Diallylgermetane. Since diallylgermetane (**76**) was produced only as a byproduct in the di-Grignard reaction of tetrachlorogermane, a better synthesis was designed. The new starting material, diallyldichlorogermane (**79**), was prepared in 18% yield by a modification of a Direct Process method by Zueva *et al.* (Scheme 39).[91] The diallyldichlorogermane then was used in the di-Grignard reaction developed for synthesis of spirodigermetane to give diallylgermetane (**76**) in 61% yield (Scheme 40).

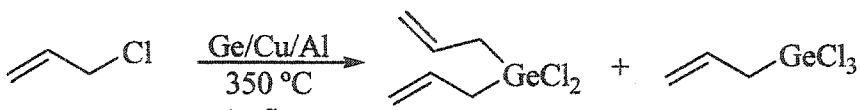

65 **79** **80**

Scheme 39. Direct Process synthesis of diallyldichlorogermane.

79 **69** **76**

Scheme 40. Synthesis of diallylgermetane.

The thermochemistry of allylsilanes has been studied quite extensively.[92-94] Two competing pathways were found to be operating (Scheme 41): a retroene elimination (path

A) and silicon-allyl bond homolysis (path B), with the retroene mechanism dominating the reaction. A retroene mechanism presents several interesting possibilities for the thermal decomposition of diallylgermetane, two of which are shown in Scheme 42.

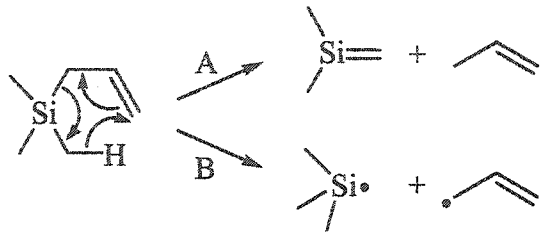

Scheme 41. Thermolysis of allylsilanes.

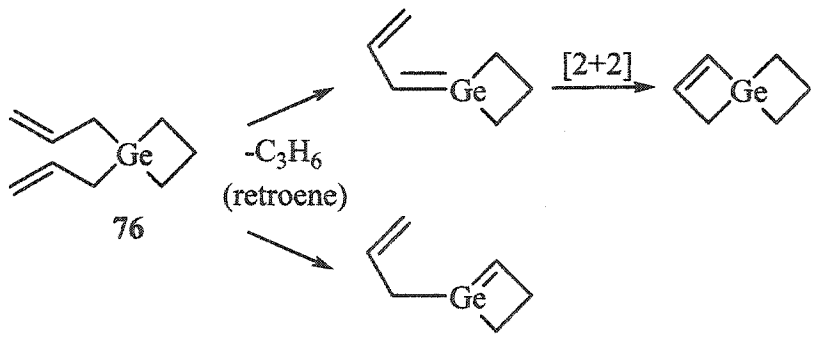

Scheme 42. Possible thermal decomposition routes for diallylgermetane.

SFR thermolysis (see Appendix A) of diallylgermetane from 430-510 °C resulted in the formation of propene and a small amount of hexadiene (Scheme 43). In marked contrast to the thermolysis of both dimethylgermetane and spirodigermetane, no cyclopropane formation was observed, even when an alumina column was used for better separation of the hydrocarbons (the difference in retention times between cyclopropane and propene on the alumna column was confirmed to be >1 minute using authentic samples). SFR thermolysis of cyclopropane alone at these temperatures failed to yield propene, ruling out the disappearance of cyclopropane by thermal decomposition. Indeed, temperatures in excess of 600 °C were needed before significant isomerization of the cyclopropane was observed.

However, just as in the case of spirodigermetane thermolysis, the E_a for decomposition of diallylgermetane (55 kcal/mol) is lower than that for dimethylgermetane (62 kcal/mol).

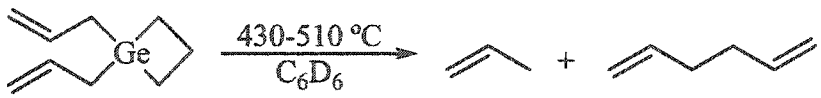

76

$E_a = 54.8 \pm 0.5$ kcal/mol
$\log A = 14.51 \pm 0.15$

Scheme 43. SFR thermolysis of diallylgermetane.

An explanation can be found in the thermochemistry of allylgermanes, such as allyltrimethylgermane. There is good evidence that allylgermanes thermally decompose *via* homolysis of the weakest bond, the allyl-germanium bond (Scheme 44).[95] In fact, SFR thermolysis of diallyldimethylgermane gave Arrhenius parameters (E_a = 53 kcal/ mol, log A = 14) that are quite close to those of diallylgermetane (see Appendix A). Thus, homolytic cleavage of an allyl-germanium bond in diallylgermetane offers a lower-energy decomposition than the germanium-carbon ring cleavage observed for dimethylgermetane.

Scheme 44. Thermolysis of allyltrimethylgermane.[95]

To test this hypothesis, flow pyrolysis of diallylgermetane (**76**) was performed in the presence of carbon tetrachloride (Scheme 45). Since carbon-chlorine bonds are efficient traps for germanium-centered radicals, the formation of chlorogermanes would suggest the formation of these intermediates. The expected products, chloro(allyl)germetane (**81**) and dichlorogermetane (**50**), were indeed formed, suggesting that homolysis of a germanium-allyl bond in diallylgermetane at least competes with ring cleavage.

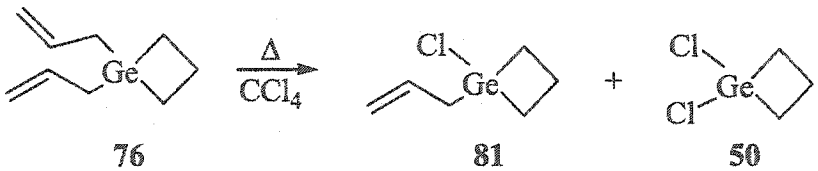

76 81 50

Scheme 45. Flow pyrolysis of diallygermetane in CCl_4.

5. Germacyclobutane. Diallylgermetane had a side benefit in that it offered an alternative route to germacyclobutane. In 1968, Roberts showed that allylgermanes can be converted to chlorogermanes with mercuric chloride (Scheme 46).[96] An added attraction to this method was that $HgCl_2$ could be a mild enough Lewis acid that electrophilic ring opening of the germacyclobutane ring could be avoided. Indeed, reaction of diallylgermetane with an excess of $HgCl_2$ in acetonitrile resulted in a 47% yield of dichlorogermetane **50** (Scheme 47). Extraction of moisture-sensitive **50** from the mercury salts proved to be challenging as the solubility of the polar dichlorogermetane is limited in hydrocarbon solvents compared to polar solvents. Accordingly, the reaction was carried out in a liquid-liquid extraction apparatus (see Appendix C). Upon completion of the reaction, extraction of the product into pentanes was accomplished in three days.

Reduction of dichlorogermetane with lithium aluminum hydride then afforded the long-awaited parent germacyclobutane **49** in quantitative yield. The product was isolated as a clear colorless liquid by low pressure distillation from the reaction mixture. The boiling point of **49** was not able to be determined accurately due to its volatility; the distillation receiver had to be cooled to –78 °C in order to collect the distilled product at ~20 torr and samples were stored in a refrigerator. In addition to peaks for the germetane ring protons (1.50 and 2.20 ppm), a germanium hydride peak was detected at 4.70 ppm by ^{1}H NMR (Figure 1). The ^{1}H NMR values for the ring protons are in good agreement with those measured for dimethylgermetane (**39**): 1.46 and 2.25 ppm.[85] The ^{13}C NMR spectrum (Figure 2) showed only resonances for the two ring carbons at 15.16 and 24.59 ppm. In the IR spectrum of **49**, the Ge–H bond stretch was evident at 2066 cm^{-1} while the GeH_2 bending and wagging frequencies appeared at 865 and 881 cm^{-1}.[82]

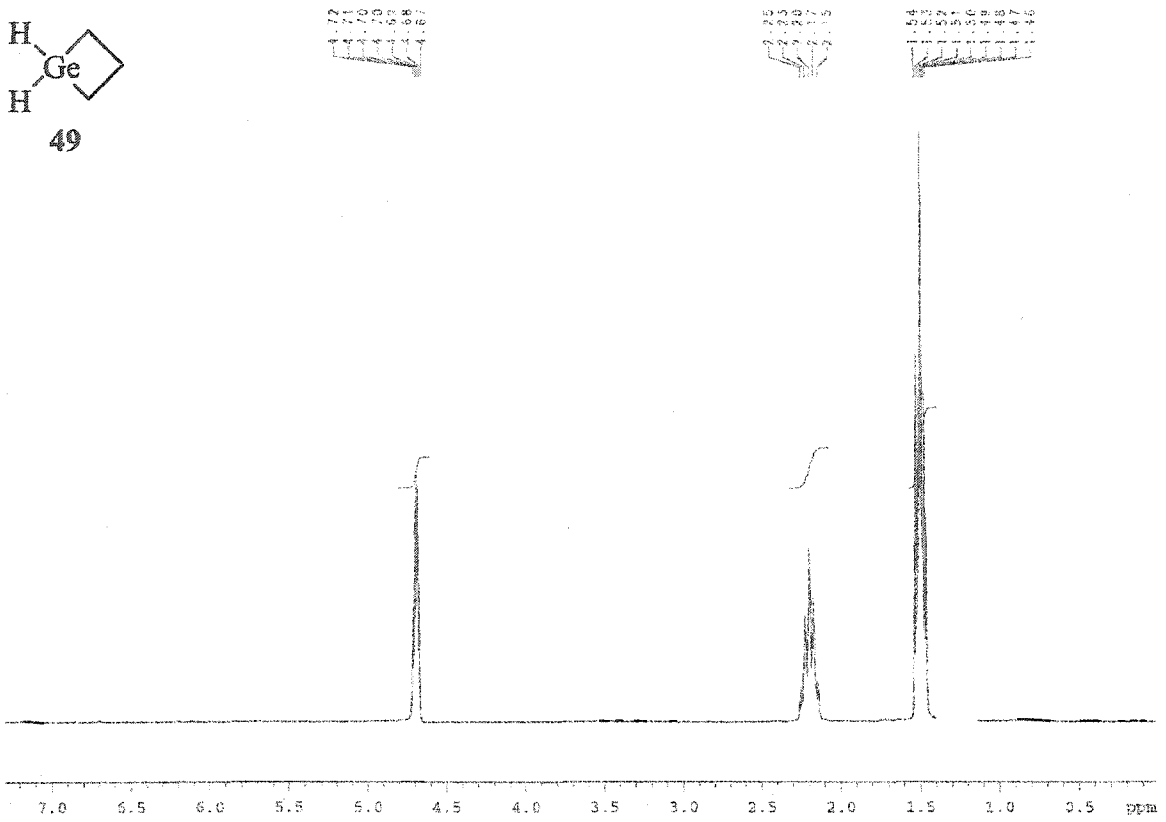

Figure 1. ^{1}H NMR spectrum of germacyclobutane (**49**).

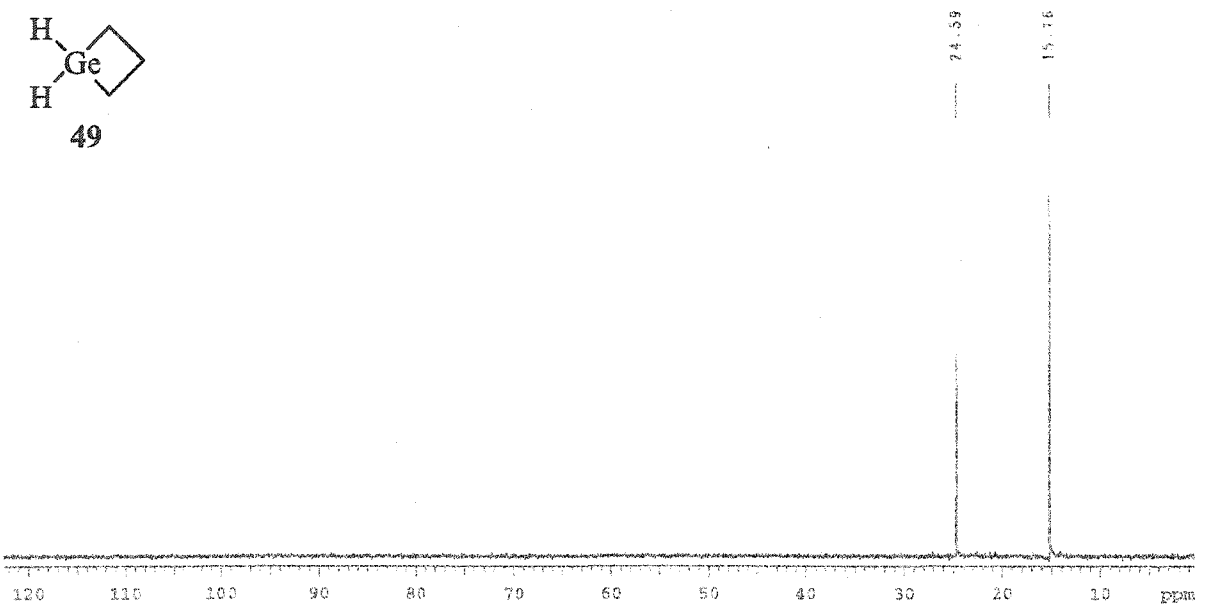

Figure 2. ^{13}C NMR spectrum of germacyclobutane (**49**).

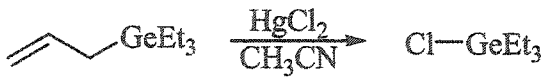

Scheme 46. Conversion of allylgermanes to chlorogermanes with $HgCl_2$.[96]

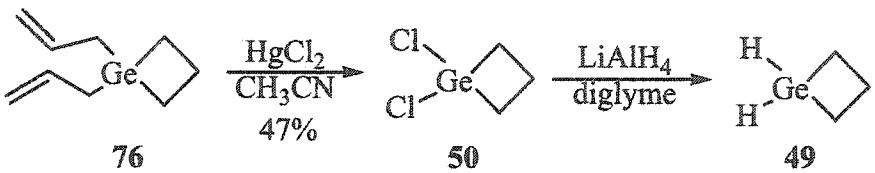

76 **50** **49**

Scheme 47. Synthesis of germacyclobutane.

Upon SFR thermolysis, germacyclobutane yielded propene as the only detected hydrocarbon product (Scheme 48). The identity of propene was confirmed by MS and identification of its bromine adduct, 1,2-dibromopropane. This sole production of propene, coupled with the significantly lower (relative to the other germetanes) E_a for germacyclobutane suggests the occurrence of a different mechanism, presumably the proposed initial [1,2]-H shift, for its decomposition. If initial ring Ge–C bond homolysis were occurring, cyclopropane also should be formed, as was the case in the thermolysis of dimethylgermetane and spirodigermetane. Sequential Ge–C homolyses also should result in the formation of significant amounts of cyclopropane through ring closure of the intermediate propane-1,3-diyl diradical.[97]

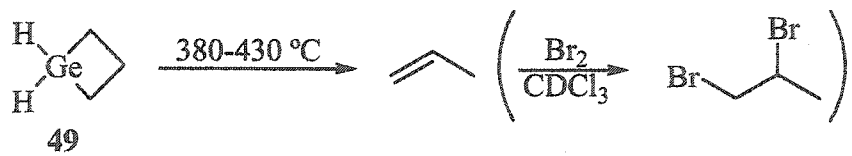

49

$E_a = 48.2 \pm 0.3$ kcal/mol

$\log A = 14.73 \pm 0.09$

Scheme 48. SFR thermolysis of germacyclobutane.

To provide evidence for the [1,2]-H shift mechanism (Scheme 49), propylgermane (**85**) was prepared and its thermochemistry examined. If a [1,2]-H shift to form propylgermylene is occurring, then production of **82** *via* a different route also should result in the formation of propene. Propylgermane was chosen as a thermal precursor to **82** because mono- and dialkylgermanes are known to lose molecular hydrogen to yield germylenes upon thermolysis.[98,99] SFR thermolysis of **85** indeed did generate propene, which was detected as above by bromine trapping. No other products were detected by GC.

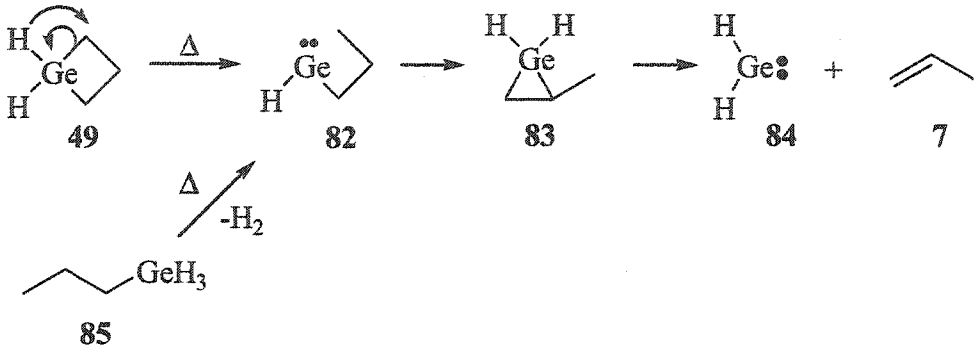

Scheme 49. Possible mechanism for germetane decomposition.

To further investigate the proposed mechanism, dideuteriogermetane (**86**) was synthesized by the lithium aluminum deuteride reduction of dichlorogermetane. Evidence for the formation of the isotopically-labelled germetane was provided by the lack of Ge–H peaks in the ^{1}H NMR spectrum and the appearance of a Ge–D stretch at 1490 cm^{-1} in the IR spectrum. The results of SFR thermolysis of 86 are presented in Scheme 50; again, propene was the only hydrocarbon produced in the reaction. To determine the amount of deuterium incorporation in the propene, a second SFR reactor was prepared in which a GC-MS was used in place of an analytical (FID) GC for product detection and analysis. Nearly 80% of the propene formed contained deuterium, based on comparison of the abundances of the *m/z* 41, 42, and 43 peaks, which represent the base peaks for propene, propene-*d*, and propene-d_2, respectively. These data are consistent with a [1,2]-migration of D from Ge to an α ring carbon. It is interesting to note that approximately 2/3 of the propene contained not just one deuterium, but *two*, consistent with a reversible migration step. Further support was provided

by comparison of the rate constants for the germacyclobutane and dideuteriogermetane thermolyses. A primary deuterium isotope effect of 1.57 (at T=410 °C), also consistent with a mechanism involving cleavage of a Ge–H (or Ge–D) bond in the rate determining step, was found.[100]

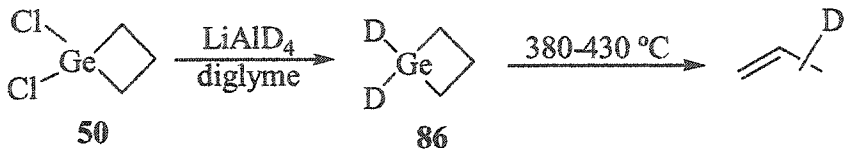

50 **86**

E_a = 49.7 kcal/mol
log A = 15.07

k_H/k_D = 1.57 (at 410 °C)

Scheme 50. Synthesis and SFR thermolysis of dideuteriogermetane.

Although these data appear to support the proposed [1,2]-H migration, they do not rule out a mechanism involving initial homolytic cleavage of a germanium-carbon bond. The intermediate diradical thus formed also could give propylgermylene upon an intramolecular hydrogen abstraction (Scheme 51). Indeed, closer inspection of the Arrhenius parameters for this reaction reveals some apparent inconsistencies. While an E_a of 48.2 kcal/mol seems too low to be consistent with Ge–C ring cleavage, especially when compared to those observed for other germacyclobutanes (*e.g.* 62 kcal/mol for dimethylgermetane), the observed log A of

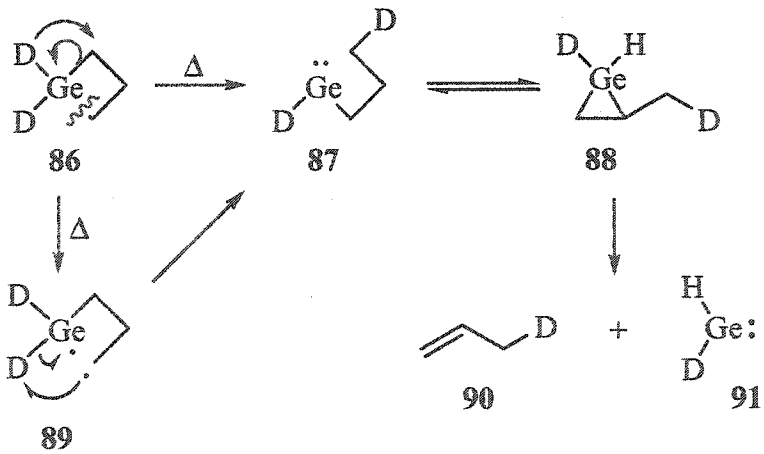

86 **87** **88** **89** **90** **91**

Scheme 51. Possible mechanisms for thermal decomposition of germacyclobutane.

14.7 is consistent with a process requiring a less constrained transition state, such as a homolytic cleavage.[101,102] It is quite possible that both processes are occurring in competition under these conditions and the Arrhenius parameters thus represent a combination of those for the competing reactions. However, log *A* values can be rather variable[102] and the E_a value of 48.2 kcal/mol is much too low to be attributed to ring cleavage.

C. Conclusions

Four new germetanes have been synthesized (Figure 3) and the thermal behavior of three of them (spirodigermetane **75**, diallylgermetane **76**, and germacyclobutane **49**) has been studied. A modified di-Grignard synthesis produces **75** and **76** in moderate yields and dichlorogermetane (**50**) and diallylgermetane themselves have proven to be useful starting materials, opening the way for the study of myriad other potentially interesting germetanes.

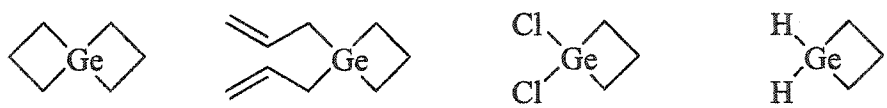

75 **76** **50** **49**

Figure 3. New germetanes.

Gas-phase thermolysis of **75** yields the same hydrocarbon products observed in previously studies systems, though with a lower energy of activation (E_a). Isodesmic calculations indicate that the ring strain in **75**, approximately double that in other monocyclic germetanes, is the likely cause for the decreased E_a. Diallylgermetane (**76**), on the other hand, produces only propene and 1,5-hexadiene upon gas-phase thermolysis. Trapping studies and comparison to the activation parameters of acyclic allylgermanes suggest that the germanium-allyl bond is weak enough to compete with ring cleavage.

The thermochemistry of the original target of this study, the parent germetanes **49**, is quite different from dimethylgermetane, as predicted. The only hydrocarbon product detected is propene, which, along with deuterium labeling studies, indicates an intramolecular hydrogen migration, much like in the case of the parent silacyclobutane, is occurring. While it is possible that the H-migration and ring-cleavage mechanisms may be in

competition with each other, the comparatively low E_a value (48.2 kcal/mol) favors the migration.

D. Experimental

Instrumentation and General Procedures. ^1H and ^{13}C NMR spectra were acquired on Varian (VXR-300 and VXR-400) spectrometers. Chemical shifts are reported as parts per million (ppm) relative to tetramethylsilane using the given solvents as standards: $CDCl_3$ (^1H 7.27 ppm, ^{13}C 77.23 ppm), C_6D_6 (^1H 7.16 ppm, ^{13}C 128.39 ppm). Fourier transform infrared (FTIR) spectra were obtained on a Bio-Rad Digilab FTS-7 spectrometer using neat samples in a 0.025 mm sealed cell. Exact masses were obtained *via* high resolution mass spectrometry (HRMS) on a Kratos MS50 mass spectrometer with a resolution of 10,000. Gas chromatography-mass spectrometry (GC-MS) data were obtained using a Hewlett-Packard 5890 Series II Plus gas chromatograph connected to an electron impact (EI) 5972 Series Mass Selective Detector operating at 70 eV. Routine analytical gas chromatography was performed using a Hewlett-Packard 5890 Series II gas chromatograph (GC) equipped with a flame ionization detector. A 30 meter J&W DB-5 capillary (0.250 mm i.d.) column was used for separation in both the analytical and GC-MS gas chromatographs. Preparative gas chromatography was carried out on a Varian Aerograph Model 920 gas chromatograph using a thermal conductivity detector. Copper tubing (210x0.5 cm) packed with Alltech 14% SE-30 on Chromosorb W-HP was used for the separations and helium was used as the carrier gas.

Pulsed stirred-flow reactor (SFR) studies were performed using an apparatus modeled after that of Baldwin *et al.*[69] The system was calibrated using the gas-phase thermal isomerization of cyclopropane to propene.[69] A quartz reaction chamber with a volume of 4 mL was heated by a tube furnace controlled with a Digi-Sense temperature controller. A helium flow rate of 30 mL/min was maintained through the reaction chamber by a MKS Model 1259B mass flow controller. Reactants and products were swept directly into a Hewlett-Packard 5890 GC, where they were separated and then analyzed by a flame ionization detector (FID). FID data were recorded on a Hewlett-Packard 3392A integrator in addition to a microcomputer. The GC was equipped with either a 30 m J&W DB-5 or a 50 m

Varian Al_2O_3/Na_2SO_4 ("alumina") megabore (0.53 mm i.d.) column. Hydrocarbon products were identified by comparison of their retention times to those of authentic samples on the alumina column. A similar apparatus was connected to the GC-MS described above for additional studies.

Tetrahydrofuran (THF) was distilled over lithium aluminum hydride (LAH) and diethyl ether was distilled over sodium/benzophenone prior to use. Other solvents and reagents were obtained commercially and used without further purification, unless indicated otherwise.

Synthesis of germanium diiodide (54). The synthesis of **54** was achieved by using Garvey's modification[103] of Foster's[104,105] route. After drying in an Abderhalden drying pistol overnight, the desired product was obtained as bright golden flakes in 90% yield.

Synthesis of 3-iodopropyltriphenylgermane (57). Germanium diiodide (5.00 g, 15.3 mmol) and diiodopropane (2.00 mL, 17.4 mmol) were placed in a 25 mL round bottom flask fitted with a magnetic stir bar and West condenser. The reaction was heated to 150 °C and stirred for 8 hours under a positive pressure of Ar. The reaction mixture turned from a pasty golden-colored liquid to a yellow-orange liquid with white precipitate. Diethyl ether (50 mL) was added, followed by 15 mL of a 3 M solution of phenylmagnesium bromide in diethyl ether (45 mmol). Stirring was continued overnight, after which the excess Grignard reagent was quenched with 10 mL water. The ether layer then was washed thrice with 10 mL saturated aqueous sodium chloride and dried over anhydrous magnesium sulfate. Concentration *in vacuo* gave a yellow oil, which, upon column chromatography (silica gel, pentanes) yielded 0.75 g (1.6 mmol, 10% yield) white powdery **57**. **^{1}H NMR** (300 MHz, chloroform-*d*) δ 1.60 (m, 2 H, Ge-C$\underline{H}_2$-CH$_2$), 2.03 (m, 2 H, CH$_2$-C$\underline{H}_2$-CH$_2$), 3.21 (t, J = 8 Hz, 2 H, I-C$\underline{H}_2$-CH$_2$), 7.42 (m, 12 H, aromatic); **^{13}C NMR** (75 MHz, chloroform-*d*) δ 10.77 (Ge-$\underline{C}$H$_2$), 15.63 (CH$_2$-$\underline{C}$H$_2$-CH$_2$), 29.58 (I-$\underline{C}$H$_2$), 128.40, 129.17, 134.94, 136.54; **GC-MS** (EI): *m/z* (% relative intensity) 397 (M^+-Ph, 2), 355 (3), 305 (100), 227 (12), 201 (2), 151 (23), 125 (3), 99 (2), 77 (3).

Attempted synthesis of 3-iodopropylgermane (58). The reaction was performed according to the procedure for the synthesis of 3-iodopropyltriphenylgermane (**57**), except that LiH (10 molar equivalents, based on GeI_2) in 100 mL diethyl ether was used in place of the phenylmagnesium bromide. GC-MS analysis indicated that the starting material had disappeared and a new product with a MS pattern consistent with **58** had formed. Removal of the solvent *in vacuo* produced a small amount of white salts in yellow oil, but GC-MS analysis of the material showed that the product had disappeared. **GC-MS** (EI): *m/z* (% relative intensity) 245 (M^+-H, 69), 201 (100), 127 (18), 119 (36), 91 (78), 77 (GeH_3, 73).

Synthesis of tetraethylgermane (67).[106,107] Tetraethylgermane was synthesized according to a modification of two literature procedures.[106,107] Germanium tetrachloride (11.4 mL, 100 mmol) was dissolved in 200 mL dry diethyl ether in a 500 mL 3-neck round bottom flask fitted with a Friedrichs condenser, magnetic stir bar, septum, and 250 mL pressure-equalizing addition funnel. The apparatus had been flushed with argon prior to the addition and the reaction was run under a positive pressure of argon. A 3.0 M solution of ethylmagnesium bromide (EtMgBr) in diethyl ether (150 mL, 450 mmol) was transferred to the addition funnel and the flask was cooled in an ice bath. The EtMgBr was added dropwise while stirring, after which the reaction was stirred overnight. The flask was again cooled in an ice bath and the reaction was quenched by slow addition of water. Another portion (100 mL) of diethyl ether was added to the reaction mixture. The organic layer was washed thrice with saturated aqueous sodium chloride solution (100 mL each) and dried over anhydrous calcium chloride. Filtration and removal of the solvent *in vacuo* yielded tetraethylgermane as a clear colorless liquid in quantitative yield. **^{1}H NMR** (300 MHz, chloroform-*d*): δ 0.72 (q, $J = 9$ Hz, 3 H, Ge-CH_2-$\underline{C}H_3$), 1.02 (t, $J = 9$ Hz, 4 H, Ge-$\underline{C}H_2$-CH_3); **^{13}C NMR** (75 MHz, chloroform-*d*): δ 3.51 (Ge-$\underline{C}H_2$-CH_3), 8.97 (Ge-CH_2-$\underline{C}H_3$).

Synthesis of chlorotriethylgermane (68).[108] A modification of Mironov and Kravchenko's monochlorination of tetramethylgermane[109] was used. A 25 mL 2-neck round bottom flask was fitted with a septum, West condenser, and magnetic stir bar; the apparatus was flushed with argon and a positive pressure of argon kept thereafter. Tetraethylgermane (3.5 g, 19

mmol) and anhydrous aluminum chloride (0.06 g, 0.4 mmol) were added to the flask and isopropyl chloride (1.8 mL, 19 mmol) added dropwise *via* syringe. The reaction was heated to 95 °C in an oil bath for one hour. Distillation yielded 1.86 g (9.53 mmol, 50% yield) chlorotriethylgermane. **^{1}H NMR** (300 MHz, chloroform-*d*): δ 1.14 (s, 15 H); **^{13}C NMR** (75 MHz, chloroform-*d*): δ 8.02, 10.42; **b.p.** 175-178 °C (lit.[108] 173-177 °C).

Synthesis of triethylgermane (61).[110] The synthesis of the title compound was based on Anderson's procedure.[110] Lithium aluminum hydride (7.4 g, 195 mmol) was dissolved in 250 mL dry diethyl ether in an argon-purged 500 mL 3-neck round bottom flask fitted with a magnetic stir bar, Friedrichs condenser, and septum. While stirring the reaction, chlorotriethylgermane (24.0 mL, 144 mmol) was added dropwise *via* syringe. Upon completion of the addition, the reaction was heated to reflux overnight. The flask then was cooled in an ice bath and the reaction was quenched by the slow addition of 200 mL slightly acidic (H_2SO_4) water. The organic layer was washed with three 100 mL portions of water and dried over anhydrous sodium sulfate. Distillation yielded 8.06 g (50.1 mmol, 35% yield) triethylgermane. **GC-MS** (EI): *m/z* (% relative intensity) 161 (M^+-H, 74), 133 (M^+-Et, 100), 103 (48), 75 (17); **b.p.** 115-117 °C (lit.[82] 122 °C, 769 torr).

Attempted synthesis of 3-chloropropyltrichlorogermane (66). This procedure was modeled after that of Huc *et al.* for hydrogermylation of terminal alkenes with $HgeCl_3$.[84] A 25 mL 3-neck round bottom flask was fitted with a magnetic stir bar, West condenser, and a 25 mL pressure-equalizing addition funnel. The apparatus was flushed with argon and 2.5 mL (22 mmol) germanium tetrachloride was added to the flask. The flask was heated to 50 °C with an oil bath and dropwise addition of a mixture of 1.7 mL (11 mmol) triethylgermane and 0.90 mL (11 mmol) allyl chloride was begun through the addition funnel. The reaction was monitored by GC-MS. Heating was continued until no allyl chloride remained (7 days). None of the intended product was detected by GC-MS, though triethylchlorogermane (**68**) was formed in significant amounts.

Attempted synthesis of bis(diethylamino)dichlorogermane (72). Anderson's procedure for the tetraamination of tetrachlorogermane was used as a model for this reaction.[87] Diethylamine (51.75 mL, 500 mmol) was dissolved in 250 mL dry diethyl ether in an argon-flushed 500 mL 2-neck round bottom flask fitted with a 50 mL pressure-equalizing addition funnel and a magnetic stir bar. The flask was cooled with an ice bath and the tetrachlorogermane (11.4 mL, 100 mmol) in 50 mL dry diethyl ether was added dropwise through the addition funnel. White "smoke" and white precipitate immediately formed. The reaction was allowed to warm to room temperature upon completion of the addition and was stirred overnight. Filtration and removal of the solvent *in vacuo* yielded an inseparable mixture of products (*vide supra*).

Attempted synthesis of dichlorogermetane (50) using Bickelhaupt's method.[85,86] Magnesium turnings (2.4 g, 100 mmol) were placed in 150 mL dry diethyl ether in a 250 mL 2-neck round bottom flask fitted with a magnetic stir bar, Friedrichs condenser, and 50 mL pressure-equalizing addition funnel. 1,3-Dibromopropane (3.42 g, 17 mmol) in 50 mL dry diethyl ether was added dropwise through the addition funnel while stirring the reaction mixture. After stirring the reaction overnight, the ether was distilled off under reduced pressure and 100 mL dry tetrahydrofuran (THF) was added. The resulting mixture was stirred for 20 minutes and then filtered. The remaining residue was rinsed 4 more times in this fashion and the THF solutions were combined. Anhydrous magnesium bromide (3.13 g, 17 mmol) was dissolved in a minimum amount of 1:1 diethyl ether:THF and added to the combined THF solutions. The resulting solution was stirred overnight, after which it was cannulated into a 500 mL pressure-equalizing addition funnel connected to a 1000 mL round bottom flask containing tetrachlorogermane (5.0 mL, 44 mmol) in 500 mL dry THF and a magnetic stir bar. The contents of the addition funnel were added dropwise (very slowly) while stirring the reaction vigorously. After stirring overnight, the reaction failed to produce any **50**, as indicated by GC-MS analysis, though the amount of tetrachlorogermane remaining had noticeably decreased.

Preparation of activated magnesium (Mg*). Rieke's procedure[88] was scaled up and used as follows. Potassium chunks (7.82 g, 200 mmol) were freshly cut and added to a solution of anhydrous magnesium chloride (10.47 g, 110 mmol) in 250 mL dry THF in a 500 mL round bottom flask fitted with a West condenser and magnetic stir bar. The reaction was heated to reflux for 3 hours, forming a dark grey colored dispersion. The mixture was allowed to cool before using.

Synthesis of 4-germaspiro[3.3]heptane (spirodigermetane, 75). A 500 mL 3-neck round bottom flask was fitted with a Friedrichs condenser, magnetic stir bar, and a 50 mL pressure-equalizing addition funnel and charged with 20.0 g (0.823 mol) -50 mesh powdered magnesium. The system was evacuated and back-filled thrice with argon, after which the system was kept under a positive pressure of argon. 250 mL dry diethyl ether was added to the flask and 13.0 mL (0.128 mol) 1,3-dibromopropane in 37 mL dry diethyl ether was added to the addition funnel. The dibromopropane solution was added dropwise while stirring until bubbling of the ether was observed. 3.0 mL (0.026 mol) tetrachlorogermane then was added to the addition funnel while continuing the dropwise addition. The reaction was stirred for three hours at room temperature. Oven-dried silica gel (150 mL) was added to the reaction mixture and stirring was continued for another ½ hour. The reaction mixture then was poured onto a large (5x25 cm) chromatography column containing a small amount of silica gel and hexanes and eluted with hexanes. The solvent was removed *in vacuo* from the eluent and the resulting yellow oily residue was chromatographed (silica gel, hexanes), yielding 0.90 g (45% yield) of spirodigermetane. **^{1}H NMR** (300 MHz, chloroform-*d*): δ 1.80 (t, J = 9 Hz, 8 H, Ge-C$\underline{H_2}$), 2.22 (pentet, J = 9 Hz, 4 H, Ge-CH_2-C$\underline{H_2}$); **^{13}C NMR** (75 MHz, chloroform-*d*): δ 21.97, 25.41; **GC-MS (EI)**: *m/z* (% relative intensity) 158 (M^+, 17), 130 (M^+-C_2H_4, 5), 116 (100), 102 (35), 88 (40), 74 (41); **HRMS**: *m/z* 158.01551 (calc. for $C_6H_{12}Ge$ 158.01517).

Synthesis of 1,1-dimethyl-1-germacyclobutane (dimethylgermetane, 39).[77] Dimethylgermetane was synthesized using the method described above for the synthesis of spirodigermetane. Dimethyldichlorogermane was used in place of tetrachlorogermane. GC-

MS (EI): *m/z* (% relative intensity) 146 (M^+, 11), 131 (M^+-Me, 9), 118 (91), 103 (42), 89 (100), 75 (19), 73 (19).

Synthesis of diallyldichlorogermane (79).[91] The synthesis of **79** was performed using a modification of the procedure by Zueva and coworkers. A contact mass consisting of 13.75 g (189.4 mmol) 100 mesh germanium powder, 11.25 g (177. mmol) 200 mesh copper powder, and 0.13 g (4.8 mmol) 20 μm aluminum powder was combined with a mortar and pestle and placed in the apparatus shown in Appendix B. The tube furnace was heated at 250 °C overnight under Ar flow (220 ml/min). The furnace temperature then was increased to 350 °C and 50.0 mL (61.3 mmol) allyl chloride was added to the apparatus *via* syringe. When the allyl chloride was gone (usually 7-8 hours), the furnace was turned off and the apparatus was allowed to cool. Vacuum distillation (6 torr) of the product mixture yielded 7.8 g (18% yield) diallyldichlorogermane and 6.9 g (17% yield) allyltrichlorogermane. For *diallyldichlorogermane*, **^{1}H NMR** (300 MHz, chloroform-*d*): δ 2.515 (d, $J = 9$ Hz, 4 H), 5.19 (m, 4 H), 5.84 (m, 2 H); **^{13}C NMR** (75 MHz, chloroform-*d*): δ 30.69, 119.07, 128.89; **GC-MS (EI)**: *m/z* (% relative abundance) 185 (25), 150 (4), 109 (65), 82 (95), 74 (6), 67 (100); **b.p.** 60-63 °C, 6 torr (lit. 85 °C, 17 torr). For *allyltrichlorogermane*, **GC-MS (EI)**: *m/z* (% relative abundance) 220 (M^+, 44), 179 (37), 144 (18), 109 (100), 74 (18); **b.p.** 33-35 °C, 6 torr (lit.[111] 153.8 °C, 743.5 torr).

Flow pyrolysis of 79 in carbon tetrachloride. A solution of 0.1 g (0.5 mmol) **79** in 3.0 mL (31 mmol) CCl_4 was pyrolyzed at 450 °C under argon flow, yielding an inseparable mixture of decomposition products. GC-MS analysis of the pyrolysate showed that *ca.* 75% of the starting germetane had decomposed, forming a mixture of chlorinated germanes, including the major products dichlorogermetane (**50**) and chloro(allyl)germetane (**81**) in 4% and 25% conversion, respectively (GC-MS).

Synthesis of 1,1-diallyl-1-germacyclobutane (diallylgermetane, 76). A 500 mL 2-neck round bottom flask was fitted with a Friedrichs condenser, magnetic stir bar, and a 25 mL pressure-equalizing addition funnel and charged with 15.0 g (0.617 mol) -50 mesh powdered

magnesium. The system was evacuated and back-filled thrice with argon, after which the system was kept under a positive pressure of argon. 250 mL dry diethyl ether was added to the flask and 5.0 mL (0.049 mol) 1,3-dibromopropane in 20 mL dry diethyl ether was added to the addition funnel. The dibromopropane solution was added dropwise while stirring until bubbling of the ether was observed. Diallyldichlorogermane (4.0 g, 0.018 mol) then was added to the addition funnel while continuing the dropwise addition. The reaction was stirred overnight at room temperature. After quenching with distilled water (200 mL) and washing with saturated aqueous ammonium chloride (200 mL), water (200 mL), and saturated aqueous sodium chloride (200 mL), the ether layer was dried over anhydrous magnesium sulfate. Upon filtration and removal of the solvent *in vacuo*, the product was isolated by gravity column chromatography on silica gel with hexanes as eluent. The reaction afforded 2.16 g (61% yield) of **76** as a clear colorless liquid. **^{1}H NMR** (300 MHz, chloroform-*d*): δ 1.55 (t, J = 9 Hz, 4 H, Ge-CH_2-C$\underline{H}_2$), 1.985 (d, J = 9 Hz, 4 H, ring Ge-C$\underline{H}_2$-CH_2), 2.18 (pentet, J = 9 Hz, 2 H, CH_2-C$\underline{H}$=CH_2), 4.92 (m, 4 H, allyl Ge-C$\underline{H}_2$), 5.91 (m, 4 H, CH_2-CH=C$\underline{H}_2$); **^{13}C NMR** (75 MHz, chloroform-*d*): δ 18.41 (ring Ge-$\underline{C}H_2$), 21.59 (ring Ge-$\underline{C}H_2$), 22.96 ($\underline{C}H_2$-CH=CH_2), 113.02 (CH_2-CH=$\underline{C}H_2$), 134.86 (CH_2-$\underline{C}$H=CH_2); **GC-MS (EI)**: *m/z* (% relative intensity) 198 (M^+, 1), 170 (M^+-C_2H_4, 3), 157 (100), 129 (38), 115 (77), 101 (32), 89 (47), 74 (8); **HRMS**: *m/z* 197.04890 (calc. for $C_9H_{16}Ge$ 197.04866).

Synthesis of 1,1-dichloro-1-germacyclobutane (dichlorogermetane, 50). In the apparatus shown in Appendix B, 20 g (74 mmol) mercuric chloride was dissolved in 40 mL dry acetonitrile. To this solution, 3.03 g (15.4 mmol) diallylgermetane (**76**) was added, immediately forming a fluffy white precipitate. The reaction was stirred for 2½ hours, after which the flask containing 50 mL dry pentanes was heated to 50 °C. The extraction was carried out for three days. Fractional distillation of the pentanes extract under reduced pressure yielded 1.33 g (47% yield) of the title compound. **^{1}H NMR** (300 MHz, chloroform-*d*) δ 2.27 (pentet, J = 9 Hz, 2 H, Ge-CH_2-C$\underline{H}_2$), 2.98 (t, J = 9 Hz, 4 H, Ge-C$\underline{H}_2$-CH_2); **^{13}C NMR** (75 MHz, chloroform-*d*) δ 18.72 (Ge-$\underline{C}H_2$), 47.02 (Ge-CH_2-$\underline{C}H_2$); **GC-MS (EI)**: (% relative intensity) 186 (M^+, 2), 158 (M^+-C_2H_4, 33), 150 (9), 144 (8), 123 (1), 109 (100), 99

(2), 88 (10), 74 (17); **HRMS**: *m/z* 185.90527 (calc. for $C_3H_6Cl_2Ge$ 185.905026); **b.p.** 67-69 °C at 23 torr.

Synthesis of 1-germacyclobutane (49). 10 mL (5 mmol LAH) of 0.5 M lithium aluminum hydride (LAH) in diglyme was added to a 25 mL side-arm round bottom flask fitted with a magnetic stir bar, rubber septum, and a short-path distillation head. A short piece of Teflon tubing was connected to the drip tip of the distillation head to extend it nearly to the inside wall of the 4 mL collection tube connected to the receiver end of the distillation head. The flask was cooled in an ice/salt bath and the collection tube was cooled in a dry ice/acetone bath. 1.42 g (7.65 mmol) dichlorogermetane (**50**) was added *via* syringe to the stirring LAH solution. The reaction was stirred for ½ hour, after which vacuum, supplied by a water aspirator, was applied for 1 hour. The ice/salt bath was removed and vacuum was applied again until no more bubbling was observed in the diglyme solution. A quantitative yield of **49**, a clear colorless liquid, was obtained. **^{1}H NMR** (300 MHz, benzene-*d*6): δ 1.50 (m, 4 H, Ge-C$\underline{H}_2$-CH_2), 2.20 (m, 2 H, Ge-CH_2-C$\underline{H}_2$), 4.70 (m, 2 H, Ge-$\underline{H}$); **^{13}C NMR** (75 MHz, benzene-*d*6): δ 15.16 (Ge-$\underline{C}H_2$), 24.59 (Ge-CH_2-$\underline{C}H_2$); **FTIR**: $\bar{\nu}$ (cm^{-1}) 2993 (w), 2938 (w), 2873 (w), 2066 (s), 2050 (s, Ge-H), 881 (w, Ge-H), 865 (w, Ge-H); **GC-MS (EI)**: *m/z* (% relative intensity) 116 (M^+-2H, 18), 101 (7), 88 (41), 74 (100); **HRMS**: *m/z* 117.98401 (calc. for C_3H_8Ge 117.983824).

Synthesis of 1,1-dideuterio-1-germacyclobutane (86). The title compound was obtained in quantitative yield using the procedure described for **49** except that lithium aluminum deuteride was used in place of lithium aluminum hydride. **^{1}H NMR** (300 MHz, benzene-*d*6): δ 1.49 (t, J = 9 Hz, 4 H, Ge-C$\underline{H}_2$-CH_2), 2.20 (pentet, J = 9 Hz, 2 H, Ge-CH_2-C$\underline{H}_2$); **^{13}C NMR** (75 MHz, benzene-*d*6): δ 14.82 (Ge-$\underline{C}H_2$), 24.57 (Ge-CH_2-$\underline{C}H_2$); **FTIR**: $\bar{\nu}$ (cm^{-1}) 2993 (w), 2934 (w), 2878 (w), 1506 (w), 1490 (w); **GC-MS (EI)**: *m/z* (% relative intensity) 116 (M^+-2D, 12), 101 (4), 90 (42), 74 (100).

Synthesis of propyltrichlorogermane.[112] Magnesium turnings (15.0 g, 617 mmol) were placed in a 500 mL 3-neck round bottom flask fitted with a magnetic stir bar, Friedrichs

condenser, and a 25 mL pressure-equalizing addition funnel. The system was evacuated and back-filled thrice with argon, after which the system was kept under a positive pressure of argon. Dry diethyl ether (250 mL) was added to the flask and 5.0 mL 1-bromopropane (55 mmol) was dissolved in 20 mL dry diethyl ether and placed in the addition funnel. A crystal of iodine was added to initiate the reaction, after which the 1-bromopropane solution was added dropwise while stirring. Stirring was continued for 2 hours after completion of the addition. The resulting Grignard reagent was filtered through a glass wool plug in Teflon tubing to a 250 mL pressure-equalizing addition funnel attached to a 1000 mL 3-neck round bottom flask fitted with a magnetic stir bar and Friedrichs condenser. Tetrachlorogermane (10.0 mL, 87.6 mmol) was dissolved in 250 mL dry diethyl ether and placed in the flask. The flask was cooled to 0 °C and the Grignard reagent was added dropwise while stirring. The reaction was stirred overnight. Removal of the solvent by distillation left 6.6 mL of crude propyltrichlorogermane. This mixture was used without further purification in the reduction reaction that follows. **GC-MS (EI)**: *m/z* (% relative intensity) 222 (M^+, 1), 207 (7), 186 (80), 184 (56), 179 (94), 150 (26), 144 (23), 109 (100), 99 (3), 87 (5), 74 (15).

Synthesis of propylgermane (85).[112] A 0.5 M solution (100 mL, 50 mmol) of lithium aluminum hydride (LAH) in diglyme was placed in a 250 mL round bottom flask fitted with a magnetic stir bar. A short-path distillation head with 100 mL pear flask attached was connected to the round bottom flask, which then was cooled in an ice/NaCl bath. The pear flask was cooled to -78 °C and the crude propyltrichlorogermane obtained in the previous synthesis was added dropwise *via* syringe. The reaction was stirred for 2 hours. The ice/NaCl bath was removed and the reaction was stirred for 2 more hours, after which a water aspirator was used to pull the propylgermane (0.26 g, 3% overall yield) into the pear flask trap. **^{1}H NMR** (300 MHz, benzene-*d*6): δ 0.72 (m, 2 H), 0.78 (t, J = 6 Hz, 3 H), 1.29 (sextet, J = 6 Hz, 2 H), 3.51 (t, J = 3 Hz, 3 H); **^{13}C NMR** (75 MHz, benzene-*d*6): δ 10.38, 16.68, 21.29; **GC-MS (EI)**: *m/z* (% relative intensity) 119 (M^+-1, 16), 116 (15), 103 (12), 89 (41), 74 (100).

Trapping of propene with bromine. A needle connected to the exit port of an SFR reactor was immersed in a solution of a few drops of bromine in chloroform-*d* in an NMR tube. Propylgermane or germacyclobutane (10 total injections in each case) was introduced into the SFR (furnace T=500 °C). NMR analysis of the resulting solution revealed the formation of 1,2-dibromopropane.[113] **^{1}H NMR** (300 MHz, chloroform-*d*): δ 1.85 (d, J = 6 Hz, 3 H), 3.58 (t, J = 9 Hz, 1 H), 3.88 (dd, J = 6 Hz, 1 H), 4.28 (m, 1 H).

E. References

(1) Willstätter, R.; Bruce, J. *Chem. Ber.* **1907**, *40*, 3979-3999.

(2) Genaux, C. T.; Walters, W. D. *J. Am. Chem. Soc.* **1951**, *73*, 4497-4498.

(3) Pritchard, H. O.; Sowden, R. G.; Trotman-Dickenson, A. F. *Proc. Roy. Soc. (London)* **1953**, *A218*, 416-421.

(4) Hoffmann, R.; Woodward, R. B. *J. Am. Chem. Soc.* **1965**, *87*, 2046-2048.

(5) Stephenson, L. M.; Brauman, J. I. *J. Am. Chem. Soc.* **1971**, *93*, 1988-1991.

(6) Karadakov, P. B.; Gerratt, J.; Cooper, D. L.; Raimondi, M. *J. Am. Chem. Soc.* **1994**, *116*, 7714-7721.

(7) Hagedorn, C. J.; Weiss, M. J.; Weinberg, W. H. *J. Phys. Chem. B* **2001**, *105*, 3838-3848.

(8) Moran, D.; Manoharan, M.; Heine, T.; Schleyer, P. v. R. *Org. Lett.* **2003**, *5*, 23-26.

(9) Frey, H. M.; Walsh, R. *Chem. Rev.* **1969**, *69*, 103-124.

(10) Frey, H. M. "The Gas Phase Pyrolyses of Some Small Ring Hydrocarbons" in *Advances in Physical Organic Chemistry*; Gold, V., Ed.; Academic Press: New York, 1966; Vol. 4.

(11) Gerberich, H. R.; Walters, W. D. *J. Am. Chem. Soc.* **1961**, *83*, 4884-4886.

(12) Butler, J. N.; Ogawa, R. B. *J. Am. Chem. Soc.* **1963**, *85*, 3346-3349.

(13) Vreeland, R. W.; Swinehart, D. F. *J. Am. Chem. Soc.* **1963**, *85*, 3349-3353.

(14) Retzloff, D.; Coull, J. *J. Chem. Phys.* **1967**, *47*, 3927-3935.

(15) Hoffmann, R.; Swaminathan, S.; G.Odell, B.; Gleiter, R. *J. Am. Chem. Soc.* **1970**, *92*, 7091-7097.

(16) Segal, G. A. *J. Am. Chem. Soc.* **1974**, *96*, 7892-7898.

(17) Barnard, J. A.; Cocks, A. T.; Lee, R. K.-Y. *J. Chem. Soc., Faraday Trans. 1* **1974**, *70*, 1782-1792.

(18) Pedersen, S.; Herek, J. L.; Zewail, A. H. *Science* **1994**, *266*, 1359-1364.

(19) Kern, F.; Walters, W. D. *Proc. Natl. Acad. Sci. U.S.* **1952**, *38*, 937-942.

(20) Genaux, C. T.; Kern, F.; Walters, W. D. *J. Am. Chem. Soc.* **1953**, *75*, 6196-6199.

(21) Wellman, R. E.; Walters, W. D. *J. Am. Chem. Soc.* **1957**, *79*, 1542-1546.

(22) Slater, N. B. *Proc. Roy. Soc. (London) A* **1953**, *218*, 224-244.

(23) Gerberich, H. R.; Walters, W. D. *J. Am. Chem. Soc.* **1961**, *83*, 3935-3939.

(24) Woodward, R. B.; Hoffmann, R. *J. Am. Chem. Soc.* **1965**, *87*, 395-397.

(25) Hoffmann, R.; Woodward, R. B. *Acc. Chem. Res.* **1968**, *1*, 17-22.

(26) Woodward, R. B.; Hoffmann, R. *Angew. Chem. Intern. Ed. Engl.* **1969**, *8*, 781-932.

(27) Woodward, R. B.; Hoffmann, R. *The Conservation of Orbital Symmetry*; Verlag Chemie: Weinheim, 1971.

(28) Salem, L.; Wright, J. S. *J. Am. Chem. Soc.* **1969**, *91*, 5947-5955.

(29) O'Neal, H. E.; Benson, S. W. *J. Phys. Chem.* **1968**, *72*, 1866-1887.

(30) Beadle, P. C.; Golden, D. M.; King, K. D.; Benson, S. W. *J. Am. Chem. Soc.* **1972**, *94*, 2943-2947.

(31) Berson, J. A. *Science* **1994**, *266*, 1338-1339.

(32) Dervan, P. B.; Uyehara, T.; Santilli, D. S. *J. Am. Chem. Soc.* **1979**, *101*, 2069-2075.

(33) Dervan, P. B.; Santilli, D. S. *J. Am. Chem. Soc.* **1980**, *102*, 3863-3870.

(34) Doubleday, J., Charles *J. Am. Chem. Soc.* **1993**, *115*, 11968-11983.

(35) Moriarty, N. W.; Lindh, R.; Karlström, G. *Chem. Phys. Lett.* **1998**, *289*, 442-450.

(36) Benson, S. W.; Kistiakowsky, G. B. *J. Am. Chem. Soc.* **1942**, *64*, 80-86.

(37) De Feyter, S.; Diau, E. W.-G.; Scala, A. A.; Zewail, A. H. *Chem. Phys. Lett.* **1999**, *303*, 249-260.

(38) Sommer, L. H.; Baum, G. A. *J. Am. Chem. Soc.* **1954**, *76*, 5002.

(39) West, R. *J. Am. Chem. Soc.* **1955**, *77*, 2339-2340.

(40) Flowers, M. C.; Gusel'nikov, L. E. *J. Chem. Soc. B* **1968**, 419-423.

(41) Butler, J. N. *J. Am. Chem. Soc.* **1962**, *84*, 1393-1398.

(42) Dasent, W. E. *Nonexistent Compounds; Compounds of Low Stability*; Marcel Dekker: New York, 1965.

(43) Roberts, J. D.; Sharts, C. M. "Cyclobutane Derivatives From Thermal Cycloaddition Reactions" in *Organic Reactions*; Cope, A. C., Ed.; John Wiley & Sons, Inc.: New York, 1962; Vol. 12.

(44) Gusel'nikov, L. E.; Nametkin, N. S. *Chem. Rev.* **1979**, *79*, 529-577.

(45) Raabe, G.; Michl, J. *Chem. Rev.* **1985**, *85*, 419-509.

(46) Schaad, L. J.; Skancke, P. N. *J. Phys. Chem. A* **1997**, *101*, 7408-7413.

(47) Gordon, M. S.; Barton, T. J.; Nakano, H. *J. Am. Chem. Soc.* **1997**, *119*, 11966-11973.

(48) Barton, T. J.; Marquardt, G.; Kilgour, J. A. *J. Organomet. Chem.* **1975**, *85*, 317-325.

(49) Golino, C. M.; Bush, R. D.; On, P.; Sommer, L. H. *J. Am. Chem. Soc.* **1975**, *97*, 1957-1958.

(50) Rotoli, P. C. *The Thermal Decomposition of 1,1-Dimethylcyclobutane.* M.S. thesis, University of Rochester, Rochester, NY, 1963.

(51) Laane, J. *J. Am. Chem. Soc.* **1967**, *89*, 1144-1147.

(52) Golino, C. M.; Bush, R. D.; Sommer, L. H. *J. Am. Chem. Soc.* **1975**, *97*, 7371-7372.

(53) Conlin, R. T.; Gill, R. S. *J. Am. Chem. Soc.* **1983**, *105*, 618-619.

(54) Jenkins, R. L.; Kedrowski, R. A.; Elliott, L. E.; Tappen, D. C.; Schlyer, D. J.; Ring, M. A. *J. Organomet. Chem.* **1975**, *86*, 347-357.

(55) Conlin, R. T.; Wood, D. L. *J. Am. Chem. Soc.* **1981**, *103*, 1843-1844.

(56) Drahnak, T. J.; Michl, J.; West, R. *J. Am. Chem. Soc.* **1981**, *103*, 1845-1846.

(57) Drahnak, T. J.; Michl, J.; West, R. *J. Am. Chem. Soc.* **1979**, *101*, 5427-5428.

(58) Conlin, R. T.; Gaspar, P. P. *J. Am. Chem. Soc.* **1976**, *98*, 868-870.

(59) Roark, D. N.; Peddle, G. J. D. *J. Am. Chem. Soc.* **1972**, *94*, 5837-5841.

(60) Barton, T. J.; Kilgour, J. A. *J. Am. Chem. Soc.* **1976**, *98*, 7746-7751.

(61) Wulff, W. D.; Goure, W. F.; Barton, T. J. *J. Am. Chem. Soc.* **1978**, *100*, 6236-6238.

(62) Barton, T. J.; Burns, S. A.; Burns, G. T. *Organometallics* **1982**, *1*, 210-212.

(63) Walsh, R. *Acc. Chem. Res.* **1981**, *14*, 246-252.

(64) Goddard, J. D.; Yoshioka, Y.; Schaefer III, H. F. *J. Am. Chem. Soc.* **1980**, *102*, 7644-7650.

(65) Yoshioka, Y.; Shaefer, H. F., III *J. Am. Chem. Soc.* **1981**, *103*.

(66) Conlin, R. T.; Kwak, Y.-W. *Organometallics* **1984**, *3*, 918-922.

(67) Davidson, I. M. T.; Ijadi-Maghsoodi, S.; Barton, T. J.; Tillman, N. *J. Chem. Soc., Chem. Commun.* **1984**, 478-480.

(68) Davidson, I. M. T.; Fenton, A.; Ijadi-Maghsoodi, S.; Scampton, R. J.; Auner, N.; Grobe, J.; Tillman, N.; Barton, T. J. *Organometallics* **1984**, *3*, 1593-1595.

(69) Baldwin, A. C.; Davidson, I. M. T.; Howard, A. V. *J. Chem. Soc., Faraday Trans. 1* **1975**, *71*, 972-979.

(70) Barton, T. J.; Tillman, N. *J. Am. Chem. Soc.* **1987**, *109*, 6711-6716.

(71) Dickenson, A. P.; Nares, K. E.; Ring, M. A.; O'Neal, H. E. *Organometallics* **1987**, *6*, 2596-2600.

(72) Dickenson, A. P.; O'Neal, H. E.; Ring, M. A. *Organometallics* **1991**, *10*, 3513-3520.

(73) Skancke, P. N.; Hrovat, D. A.; Borden, W. T. *J. Am. Chem. Soc.* **1997**, *119*, 8012-8014.

(74) Skancke, P. N. *J. Phys. Chem. A* **1997**, *101*, 5017-5021.

(75) Nametkin, N. S.; Gusel'nikov, L. E.; Ushakova, R. L.; Orlov, V. Y.; Kuz'min, O. V.; Vdovin, V. M. *Proc. Acad. Sci. USSR* **1970**, *194*, 741-743.

(76) Barton, T. J.; Kline, E. A.; Garvey, P. M. *J. Am. Chem. Soc.* **1973**, *95*, 3078.

(77) Namavari, M.; Conlin, R. T. *Organometallics* **1992**, *11*, 3307-3312.

(78) Khabashesku, V. N.; Kudin, K. N.; Tamás, J.; Boganov, S. E.; Margrave, J. L.; Nefedov, O. M. *J. Am. Chem. Soc.* **1998**, *120*, 5005-5016.

(79) Toltl, N. P.; Leigh, W. J. *J. Am. Chem. Soc.* **1998**, *120*, 1172-1178.

(80) Toltl, N. P.; Stradiotto, M.; Morkin, T. L.; Leigh, W. J. *Organometallics* **1999**, *18*, 5643-5652.

(81) Damrauer, R.; Davis, R. A.; Burke, M. T.; Karn, R. A.; Goodman, G. T. *J. Organomet. Chem.* **1972**, *43*, 121-125.

(82) Lesbre, M.; Mazerolles, P.; Satgé, J. *The Organic Compounds of Germanium*; Wiley: New York, 1971.

(83) Lesbre, M.; Mazerolles, P.; Manuel, G. *Compt. Rend.* **1963**, *257*, 2303-2305.

(84) Huc, V.; Boussaguet, P.; Mazerolles, P. *J. Organomet. Chem.* **1996**, *521*, 253-260.

(85) Seetz, J. W. F. L.; Heisteeg, B. J. J. v. d.; Schat, G.; Akkerman, O. S.; Bickelhaupt, F. *J. Organomet. Chem.* **1984**, *277*, 319-322.

(86) Seetz, J. W. F. L.; Hartog, F. A.; Böhm, H. P.; Blomberg, C.; Akkerman, O. S.; Bickelhaupt, F. *Tetrahedron Lett.* **1982**, *23*, 1497-1500.

(87) Anderson, H. H. *J. Am. Chem. Soc.* **1952**, *74*, 1421-1423.

(88) Rieke, R. D.; Bales, S. E. *J. Am. Chem. Soc.* **1974**, *96*, 1775-1781.

(89) Hehre, W. J.; Ditchfield, R.; Radom, L.; Pople, J. A. *J. Am. Chem. Soc.* **1970**, *92*, 4796-4801.

(90) Ponomarev, D. A.; Takhistov, V. V. *J. Chem. Educ.* **1997**, *74*, 201-203.

(91) Zueva, G. Y.; Khaustova, T. I.; Serezhkina, N. V.; Ponomarenko, V. A. *Bull. Acad. Sci. USSR., Div. Chem. Sci.* **1979**, *28*, 2599-2601.

(92) Block, E.; Revelle, L. K. *J. Am. Chem. Soc.* **1978**, *100*, 1630-1632.

(93) Barton, T. J.; Burns, S. A.; Davidson, I. M. T.; Ijadi-Maghsoodi, S.; Wood, I. T. *J. Am. Chem. Soc.* **1984**, *106*, 6367-6372.

(94) Auner, N.; Davidson, I. M. T.; Ijadi-Maghsoodi, S. *Organometallics* **1985**, *4*, 2210-2213.

(95) Engel, J. P. *Gas Phase Thermochemistry of Organogermanium Compounds.* Ph.D. dissertation, Iowa State University, Ames, IA, 1993.

(96) Roberts, R. M. G. *J. Organomet. Chem.* **1968**, *12*, 97-103.

(97) Wentrup, C. *Reactive Molecules*; Wiley: New York, 1984.

(98) Dzarnoski, J.; O'Neal, H. E.; Ring, M. A. *J. Am. Chem. Soc.* **1981**, *103*, 5740-5746.

(99) Classen, N. R. *Synthesis and gas phase thermochemistry of germanium-containing compounds.* Ph.D. dissertation, Iowa State University, Ames, IA, 2002.

(100) Lowry, T. H.; Richardson, K. S. *Mechanism and Theory in Organic Chemistry*; Third ed.; Harper & Row: New York, 1987.

(101) Benson, S. W. *Thermochemical Kinetics*; 2nd ed.; John Wiley & Sons: New York, 1976.

(102) Trotman-Dickenson, A. F. *Gas Kinetics: An Introduction to the Kinetics of Homogeneous Gas Reactions*; Butterworths Scientific Publications: London, 1955.

(103) Garvey, P. M. *Generation and Reactions of Compounds Containing a Germanium-Carbon (p-p)π Double Bond.* M.S. thesis, Iowa State University, Ames, IA, 1973.

(104) Foster, L. S.; Williston, A. F.; Johnson, W. C. "Germanium(IV) Iodide" in *Inorganic Syntheses*; Fernelius, W. C., Ed.; McGraw-Hill: New York, 1946; Vol. II, pp 112-114.

(105) Foster, L. S.; Moeller, T.; Heneghan, L. F. "Germanium(II) Iodide (Germanium diiodide)" in *Inorganic Syntheses*; Audrieth, L. F., Ed.; McGraw-Hill: New York, 1950; Vol. III, pp 63-64.

(106) Tabern, D. L.; Orndorff, W. R.; Dennis, L. M. *J. Am. Chem. Soc.* **1925**, *47*, 2039-2044.

(107) Kraus, C. A.; Flood, E. A. *J. Am. Chem. Soc.* **1932**, *54*, 1635-1644.

(108) Vyazankin, N. S.; Razuvaev, G. A.; D'yachkovskaya, O. S. *J. Gen. Chem.* **1963**, *33*, 607-610.

(109) Mironov, V. F.; Kravchenko, A. L. *Bull. Acad. Sci. USSR, Div. Chem. Sci.* **1965**, *6*, 988-995.

(110) Anderson, H. H. *J. Am. Chem. Soc.* **1957**, *79*, 326-328.

(111) Petrov, A. D.; Mironov, V. F.; Golgy, I. E. *Bull. Acad. Sci. USSR, Div. Chem. Sci.* **1956**, 1169-1172.

(112) Johnson, O. H.; Jones, L. V. *J. Org. Chem.* **1952**, *17*, 1172-1176.

(113) Pouchert, C. J.; Behnke, J. *The Aldrich Library of ^{13}C and ^{1}H FT NMR Spectra. Edition I.*; Aldrich Chemical Company, Inc., 1993.

II. DIGERMANE ADDITIONS TO ACETYLENES

A. Introduction

1. Disilane additions to acetylenes. Woodward-Hoffmann orbital symmetry theory[1,2] has become one of the cornerstones of organic chemistry. It's ability to predict the stereochemical outcomes of concerted reactions has made it a powerful tool for understanding the electronic aspects of pericyclic reactions. For example, a concerted [2+2] mechanism for thermal decomposition of cyclobutane, described in the previous chapter, was able to be ruled out based on orbital symmetry rules. The orbital interactions involved in [2+2] cycloadditions are shown in Figure 1.

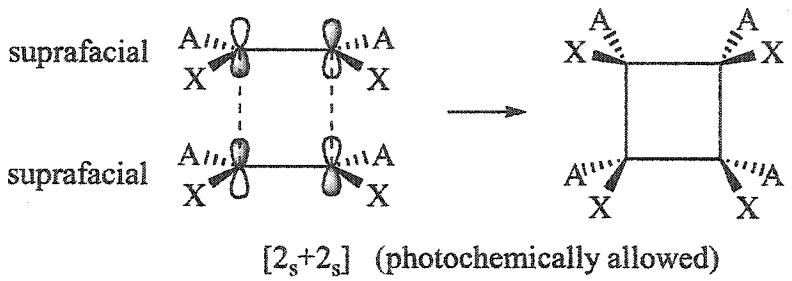

$[2_s+2_s]$ (photochemically allowed)

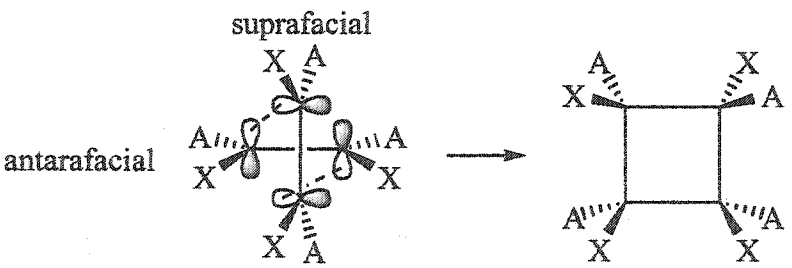

$[2_s+2_a]$ (thermally allowed)

Figure 1. Orbital interactions in [2+2] cycloadditions.

These cycloadditions recently have become of interest in organosilicon chemistry due to the reactive nature of the Si–Si single bond. It is well known that a Si–Si sigma bond behaves remarkably like a C–C pi bond.[3] For example, halogens "add" across a Si–Si single

bond, cleaving it in much the same way as halogens add to alkenes (Scheme 1).[4] The Si–Si bond $\sigma \rightarrow \sigma^*$ transition occurs around 190 nm ($Me_3Si–SiMe_3$)[5] as compared to the $\pi \rightarrow \pi^*$ transition at 165 nm for ethylene.[6]

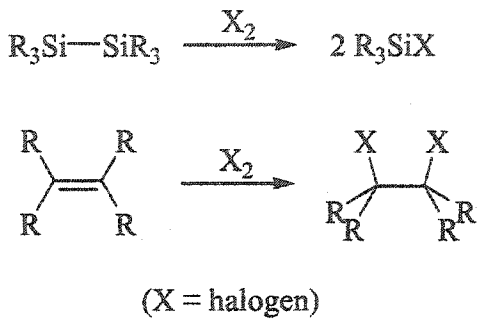

Scheme 1. Reaction of halogens with Si–Si and C=C bonds.

However, with the exception of recent work in the Barton group (*vide infra*), the only [2+2] cycloadditions of disilanes studied were those involving transition metal (*e.g.*, palladium) catalysis.[7,8] The first such report was by Sakurai *et al.*, who showed that cyclic disilanes (**1**) in the presence of a Pd(0) or Pd(II) catalyst added in a *cis* fashion to substituted acetylenes to yield disilacycloalkenes (**2**) (Scheme 2).[9] Since then, various other intra- and intermolecular catalytic Si–Si additions have been explored, including additions to both alkenes[10,11] and alkynes.[12-14]

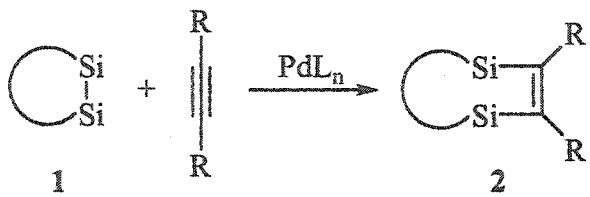

Scheme 2. Catalytic Si–Si addition to substituted acetylenes.

Despite the Si–Si sigma bond's chemical similarity to C–C pi bonds, only fairly recently have their thermal and photochemical [2+2] cycloadditions been investigated.[15-17] The first example of such a reaction was the flow pyrolysis of disilacycloöctyne 3 Scheme 3).[15] The thermally-allowed [2_s+2_a] cycloaddition gave bicyclic compound 4 and tetraphenylbutatriene (**5**) in 70% yield. Semiempirical (AM1) calculations showed that the

expected $[2_s+2_a]$ transition state geometry was 14 kcal/mol lower in energy than the forbidden $[2_s+2_s]$ geometry while *ab initio* calculations on an intermolecular model system gave an activation entropy ($\Delta S^{\ddagger}$) of -35.16 cal/mol·K. AM1 calculations on **3** also revealed that the relative orientation of the Si–Si and C≡C bonds in **3** is very close to that in the $[2_s+2_a]$ transition state. Thus, it was postulated that the main barrier for the bimolecular reaction could be due to entropic factors.

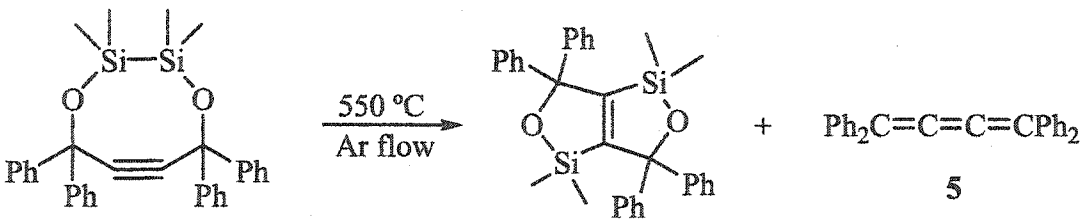

3 **4** **5**

Scheme 3. Flow pyrolysis of **3**.

In order to test this hypothesis, flow pyrolyses (Scheme 4) of acyclic congener **6** and of hexamethyldisilane (**9**) with phenylacetylene (**10**) were performed. In the latter case, no reaction was observed, possibly due to the large value of $\Delta S^{\ddagger}$, though these data do not provide definitive proof. In the case of acyclic **6**, in which free rotation frees it from being constrained in a $[2_s+2_a]$ geometry, silane **7** and trisilane **8** were formed exclusively from a silylene extrusion and insertion.

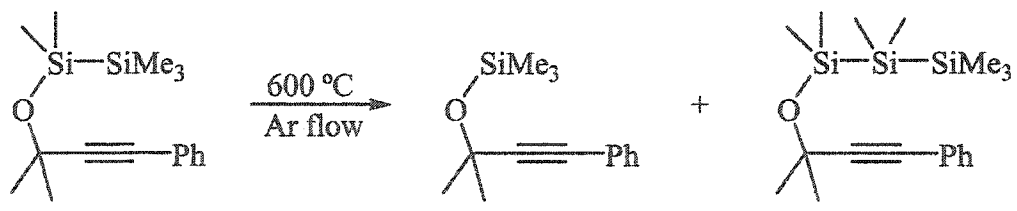

6 **7** **8**

9 **10**

Scheme 4. Flow pyrolyses of acyclic and intermolecular analogues of **3**.

Two different disilacycloöctynes also were pyrolyzed to test the generality of the cycloaddition (Scheme 5). Hexasilacycloöctyne **13** did not undergo an intramolecular [2+2] addition, but instead thermally extruded dimethylsilylene, as had been previously observed for this[18] and other[19,20] polysilacycloalkynes. Dibenzodisilacycloöctyne **11**, on the other hand, did yield the apparent $[2_s+2_a]$ cycloaddition product **12** upon flow pyrolysis at 550 °C. This isomer was found to be strongly photoluminescent (emission $\lambda_{max} = 425$ nm) with a rather impressive quantum yield ($\Phi_f = 0.68$), making it a potential material for organic light-emitting diodes (LEDs).

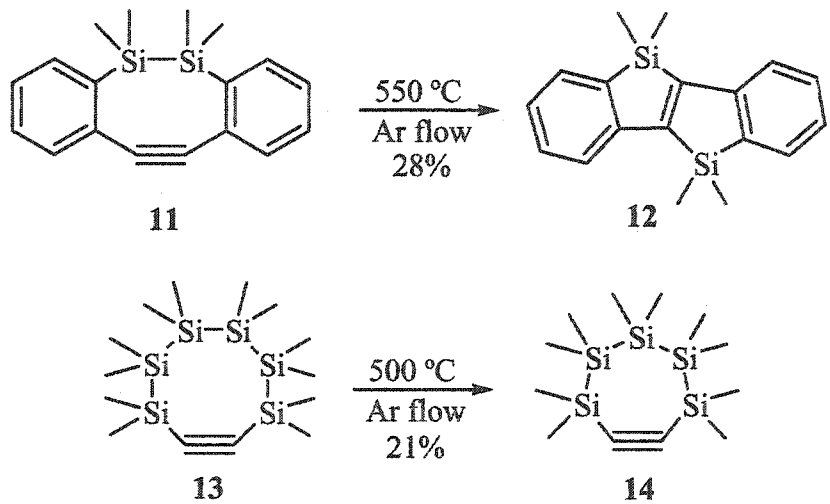

Scheme 5. Other disilacycloöctyne pyrolyses examined.

The photochemical Si–Si addition next was explored. However, UV (254 nm) photolysis of **3** did not result in the expected product (**16**) of a photochemically-allowed intramolecular $[2_s+2_s]$ addition (Scheme 6). Instead, isomer **15** and tetraphenylbutatriene (**5**) were isolated in 85% and 10% yields, respectively. A diradical mechanism initiated by homolytic Si–Si bond cleavage (Scheme 7) was proposed to explain the formation of **15**. The formation of tetraphenylbutatriene is easily explained by extrusion of two equivalents of dimethylsilanone (**17**) from the expected photoadduct **16** (Scheme 6). This explanation is supported by the results of catalytic decomposition of **3**. As catalytic [2+2] cycloadditions of Si–Si single bonds to C–C triple bonds typically yield *cis* adducts (*vide supra*), the

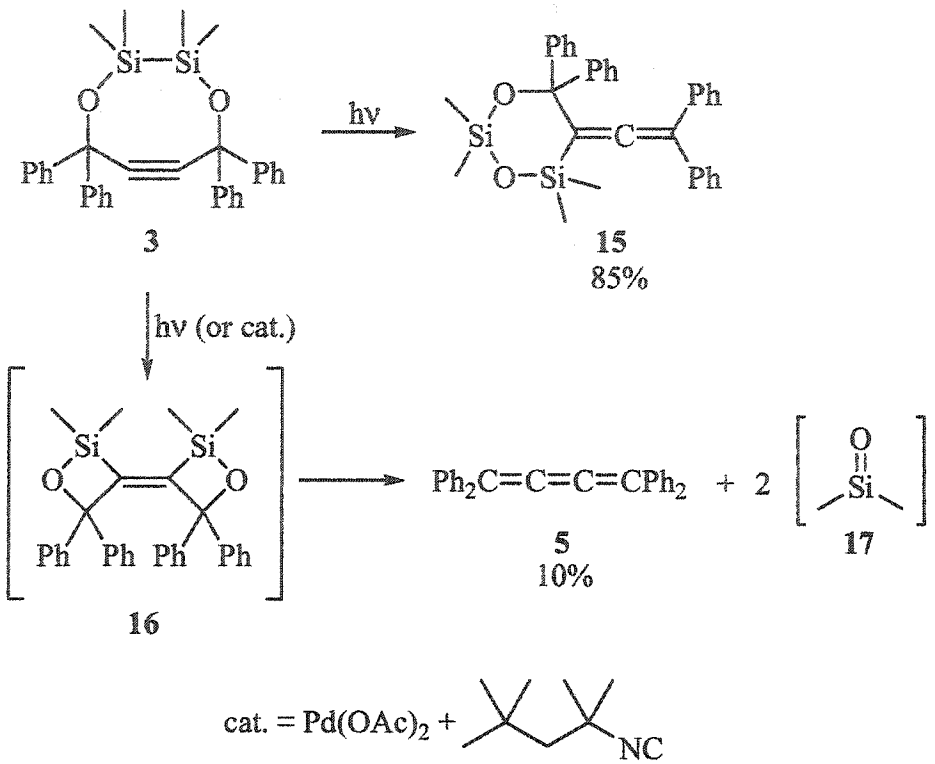

Scheme 6. Photolysis of **3**.

reaction of **3** with a Pd(II) catalyst also should give tetraphenylbutatriene as a product. This was in fact the case; addition of catalytic amounts of $Pd(OAc)_2$ and 1,1,3,3-tetramethylbutyl isocyanide gave **5** as the sole product in 100% yield after column chromatography.

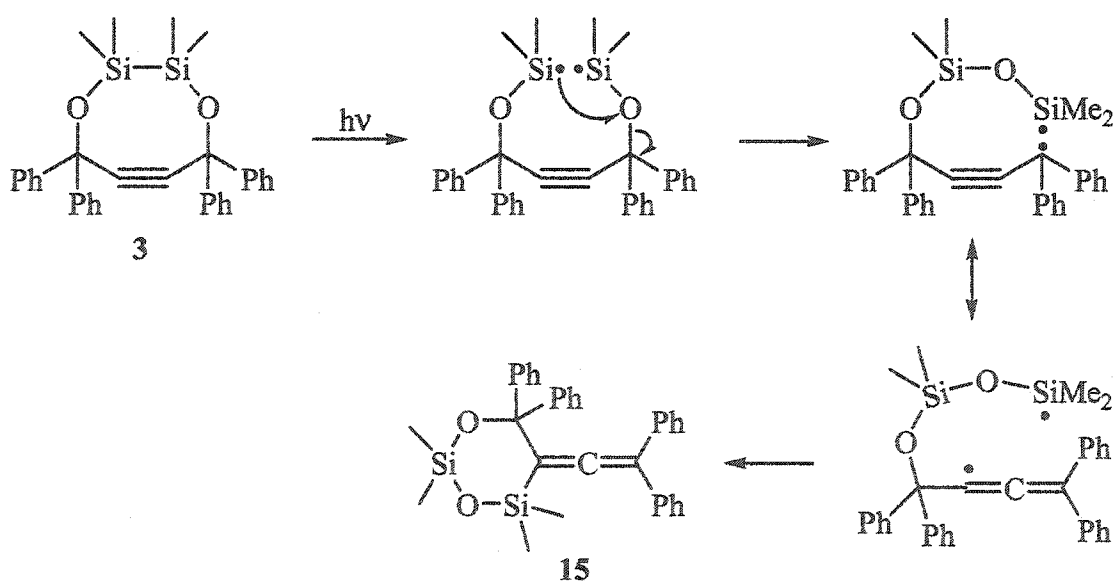

Scheme 7. Proposed mechanism for formation of photoisomer **15**.

Photolysis of cyclic hexasilaalkyne **13** expectedly[18] yielded the same ring-contracted product **14** obtained in its thermolysis (Scheme 5). The surprising result came upon photolysis of **11** (Scheme 8). Instead of the allowed $[2_s+2_s]$ isomer **18**, only thermoisomer **12** was formed, and in 92% yield! These results were remarkable because, if the reaction indeed were a concerted process, it would be the first example of a forbidden photochemical $[2_s+2_a]$ cycloaddition.[1,2]

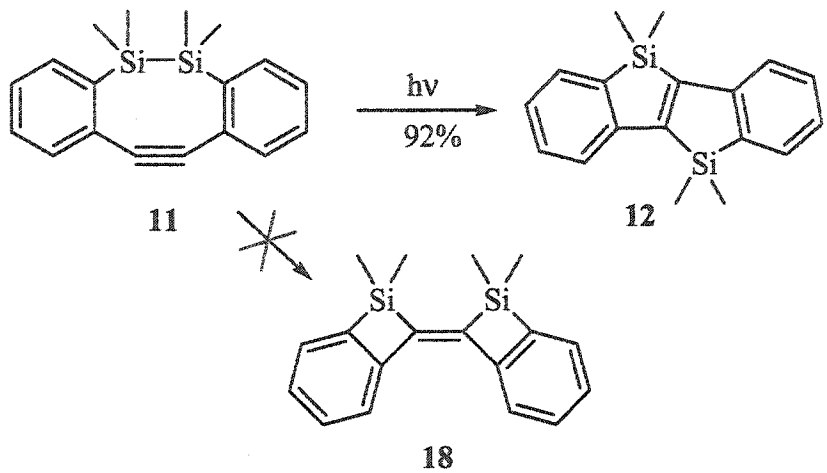

Scheme 8. Photolysis of **11**.

Trapping experiments were performed in order to shed more light on the mechanism of this puzzling rearrangement (Scheme 9). The possibility of a homolysis mechanism was explored first, but photolysis of **11** in neopentyl chloride failed to yield **20**, the expected product of intermolecular reaction with diradical **19**. Likewise, a silene intermediate (**21**) formed by photochemically-induced 1,3-silyl migration, a precedented[21] reaction, was not trapped in the methanol-solvated photolysis. Instead, methoxysilane **23** was obtained in 76% yield (24% **12**), suggesting an electron-transfer mechanism (Scheme 10), though the failure to trap both **19** or **21** does not rule out a mechanism involving either homolysis or 1,3-silyl migration.

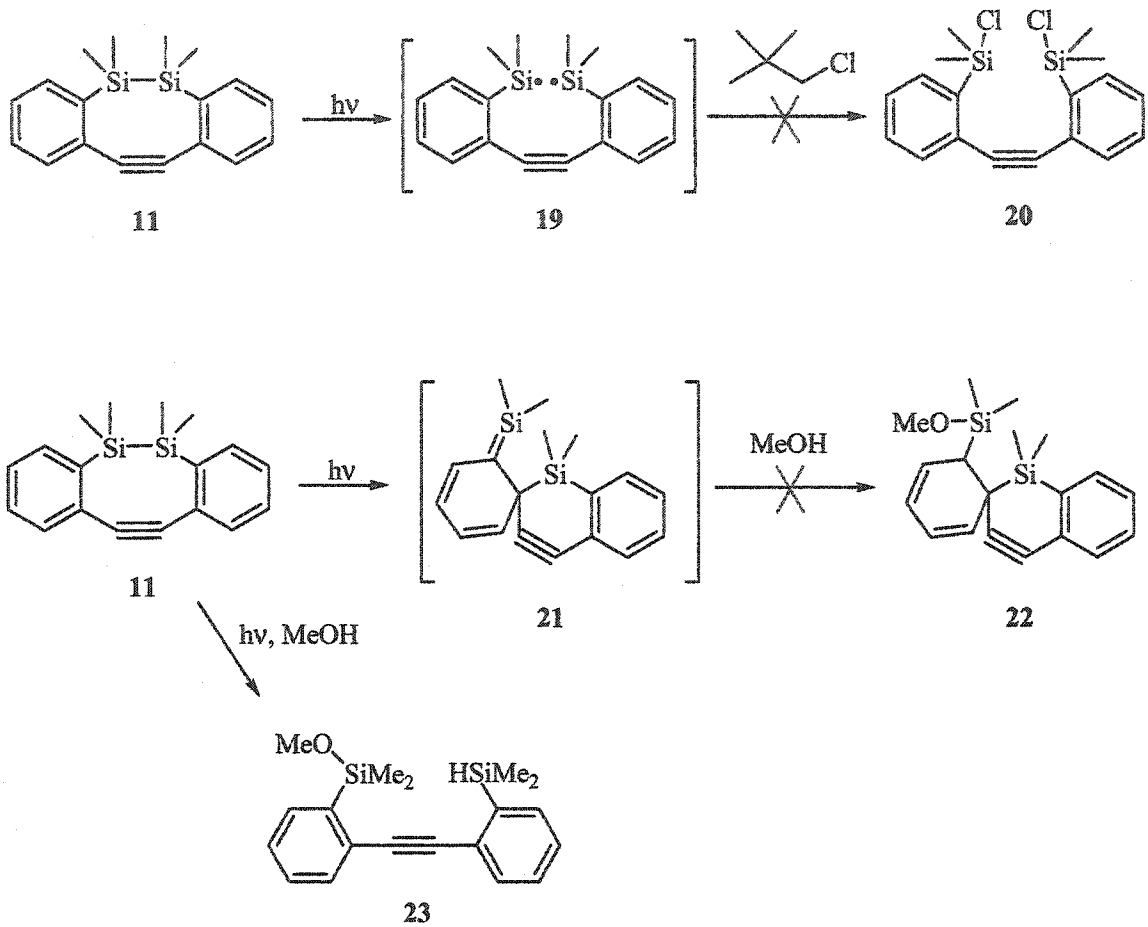

Scheme 9. Trapping experiments in the photolysis of **11**.

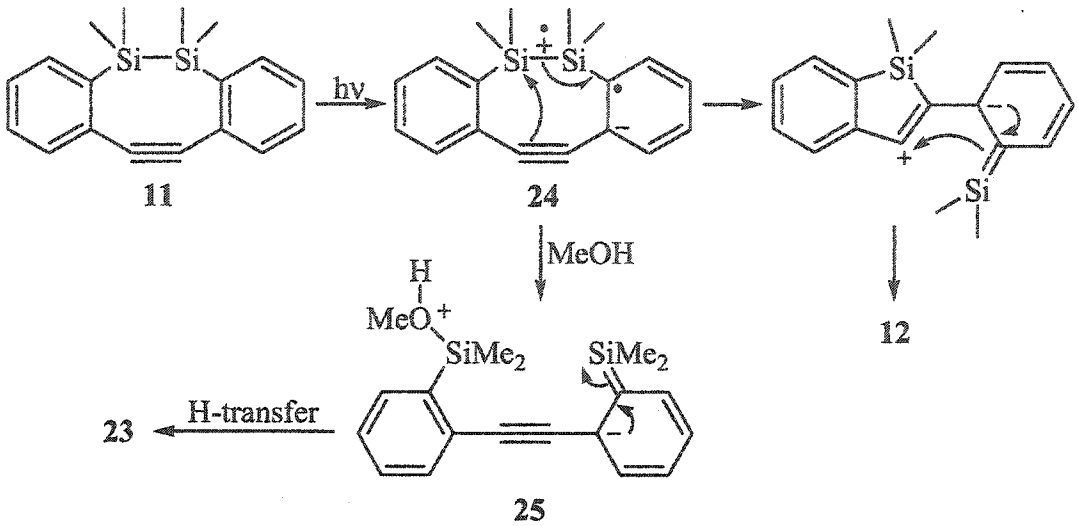

11 24 12 23 25

Scheme 10. Proposed electron-transfer mechanism for photolytic formation of **23**.

Acyclic disilane **26** also produced some interesting results upon UV irradiation (Scheme 11). While isomer **27** conceivably could originate from an allowed photochemical [2_s+2_s] cycloaddition of **26**, an electron-transfer mechanism, as proposed in the case of **11**, could be responsible for the formation of both isomers (Scheme 12). The results are inconclusive, however, as photolysis in methanol failed to trap zwitterion **31** and the reaction of **28** with methanol yielded the same product that would be formed upon trapping of zwitterion **30**. The formation of **27** from rearrangement of **28** was ruled out by photolysis of **28** alone; no **27** was formed in the reaction.

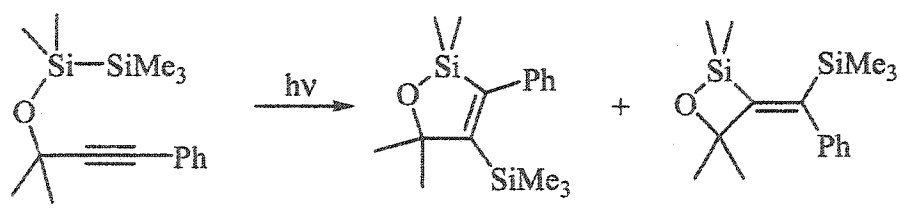

26 **27** 84% **28** 16%

Scheme 11. Photolysis of **26**.

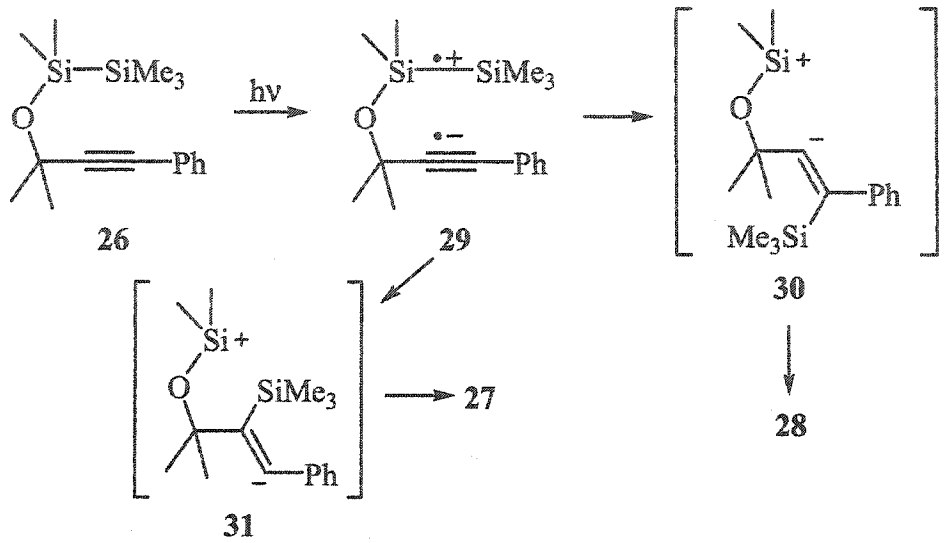

Scheme 12. Proposed electron-transfer mechanism for photolytic formation of **27** and **28**.

2. Tri- and tetrasilane additions to acetylenes. Due to the promise of disilole **12** for use in organic LEDs, expanding the system to increase its conjugation was examined.[17] To this effect the original precursor (**11**) was modified to include another dimethylsilylene moiety and C–C triple bond (**32**). Both flow pyrolysis and UV photolysis of **32** gave the

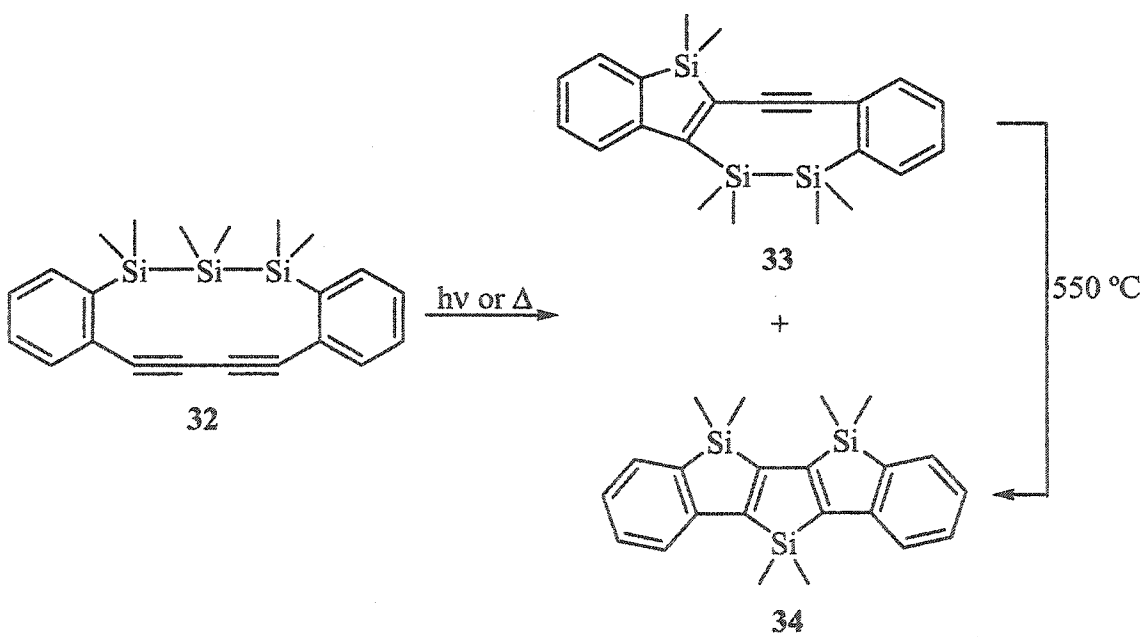

Scheme 13. Photolysis and thermolysis of **32**.

expected isomer **34** as well as **33**. The latter isomer was confirmed as an intermediate in the formation of **34** by independent pyrolysis of isolated **33**. Trisilole **34** formed bright green crystals and produced a fluorescent green solution in both hexanes and ethanol. This compound, like its disilole cousin, also had remarkable photophysical properties with a fluorescence quantum yield (Φ_f) in aqueous solution (quinine sulfate standard) of 0.57 and a λ_{max} of 426 nm.

The ring system was expanded further to include yet another silicon (**35**). Subsequent irradiation (254 nm) of this compound yielded a single isomer (**36**) in 88% yield after *ca.* 1.5 hrs. Continued irradiation resulted in the formation of another isomer (**37**) and the product of an apparent silylene extrusion, trisilole **34**, after 91 hours. These data are not surprising in light of the results obtained in the cyclic trisilanyl case. It is quite conceivable that the reaction proceeds by sequential formal Si–Si additions, first forming **36** and then **37**, which then can extrude a silylene to yield the trisilole. Isomer **33** was found to have blue (λ_{max} = 376 nm) photoluminescence, but its quantum yield (aqueous, quinine sulfate standard) was surprisingly low (Φ_f = 0.032), considering the vivid color produced upon irradiation.

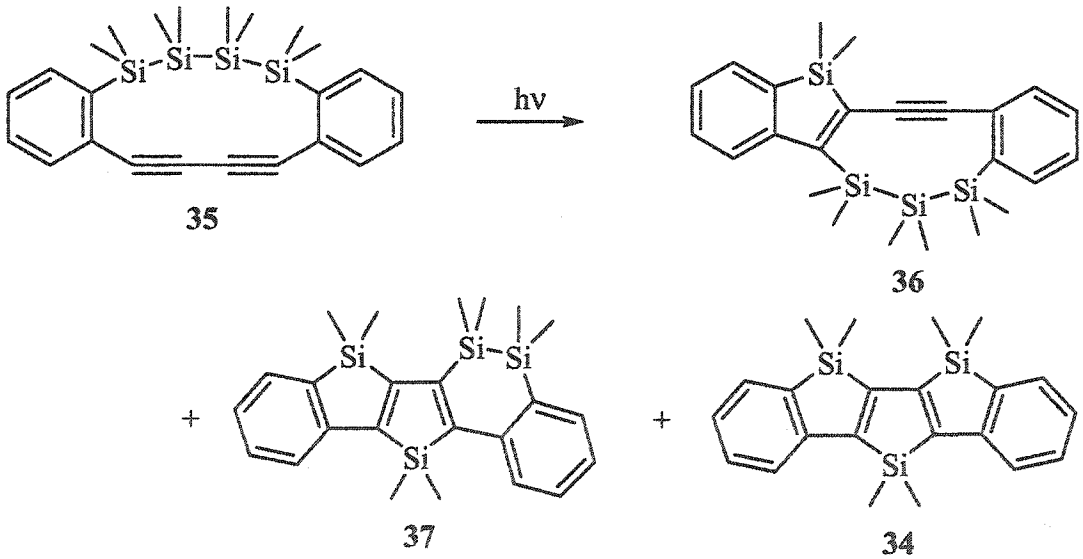

Scheme 14. Photolysis of **35**.

Flow pyrolysis of cyclic tetrasilane **35**, on the other hand, did produce some rather unexpected results (Scheme 15). In addition to the photoproducts **36** and **37**, two new

isomers (**38** and **39**) were formed with only trace amounts of trisilole **34**. Flow pyrolysis of isolated **36** produced not only isomers **37** and **38**, consistent with sequential thermally-allowed [2_s+2_a] cycloadditions, but also cumulene **39**; the formation of **39** was explained by two formal silyl shifts, one 1,2 and the other 1,4 (Scheme 16).

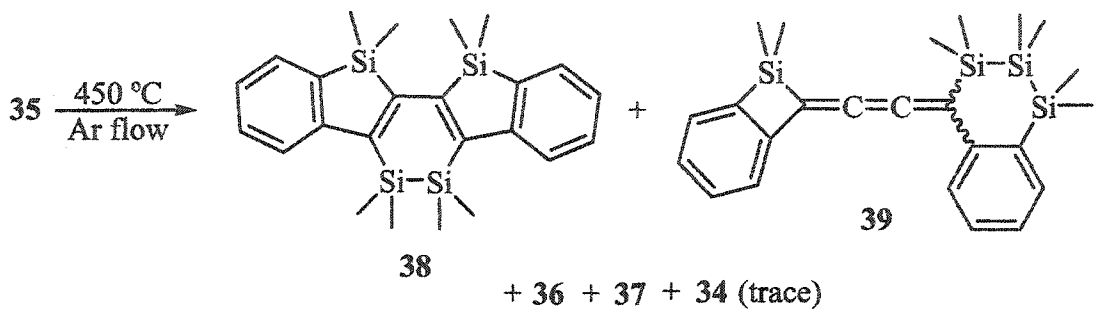

Scheme 15. Flow pyrolysis of **35**.

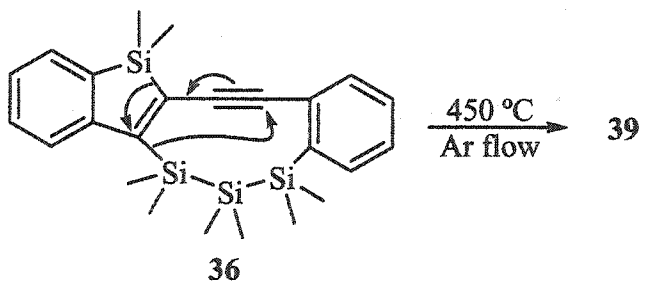

Scheme 16. Proposed mechanism for formation of **39**.

Intermolecular reactions also were initially attempted. As was the case with the disilanyl system **9**,[15] no addition products were observed upon either photolysis (254 nm) or flow pyrolysis (450 °C) of decamethyltetrasilane (**40**)/diphenylbutadiyne (**41**) mixtures (Scheme 17).

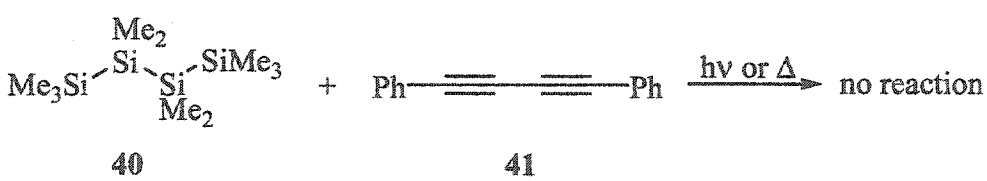

Scheme 17. Attempted intermolecular reactions.

B. Results and Discussion

As was the case with disilane additions, the only reported digermane additions to unsaturated C–C bonds are palladium- or platinum-catalyzed.[22-24] The intriguing results of photo- and thermochemical additions of Si–Si bonds naturally leads to the question of how the Ge–Ge sigma bond behaves under similar conditions. Accordingly, the germanium analogues of the disilanyl compounds previously studied were examined and the remainder of this dissertation comprises the results of these investigations.

1. Digermadibenzocycloöctyne. The first molecule studied was digermadibenzocycloöctyne **45**. The synthesis of **45**, shown in Scheme 18, is straightforward and begins with a modification of Bulten and Drenth's metathesis reaction.[25] Hexaethyldigermane (**42**) is dichlorinated by refluxing with two equivalents of tin tetrachloride in nitromethane for 22 hours to form 1,2-dichlorotetraethyldigermane (**43**) in 30% yield. It was found that the reaction conditions could be controlled to effect

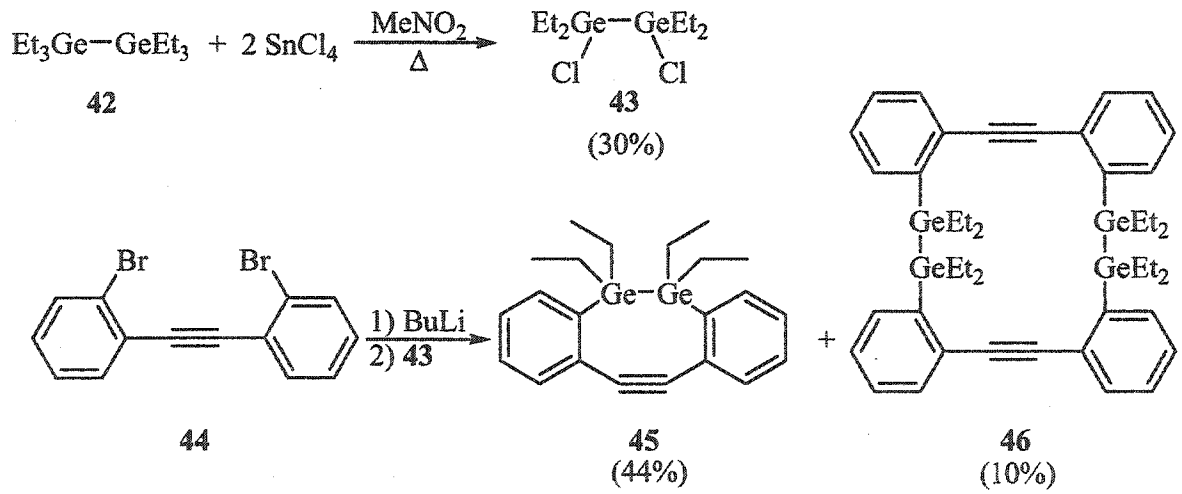

Scheme 18. Synthesis of **45**.

monochlorination, as will be described below. Ring formation was carried out according to the reported procedure[15] with dibromotolane (44) and butyl lithium to yield crystalline 45 in 44 % yield. The identity of 45 was confirmed by comparison of its ^{1}H and ^{13}C NMR spectra to those of the silicon analogue. The ^{13}C NMR spectrum was particularly diagnostic as the six aromatic carbon resonances from 127.00 to 142.74 ppm and the ethynyl carbon resonance

at 10.05 were very close to those of **11**.[15] In addition to the desired product, a second product with identical NMR spectral characteristics also was isolated in 10% yield. X-ray crystallography identified the product as the 16-membered ring dimer **46** (see Appendix D). Attempted catalytic cyclization using palladium(II) acetate and tetramethylbutyl isocyanide failed to produce any reaction, even after refluxing for five days.

Upon both UV photolysis and flow pyrolysis, **45** yielded the expected isomer **47** as the sole product in 92% and 21% conversion, respectively (Scheme 19). The ^{1}H and ^{13}C NMR spectra of **47** were quite similar to those of the silicon analogue and X-ray crystallography confirmed its structure (see Appendix D). The colorless crystals of **47** emit a beautiful purplish-blue light upon UV irradiation. Fluorescence quantum yield measurements (*vide infra*) in cyclohexane with 9,10-diphenylanthracene as standard gave a value of $\Phi = 0.85 \pm 0.01$ at $\lambda = 352$ nm. While this is a remarkably high value (*cf.* $\Phi = 0.68$ for the silicon analogue) the potential applications of this material may be prohibited by the high cost of germanium compounds.

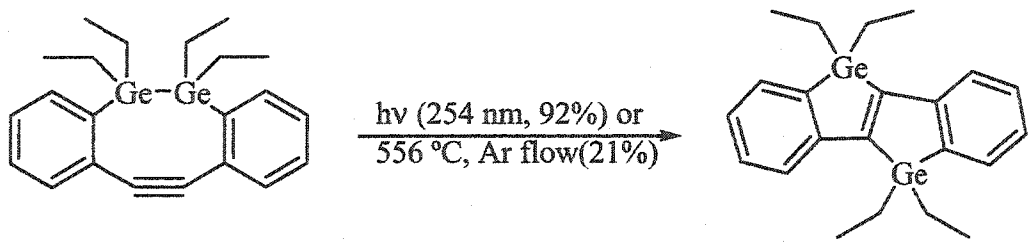

45 **47**

Scheme 19. Formation of **47** by photolysis and flow pyrolysis.

2. Acyclic digerma- and disilabenzoalkynes. The related acyclic compound **50** next was synthesized using a similar procedure to that for the cyclic compound (Scheme 20). The metathesis reaction described above, when carried out using one equivalent of tin tetrachloride and refluxing for only 2½ hours, yielded monochlorinated digermane **48** in a significantly greater yield. The mono- and dichlorination reactions are quite easily monitored by GC-MS as the two products are well separated on a DB-5 column and have MS patterns which are characteristic due to the presence of either one or two chlorine atoms. The lower yield of the dichlorination reaction most likely is due to the increased reflux time

allowing for the production of polychlorinated and oligomeric side products. Reflux times between 2½ and 22 hours were attempted, but complete dichlorination was not achieved and the resulting mixtures of **43** and **48** proved to be difficult to separate due to their similar boiling points. Sealed tube reactions also were tried in order to reduce reaction times and to improve yields, but were unsuccessful, yielding complex mixtures of products.

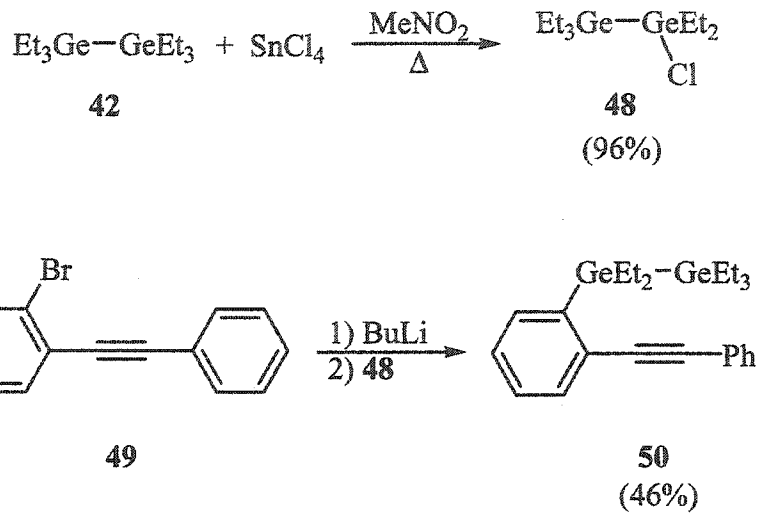

Scheme 20. Synthesis of **50**.

The structure of **50** was assigned based on its spectral data. The ^{1}H NMR only showed two sets of overlapping multiplets: alkylgermane protons in the range from 0.90-1.53 ppm and aromatic protons from 7.29-7.59 ppm. ^{13}C NMR, however, resolved the alkylgermane carbons into four resonances at 5.99, 6.75, 10.22, and 10.33 ppm, indicating the presence of two inequivalent Ge-Et groups. Ten inequivalent aromatic carbon resonances, corresponding to the phenyl and benzo carbons, also were present at 124.24, 128.07, 128.23, 128.79, 129.02, 129.50, 131.88, 133.53, 135.39, and 144.26 ppm. The peaks for the two ethynyl carbons appeared at 91.10 and 91.12 ppm. While the GC-MS spectrograph did not contain a peak for the molecular ion (*m/z* 468), but rather one corresponding to loss of an ethyl group (*m/z* 439), this is consistent with MS fragmentation patterns observed with other terminal ethyldigermanes, in which the molecular ion peak is either nonexistent or very weak (e.g., **48** and **62**).

Photolysis of **50** in hexanes gave a single isomeric product in 96% yield after 1½ hours (Scheme 21). The product was assigned the structure of germaindene **51** after inspection of the spectral data. In particular, the peaks corresponding to the sp^2 carbons in the ^{13}C NMR spectrum appeared in the same location as those for **47**, though the lower symmetry of **51** was evident from the greater number of inequivalent carbons. If isomer **52** were formed instead, an sp^2 carbon resonance would be expected to appear further downfield due to stronger deshielding from two germanium atoms being connected the same carbon. In addition, one can envision a through-space interaction between the ethyl protons on the geminal carbons on **52**, while this interaction should be negligible in **51**. Accordingly, ^1H-^1H nuclear Overhauser effect (NOE) spectroscopy experiments were performed. No inter-germanium ethyl cross-peaks were found, though CH_2-CH_3 interactions were evident within individual germanium-ethyl groups. While the absence of an NOE by itself does not rule out structure **52**, coupled with the ^{13}C NMR data, it is consistent with the assignment of structure **51**. As the product is a liquid at room temperature, the structure could not be determined definitively by X-ray crystallography.

To see if the electron-transfer mechanism proposed for the cyclic silicon analogue **26** could be operating in this case (Scheme 22), the photolysis also was performed in methanol. However, due to the poor solubility of **50** in methanol, several drops (~21 molar equivalents) of ethyl acetate were added to help dissolve the starting material. No reaction occurred after 7½ hours of irradiation at 254 nm, possibly due to absorption by the significantly more concentrated ethyl acetate. When the ethyl acetate was replaced with diethyl ether, only germaindene **51** was formed, albeit at a much slower rate. Two separate photolyses, one in hexanes and the other in methanol/diethyl ether were performed simultaneously and confirmed the rate inhibition in methanol. A possible explanation for the absence of methanol-trapped product is an inability of the intermolecular reaction with methanol to compete with the intramolecular rearrangement. The rate retardation in methanol cannot be due to decreased absorption by the starting material through interference with methanol or diethyl ether as neither of the latter have significant absorption at these wavelengths.[6] It is possible that reversible complex (*e.g.*, exciplex) formation of the dipolar intermediate **53**

with methanol is competing with product formation, thereby slowing down the overall rate.[26] Such dipole-dipole stabilized exciplexes involving aliphatic alcohols are known to form.[27]

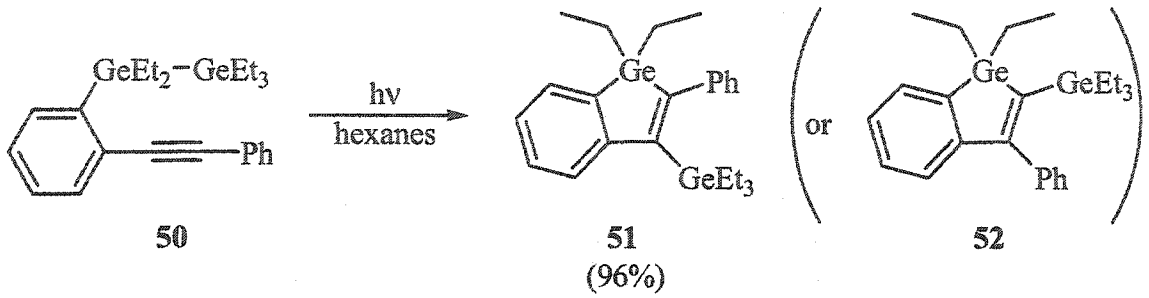

50 **51** (96%) **52**

Scheme 21. UV photolysis of **50**.

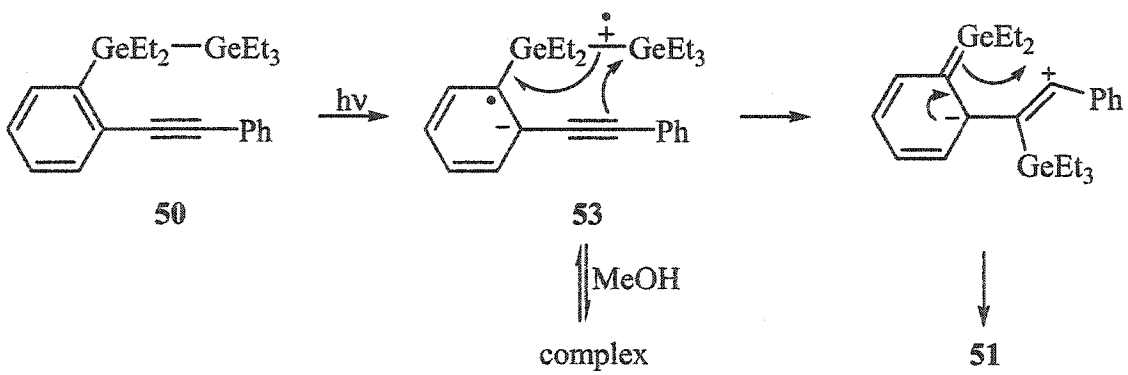

50 **53** complex **51**

Scheme 22. Possible mechanism for photolytic formation of **51**.

While the Pd(II)-catalyzed reaction of **50** gave the photoisomer **51** in 98% yield, flow pyrolysis at temperatures from 456 to 657 °C failed to produce any isolable products. Only the starting material was recovered in the lower temperature ranges while complete decomposition occurred at the higher temperatures. This lack of thermal reactivity is not surprising, considering the high activation entropy ($\Delta S^{\ddagger}$) calculated by Ma[15] (discussed in the introduction) and the fact that the molecule is no longer locked in a position that facilitates a $[2_s+2_a]$ cycloaddition.

In order to carry out comparative studies, the silicon analogue (**54**) was synthesized in a manner similar to that for the synthesis of **50** (see experimental section). Both flow

pyrolysis and UV photolysis of **54** yielded a single isomeric product (Scheme 23) in 38 and 78% conversions, respectively. Based on the similarity of its NMR spectra to those of germanium analogue **51**, the product was assigned the structure **55**. The pyrolytic formation of **55** is in contrast to the reluctance of the germanium compound to undergo the same isomerization thermally. One explanation for this phenomenon is that, at the temperatures required to overcome the large $\Delta S^{\ddagger}$ for the cyclization, other reaction modes (*e.g.*, germylene elimination) become available to the germanium system, resulting in decomposition of the starting material.

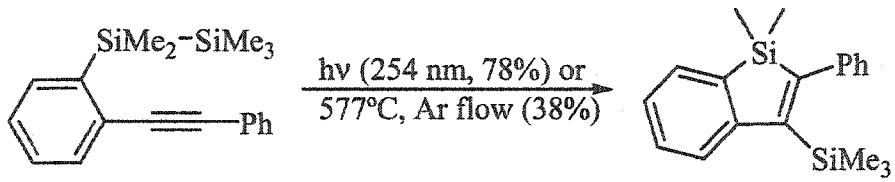

54 **55**

Scheme 23. Flow pyrolysis and UV photolysis of **54**.

3. Dioxadigermacycloöctyne. The synthesis of **58** was carried out according to the scheme used by Ma in the synthesis of the disilyl derivative (Scheme 24). Dilithioacetylene, prepared *in situ* by the reaction[28] of three equivalents of butyl lithium with trichloroethylene (**56**), was reacted with two equivalents of benzophenone to yield diol **57**. Deprotonation of **57** with butyl lithium, followed by addition of dichlorodigermane **43** gave the desired product (**58**) in 13% yield. The symmetry of this molecule and its structural similarity to silicon analogue **3** are evident from its NMR spectra. Both the ^{1}H and ^{13}C NMR data revealed the presence of a single unique Ge-Et group at 0.99 and 8.86/12.03 ppm, respectively. In the ^{13}C NMR spectrum, the quaternary sp^3 carbon resonance appears at 77.72 ppm while the two acetylenic carbons give rise to a single peak at 95.35 ppm.

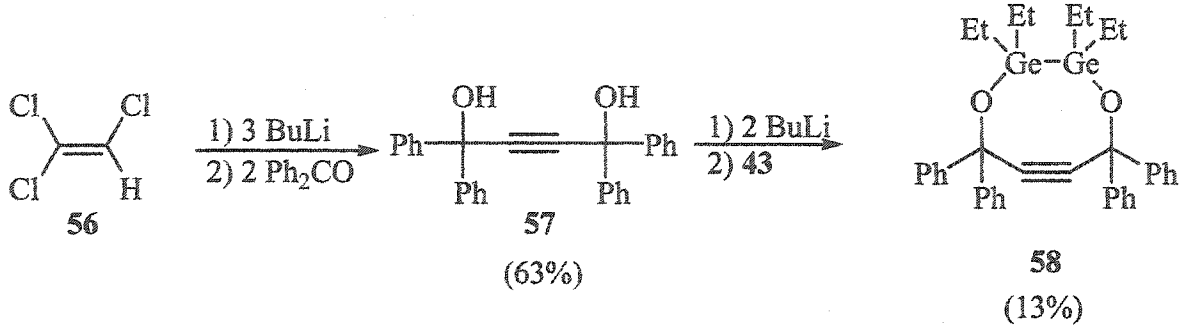

Scheme 24. Synthesis of **58**.

Irradiation of **58** in hexanes for seven hours at 254 nm yielded a single isomer (**59**) in 81% yield (Scheme 25). The ^{1}H NMR spectrum of **59** was relatively unremarkable, with only peaks corresponding to aromatic and germanium-ethyl protons appearing. The ^{13}C NMR spectrum, however, confirmed the presence of two inequivalent germanium-ethyl groups and three unique phenyl groups. Particularly diagnostic is the peak at 203.29 ppm, corresponding to the central allenic carbon.

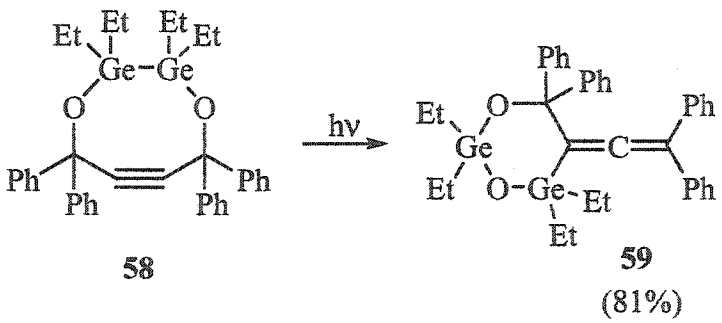

Scheme 25. UV photolysis of **58**.

No tetraphenylbutatriene was detected in the photolysis by GC-MS, so the diradical mechanism proposed for silicon analogue **3** (see Scheme 7) apparently is occurring in exclusion of a photochemical $[2_s+2_s]$ cycloaddition. Attempted reaction with catalytic palladium(II) acetate and tetramethylbutyl isocyanide also failed to effect a cycloaddition reaction; the starting material remained unchanged after refluxing for 81½ hours.

Flow pyrolysis of **58** also produced some unexpected results (Scheme 26). At 531 °C, no starting material remained and the only product detected by GC-MS was benzophenone (**60**). Decreasing the reaction temperature to 507 °C also resulted in the formation of benzophenone, but undecomposed starting material remained in this case. Sealed tube pyrolysis failed to produce any GC-detectable germanium-containing products, including starting material, or benzophenone after 14 hours of heating at 194 °C. The benzophenone produced in the 531 °C pyrolysis was purified by column chromatography, revealing that only 0.73 molar equivalents (based on starting material) were isolated in the reaction. Two plausible explanations for these data are that 1) the thermal $[2_s+2_a]$ cycloaddition occurs but only at temperatures where the products are thermally unstable, resulting in complete decomposition of the product, or 2) the cycloaddition does not have a chance to occur because the activation barrier for cyclization is higher than that for decomposition. The appearance of **60** is puzzling and possibly is a product of some complex decomposition mechanism.

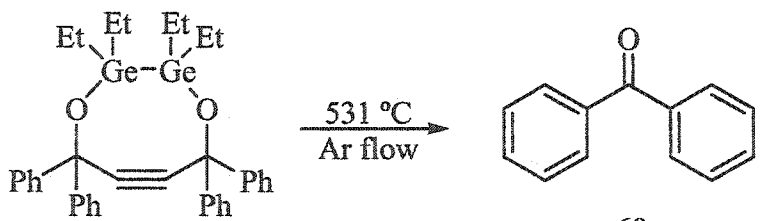

58 **60**

Scheme 26. Flow pyrolysis of **58**.

4. Acyclic germaoxaalkynes. Although the synthesis of **62** (Scheme 27), analogous to that for formation of cyclic **58**, was straightforward and occurred without difficulty, the isolation proved to be somewhat troublesome. Upon completion of the reaction, the expected product was identified by GC-MS and appeared to be produced in good yield. However, several standard purification techniques, including column chromatography with a variety of solvents, were attempted, but resulted in complete disappearance of the product. The only

method that gave a pure product without total sample loss was preparative-scale gas chromatography (prep-GC).

61 **62**

Scheme 27. Synthesis of **62**.

When a solution of **62** in hexanes was irradiated at 254 nm for 7½ hours, complete conversion to a single non-isomeric product occurred. The results of GC-MS analysis of the product indicated that it contained only one germanium atom. Like the starting material, this product proved to be difficult to isolate and prep-GC once again proved to be the only successful technique. Spectral analysis identified the product as germaoxacyclopentene **63**. Integration of the Ge-Et multiplet in the ^{1}H NMR revealed the presence of a single unique Ge-Et group. The Ge-containing fragments, including the molecular ion, in the GC-MS spectrogram also showed the existence of only a single Ge atom in the product. The vinyl proton resonance at 6.94 ppm is consistent with a vinyl proton vicinal to an alkylgermane.[29]

A possible mechanism for the formation of **63** is shown in Scheme 28. Initial Ge–Ge bond homolysis would yield triethylgermyl radical **65** and alkoxygermyl radical **64**, which undergoes an intramolecular addition reaction to yield vinyl radical **66**. This radical then could abstract a hydrogen atom from the solvent, for example, to yield the final product. Evidence for the formation of triethylgermyl radical was provided by photolysis of **62** in a 50:50 mixture of hexanes and chlorobutane. After 1½ hours, both **63** (in *ca.* 40% conversion) and chlorotriethylgermane (**71**) were formed, consistent with trapping of **65**.

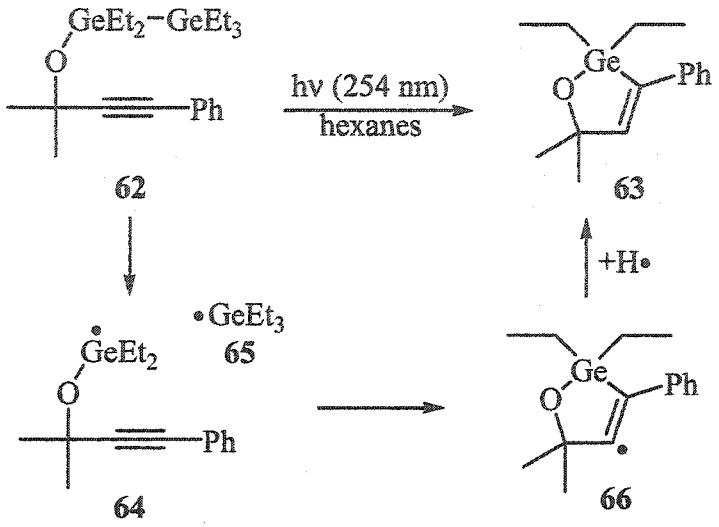

Scheme 28. Possible mechanism for photochemical formation of **63**.

The thermal behavior of **62** was no less remarkable. Flow pyrolysis at 531 °C produced three products (95% decomposition): hexaethyldigermoxane (**67**), isopropylphenylacetylene (**68**), and propadiene **69** (Scheme 29). The identity of **67** was confirmed by independent synthesis (see experimental section) and **68** and **69** by NMR and GC-MS.

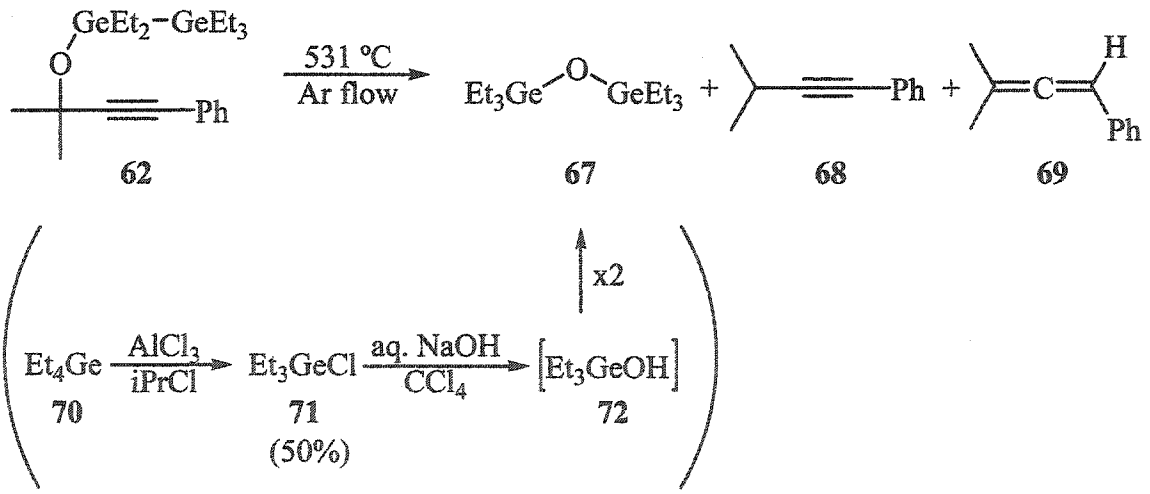

Scheme 29. Flow pyrolysis of **62**.

Initially, it was postulated that the products resulted from a mechanism involving initial elimination of diethylgermylene (Scheme 30). While flow pyrolysis in deuterated toluene failed to produce any deuterium-incorporated products, it still is possible, though unlikely, that this decomposition is a surface reaction and, as such, hydrogen abstraction (whether inter- or intramolecular) may occur on the surface of the fused silica chips in the reaction tube.

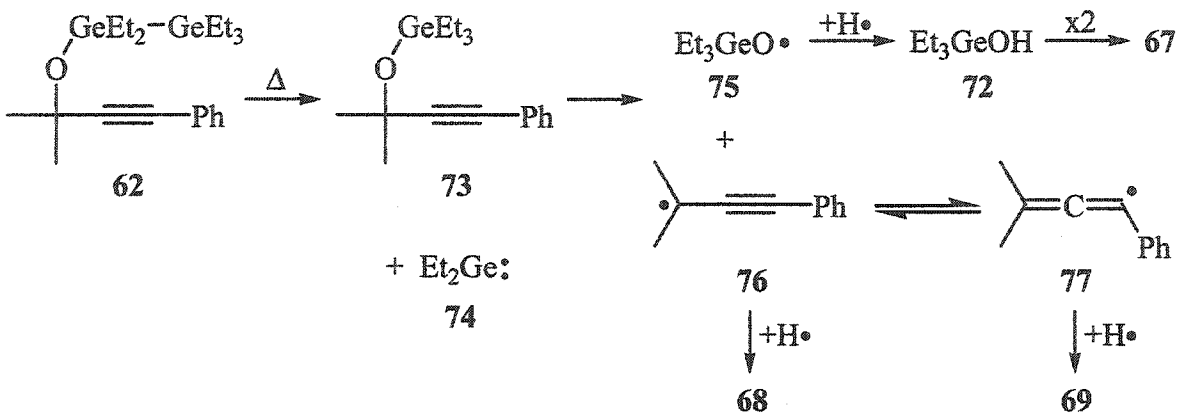

Scheme 30. Possible mechanism for **62** pyrolysis.

Sealed tube pyrolysis of 62 at 200 °C for 20 hours yielded only 73 in both nonane and deuterated toluene. While this result appeared to support the mechanism presented in Scheme 30, synthesis (Scheme 31) and subsequent flow pyrolysis of 73 (and the silicon

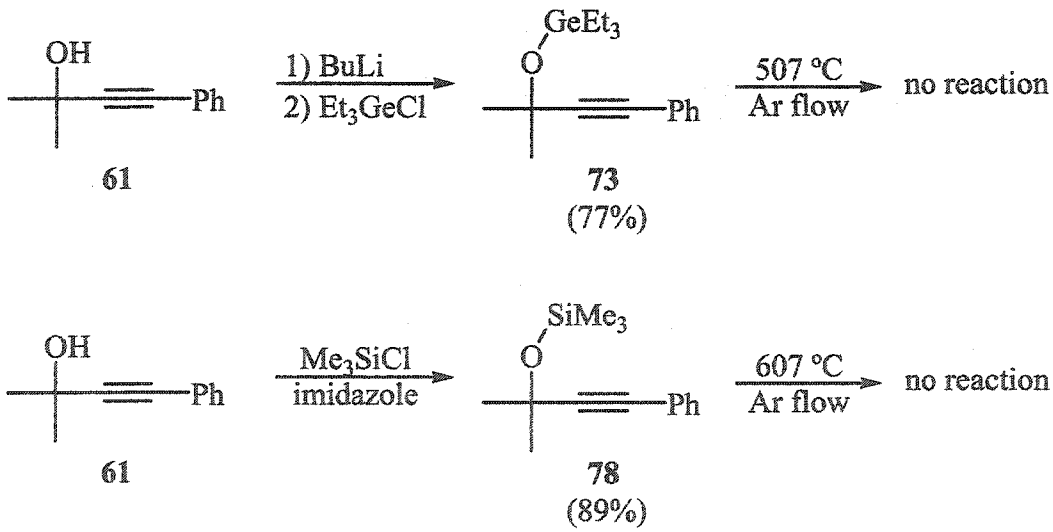

Scheme 31. Syntheses and flow pyrolyses of **73** and **78**.

analogue **78** for comparison) under the same conditions failed to produce any reaction at all. Apparently, flow pyrolysis and sealed tube pyrolysis cause the starting material to decompose *via* different mechanisms; diethylgermylene elimination is a likely candidate for the sealed tube process.

The reaction of **62** with a catalytic amount of Pd(II) acetate and tetramethylbutyl isocyanide resulted in complete conversion of the starting material after 14 hours in refluxing hexanes. Once again, all attempts at isolation of the product resulted in complete loss of the material. The only clean data able to be obtained was from GC-MS, which indicated that the product was in fact an isomer of the starting material. A possible structure for the isomer, based on the results for silicon analogue **11**,[15] is germaoxetane **79** (Scheme 32). Considering the relative instability of the starting material, it would not be unreasonable to expect that a strained molecule such as **79** also would be unstable.

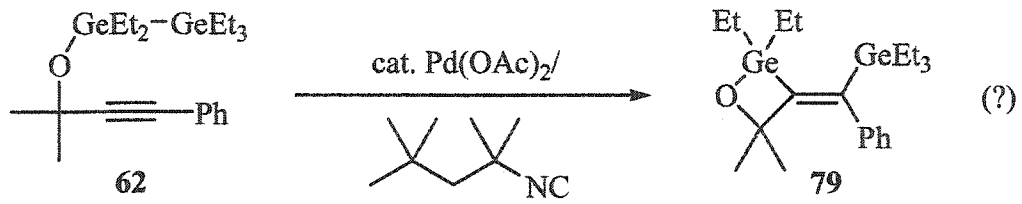

Scheme 32. Catalytic reaction of **62**.

5. Intramolecular experiment. Finally, an intermolecular thermal Ge–Ge addition to a C–C triple bond was attempted. It was decided to perform a sealed tube pyrolysis instead of a flow pyrolysis in order to minimize as much as possible the entropic factors associated with the reaction (Scheme 33). After 18 hours at 200 °C, no reaction was observed between hexaethyldigermane (**42**) and tolane (**80**), again probably due to a large $\Delta S^{\ddagger}$ for the reaction.

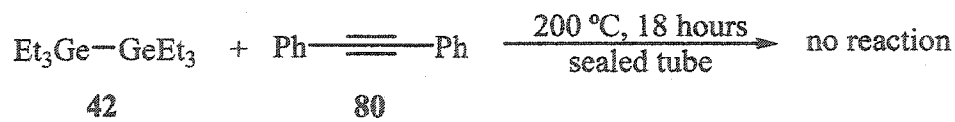

Scheme 33. Attempted intramolecular reaction between **42** and **80**.

C. Conclusions

The thermal, photochemical and catalytic additions of several digermanes to acetylenes have been explored and are summarized in Schemes 34 and 35. Both cyclic (**45**) and acyclic (**50**) digermabenzoalkynes behaved quite similarly to their silicon analogues, producing trans-addition products **47** and **51**, respectively. These results are remarkable in that they provide the first examples of both thermo- and photochemical additions of Ge–Ge bonds to acetylenes. Although the mechanisms for these cycloaddition reactions is not yet fully understood, it is likely that the same process is occurring in both the silicon and germanium systems.

Cyclic digermadioxaalkyne **58** also underwent thermo- and photochemistry similar to that of its silicon analogue **3**. Allenic isomer **59** (*cf.* **15**, Scheme 6) was produced photochemically, though in exclusion of any other detectable germanium-containing or hydrocarbon products. The only product isolated from thermal reaction of **58** was benzophenone (**60**), which may explained by decomposition of an intermediate germanium compound similar to thermal silicon intermediate **16** (Scheme 6). As was the case for hexamethyldisilane (**9**), intramolecular thermal reaction between a digermane (**42**) and an acetylene (**80**) did not occur, consistent with a large entropy of activation for the reaction.

The chemistry of acyclic digermaoxaalkyne **62** proved to be especially rich and equally perplexing (Scheme 35). Photolysis yielded cyclized product **63**, possibly resulting from initial loss of a triethylgermyl radical. Thermally, the results obtained were quite different, depending on the method of thermolysis. Flow pyrolysis yielded hexaethyldigermoxane (**67**) and hydrocarbons **68** and **69** while sealed tube pyrolysis gave germylene extrusion product **73**, resembling the thermochemistry of the silicon analogue. Catalytically, an nonisolable isomer, tentatively assigned the structure **79**, was produced. Trapping studies with deuterated toluene were inconclusive as no deuterium incorporation was observed in any of the products.

The results presented here represent the first investigations into an unexplored area of organogermanium chemistry. Further studies into these new cycloaddition reactions, particularly into their mechanisms, will provided a deeper understanding of the organic chemistry of germanium.

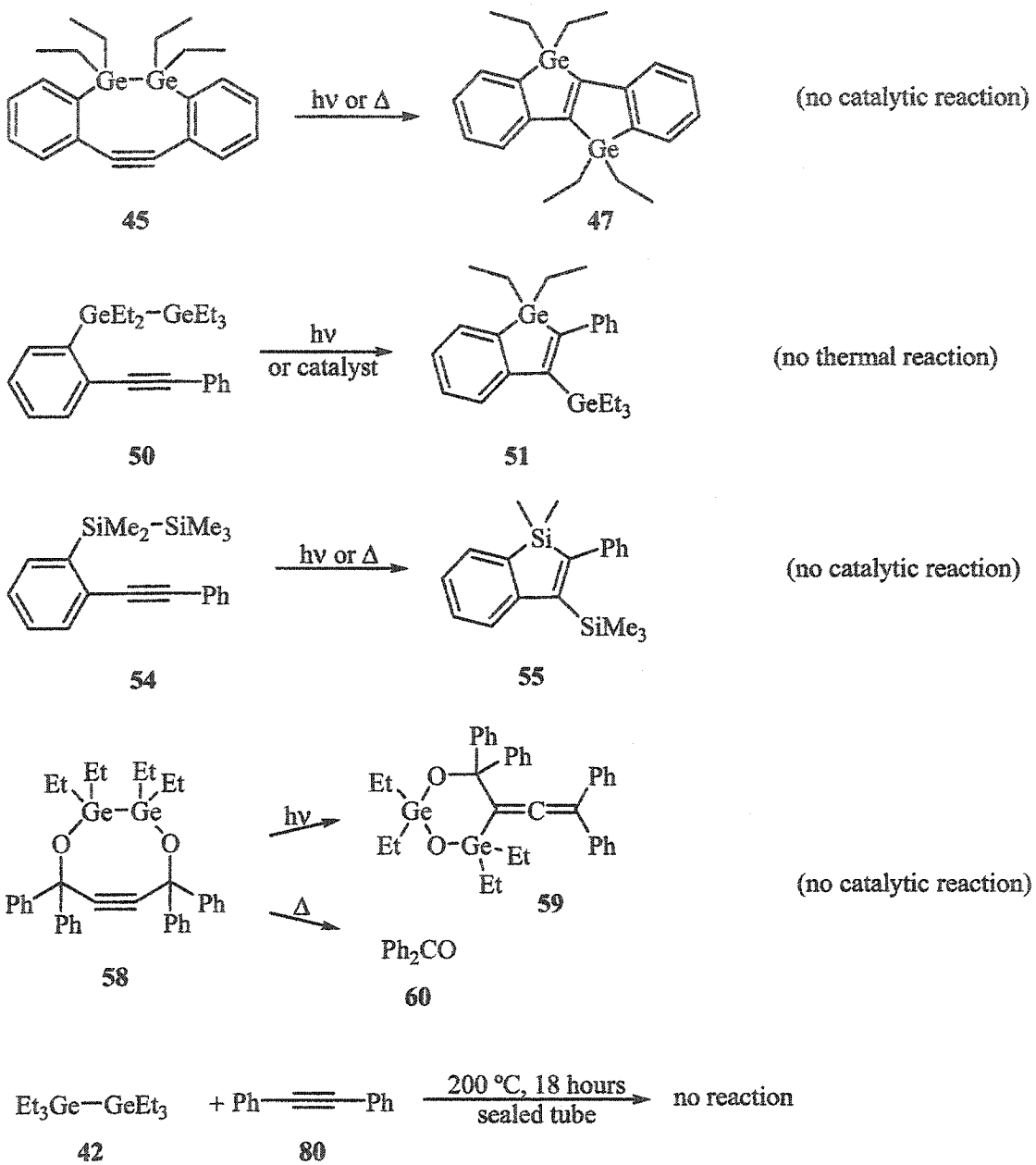

Scheme 34. Summary of reactions.

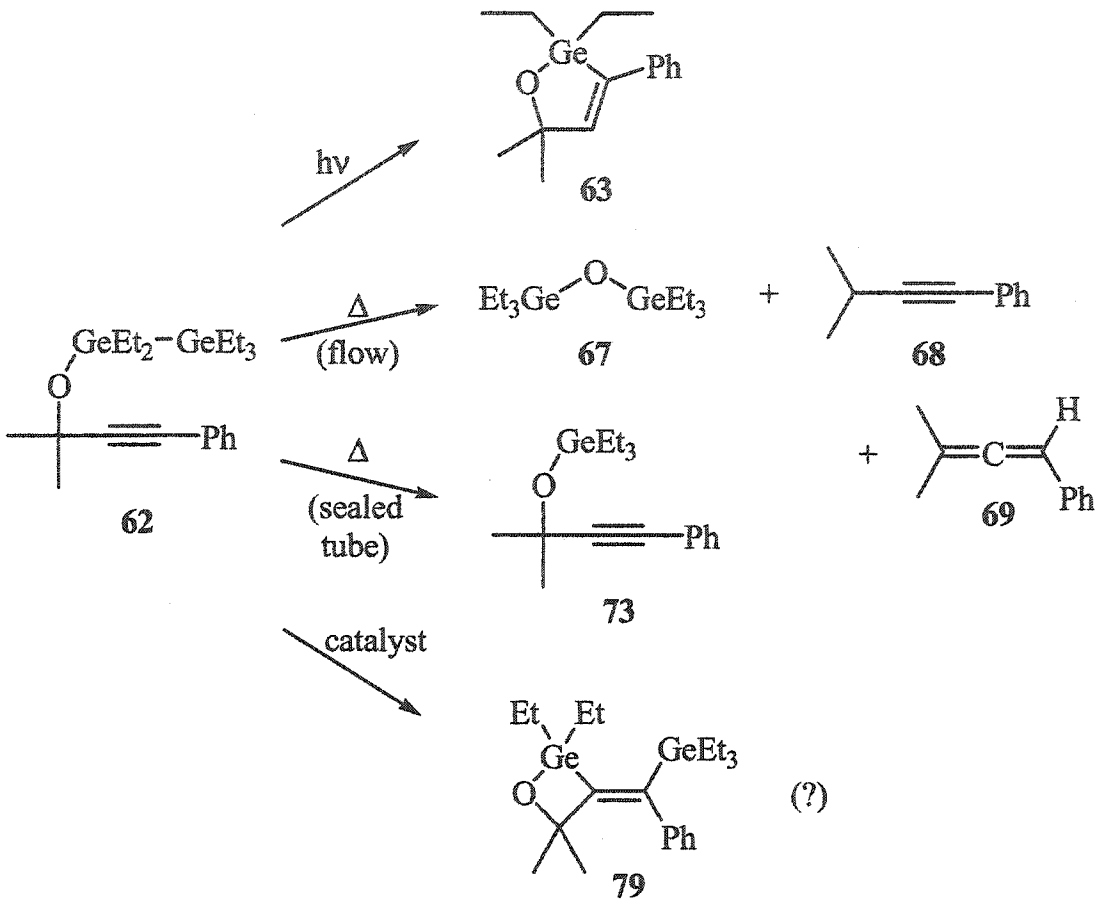

Scheme 35. Summary of reactions of **62**.

D. Experimental

Instrumentation and General Procedures. ^{1}H and ^{13}C NMR spectra were acquired on Varian (VXR-300 and VXR-400) spectrometers. Chemical shifts are reported as parts per million (ppm) relative to tetramethylsilane using the given solvents as standards: $CDCl_3$ (^{1}H 7.27 ppm, ^{13}C 77.23 ppm), CD_2Cl_2 (^{1}H 5.32 ppm, ^{13}C 54.00 ppm), C_6D_6 (^{1}H 7.16 ppm, ^{13}C 128.39 ppm). Fourier transform infrared (FTIR) spectra were obtained on a Bio-Rad Digilab FTS-7 spectrometer using neat samples in a 0.025 mm sealed cell. Ultraviolet-visible (UV-vis) spectroscopy was performed using a Hewlett-Packard 8452A diode array spectrophotometer. UV emission spectroscopy and fluorescence quantum yield experiments were carried out on a Jobin Yvon-Spex FluoroMax-2 spectrofluorometer equipped with DataMax-Std version 2.20 acquisition software and GRAMS version 3.04 Level II post-

processing software. Mass spectrometry was performed with a Finnigan TSQ700 mass spectrometer. Exact masses were obtained *via* high resolution mass spectrometry (HRMS) on a Kratos MS50 mass spectrometer with a resolution of 10,000. X-ray crystallographic data were obtained at the Iowa State Molecular Structure Laboratory.

Photolysis experiments were carried out in a Rayonet photochemical reactor equipped with fourteen 5W low pressure Hg lamps (253.7 nm). In a typical experiment, 60-100 mmol of starting material were dissolved in 50 mL of solvent in a valve-sealed 28x2 cm fused silica tube; the solution was degassed with 6 freeze-pump-thaw cycles and sealed under vacuum.

In a typical flow pyrolysis experiment, a vertical 50x2 cm (30 cm hot zone) fused silica tube was packed with fused silica chips and equipped with a drip tip, 250 mL round bottom flask, septum, and mineral oil bubbler. The tube was heated in a Lindberg tube furnace overnight under Ar flow (60 mL/min) to a temperature *ca.* 100 °C in excess of the pyrolysis temperature. The desired temperature was controlled by a Digi-Sense temperature controller connected to a thermocouple probe located inside the tube furnace at the center of the hot zone. The tube then was cooled down and allowed to equilibrate at the pyrolysis temperature. A Graseby 3300 medical syringe pump was used to add a solution of 60 mmol of starting material in 20 mL solvent at a rate of 1 mL/min. The pyrolysate was collected in the round bottom flask, which was cooled in a cold bath appropriate for the solvent used (e.g. -78 °C for hexanes, 0 °C for benzene).

Sealed tube pyrolyses were performed in 10x1.5 cm Pyrex tubes immersed in mineral oil baths heated by a hot plate to the desired temperature. The samples were prepared by dissolving the starting material(s) in the appropriate solvent and then degassing with 3 freeze-pump-thaw cycles. The tubes were flame-sealed under vacuum before pyrolysis.

Gas chromatography-mass spectrometry (GC-MS) data were obtained using a Hewlett-Packard 5890 Series II Plus gas chromatograph connected to an electron impact (EI) 5972 Series Mass Selective Detector operating at 70 eV. Routine analytical gas chromatography was performed using a Hewlett-Packard 5890 Series II gas chromatograph (GC) with flame ionization detector. A 30 meter J&W DB-5 capillary (0.250 mm i.d.) column was used for separation in both the analytical and GC-MS gas chromatographs. Preparative gas chromatography was carried out on a Varian Aerograph Model 920 gas

chromatograph (oven T = 205 °C, injector T = 230 °C) using a thermal conductivity detector (T = 250 °C). Copper tubing (210x0.5 cm) packed with Alltech 14% SE-30 on Chromosorb W-HP was used for the separations and helium (58 mL/min, reference: 21 mL/min) was used as the carrier gas.

Unless otherwise indicated, all reactions were run under a positive pressure of argon maintained by a continuous flow through a mineral oil bubbler. Tetrahydrofuran (THF) was distilled over lithium aluminum hydride (LAH) and diethyl ether was distilled over sodium/benzophenone prior to use. Other solvents and reagents were obtained commercially and used without further purification, unless indicated otherwise. Melting points were obtained using a Mel-Temp II melting point apparatus and are uncorrected.

Synthesis of 2,2'-dibromodiphenylacetylene (dibromotolane, 44). Ma's procedure[15] was used to synthesize the title compound. 1,2-Bromoiodobenzene (25 g, 88 mmol) and o-bromophenylacetylene (18.4 g, 100 mmol) were dissolved in 250 mL triethylamine in a 500 mL 20-neck round bottom flask fitted with a magnetic stir bar. Copper(I) iodide (0.54 g, 2.8 mmol) and bis(triphenylphosphino)palladium(II) chloride (0.53 g, 760 mmol) were added and the flask was covered in aluminum foil. After stirring for six hours, the reaction was quenched with 100 mL aqueous ammonium chloride. The organic layer was separated and passed through a short silica gel column to remove the catalysts and the solvent was removed *in vacuo* to give brownish yellow crystals. The crystals were recrystallized in hexanes to yield the desired product in 78% yield. **GC-MS (EI)**: 336 (M^+, 100), 176 (79), 168 (6), 150 (15), 137 (4), 126 (5), 110 (4), 99 (7), 88 (21), 75 (10), 51 (4); **m.p.** 80-81 °C (lit.[30] 81-83 °C).

Synthesis of *sym*-dichlorotetraethyldigermane (43). The title compound was synthesized according to a modification of the procedure by Bulten and Drenth.[25] A mixture of 3.80 g (11.9 mmol) hexaethyldigermane and 25 mL nitromethane was placed in an Ar-flushed 50 mL round bottom flask fitted with a West condenser, magnetic stir bar, and side arm. After the addition of 2.80 mL (23.9 mmol) tin tetrachloride *via* syringe, the reaction mixture was heated with a mineral oil bath to 85-90 °C for 22 hours. The resulting mixture was distilled,

yielding 1.2 g (30% yield) of the desired product. **GC-MS (EI)**: *m/z* (% relative intensity) 332 (M^+, 5), 303 (M^+-Et, 7), 275 (9), 217 (5), 184 (8), 167 (62), 132 (100), 109 (61), 103 (66), 75 (24); **b.p.** 60-63 °C, 0.1 torr (lit. 144-146 °C, 18 torr).

Synthesis of 5,5,6,6-tetraethyl-5,6-digermadibenzo[*c*,*g*]cycloöctyne (45). This procedure was based on the synthesis of the silicon analogue by Ma.[15] A 1000 mL 2-neck round bottom flask was fitted with a rubber septum, magnetic stir bar, and a Friedrichs condenser and charged with 5.05 g (15.0 mmol) dibromotolane **44** in 500 mL dry tetrahydrofuran (THF). The flask was cooled to -78 °C in a dry ice/acetone bath and 15.8 mL (30.0 mmol) of a 1.9 M solution of butyl lithium in hexanes was added dropwise *via* syringe while stirring. The reaction was stirred for 1½ hours, after which 5.00 g (15.0 mmol) dichlorodigermane **43** was added dropwise *via* syringe. After stirring overnight, the reaction was quenched with 250 mL saturated aqueous ammonium chloride. The aqueous layer was extracted with diethyl ether, which was then combined with the original THF layer. The combined ethereal fraction was washed sequentially with water and saturated aqueous sodium chloride and dried over anhydrous magnesium sulfate. The crude product, after filtration and removal of the solvent *in vacuo*, was purified by column chromatography (silica gel, hexanes) and crystallization, to yield 2.91 g (44% yield) of the desired product (see Appendix D for X-ray crystallography data). **^{1}H NMR** (300 MHz, CD_2Cl_2): δ 1.06 (t, J = 6 Hz, 12 H, Ge-CH_2-$\underline{C}H_3$), 1.37 (q, J = 6 Hz, 8 H, Ge-$\underline{C}H_2$-CH_3), 6.91-7.35 (m, 8 H, aromatic); **^{13}C NMR** (75 MHz, CD_2Cl_2): δ 6.90 (Ge-$\underline{C}H_2$-CH_3), 10.05 (Ge-CH_2-$\underline{C}H_3$), 93.42 ($\underline{C}\equiv\underline{C}$), 127.00, 127.98, 130.09, 132.43, 135.08, 142.74; **GC-MS (EI)**: *m/z* (% relative intensity) 438 (M^+, 26), 409 (M^+-Et, 100), 381 (25), 351 (31), 323 (54), 277 (12), 251 (68), 225 (18), 178 (41), 161 (15), 151 (22), 99 (12), 75 (6); **HRMS**: *m/z* 438.06333 (calc. for $C_{22}H_{28}Ge_2$ 438.062883); **UV-vis** (hexanes): λ_{max} (nm) 202, 232, 292, 308; **m.p.** 178-180 °C. In addition to the expected digermadibenzocycloöctyne, 0.66 g (10% yield) of colorless prismatic crystals also were isolated. While ^{1}H and ^{13}C NMR spectroscopies were identical to those of **45** (*vide supra*), MS and X-ray crystallography identified the new crystalline substance as the 16-membered ring dimer 5,5,6,6,13,13,14,14-octaethyl-5,6,13,14-tetragermatetrabenzo[*c*,*g*,*k*,*o*]-cyclohexadecyne (**46**). **MS (EI)**: *m/z* (% relative intensity) 847 (M^+-Et, 100), 715 (52), 658

(16), 569 (15), 555 (25), 525 (14), 499 (23), 427 (21), 422 (86), 409 (32), 353 (67), 322 (35), 277 (20), 250 (25), 133 (15), 101 (16), 73 (2); **m.p.** 161-163 °C.

Photolysis of 45. A solution of 2.91 g (6.65 mmol) of **45** in 50 mL HPLC-grade hexanes was irradiated at 254 nm for 48 hours. Removal of the solvent followed by crystallization in hexanes yielded prismatic crystals of 3,3,3',3'-tetraethyl-3,3'-digermaindeno[2,1-*a*]indene (**47**) as the sole product in 92% conversion: **^{1}H NMR** (400 MHz, $CDCl_3$): δ 1.24 (t, J = 4 Hz, 12 H, Ge-CH_2-$C\underline{H}_3$), 1.28 (q, J = 4 Hz, 8 H, Ge-$C\underline{H}_2$-CH_3), 7.13-7.56 (m, 8 H, aromatic); **^{13}C NMR** (100 MHz, $CDCl_3$): δ 6.59 (Ge-$\underline{C}H_2$-CH_3), 9.66 (Ge-CH_2-$\underline{C}H_3$), 126.03, 126.31, 129.38, 133.04, 141.39, 150.37, 161.25; **GC-MS (EI)**: *m/z* (% relative intensity) 438 (M^+, 83), 409 (M^+-Et, 91), 381 (11), 351 (40), 323 (58), 291 (3), 277 (27), 263 (14), 251 (100), 235 (3), 223 (21), 202 (29), 191 (25), 178 (60), 165 (76), 151 (32), 123 (6), 99 (20), 75 (11); **UV-vis** (cyclohexane): λ_{max} (nm) (ε (L mol^{-1} cm^{-1})) 222 (11977), 246 (17827), 256 (17917), 302 (7091), 316 (8624), 338 (11897), 350 (13854), 366 (9650); **m.p.** 99-101 °C.

Fluorescence quantum yield of 47. The secondary method for determination of fluorescence quantum yields was used as described by Eaton.[31] Spectrometric grade cyclohexane was used as the solvent for both the sample and the standard (9,10-diphenylanthracene). Concentrations were adjusted so that the absorbances at the excitation wavelength (352 nm) were < 0.1 and then the solutions were degassed by argon bubbling for 10-15 minutes. Three measurements were performed on each of three freshly-made and -degassed solutions of both standard and sample. Integration of the areas under the fluorescence spectra were used in the following equation to obtain the quantum yield of the sample (Φ_u):

$$\Phi_u = \Phi_s\left[\frac{(A_s F_u \eta_u^2)}{(A_u F_s \eta_s^2)}\right]$$

where Φ is the quantum yield, A is the absorbance at the excitation wavelength, F is the integrated area under the fluorescence curve, and η is the index of refraction of the solvent. The sample and standard solutions are denoted by the subscripts u ("unknown") and s,

respectively. The nine quantum yields (Φ_u) calculated were averaged to yield an average quantum yield of 0.85 ± 0.01 for **47**.

Flow pyrolysis of 45. Flow pyrolysis was carried out at 556 °C on a 10 mL column chromatography fraction of **45** in HPLC-grade hexanes. The same isomeric product obtained in the photolysis of **45** (germaindene **47**, *vide supra*) was formed in 21% conversion.

Catalytic reaction of 45. To a 25 mL round bottom flask fitted with a magnetic stirrer and West condenser was added 60 mg (0.13 mmol) **45** in 10 mL HPLC-grade hexanes. Palladium(II) acetate (3 mg, 0.013 mmol) and 6 mg (0.04 mmol) 1,1,3,3-tetramethylbutyl isocyanide then were added and the reaction was stirred overnight. The reaction was monitored by GC-MS. No reaction occurred, so the reaction was heated to reflux; no reaction occurred after refluxing for 5 days.

Synthesis of chloropentaethyldigermane (48).[25] The title compound was synthesized according to the method used for the synthesis of *sym*-dichlorotetraethyldigermane (**43**) above with only two modifications: half as much $SnCl_4$ is used and the reaction is refluxed for only 2½ hours. The resulting mixture was distilled gives the desired product in 96% yield. **GC-MS (EI)**: *m/z* (% relative intensity) 326 (M^+, 4), 297 (M^+-Et, 15), 269 (6), 239 (3), 209 (3), 181 (8), 161 (100), 133 (100), 103 (56), 89 (3), 75 (17); **b.p.** 65-68 °C, 0.1 torr (lit.[25] 146-147 °C, 18 torr).

Synthesis of (*o*-bromophenyl)phenylacetylene (bromotolane, 49). Sashida's procedure[32] was modified and carried out as follows. Phenylacetylene (10 mL, 91 mmol) and *o*-bromoiodobenzene (25.01 g, 88.40 mmol) were dissolved in a mixture of 100 mL benzene and 100 mL triethylamine. The solution was placed in a 500 mL 2-neck round bottom flask fitted with a magnetic stir bar, Friedrichs condenser, and rubber septum. Bis(triphenylphosphine)palladium dichloride (0.69 g, 0.98 mmol) and 0.39 g (2.0 mmol) copper(I) iodide then were added while stirring and the flask was covered in aluminum foil. After stirring overnight, 100 mL diethyl ether was added and the reaction was quenched with

100 mL saturated aqueous ammonium chloride. The solvent was removed *in vacuo* from the organic layer. Column chromatography (silica gel, hexanes) of the resulting liquid yielded 22.13 g (86.07 mmol, 97% yield) of clear pale yellow liquid **49**. **GC-MS (EI)**: *m/z* (% relative intensity) 258 (M+2, 84), 256 (M^+, 88), 176 (M^+-Br, 100), 151 (35), 126 (9), 111 (5), 98 (12), 88 (27), 75 (13), 63 (6), 51 (8).

Synthesis of 1,1,2,2,2-pentaethyl-1-(2-phenylethynyl)phenyldigermane (50). A 500 mL 2-neck round bottom flask was fitted with a rubber septum, magnetic stir bar, and a Friedrichs condenser and charged with 1.74 g (6.77 mmol) *o*-bromotolane **49** in 250 mL dry THF. The flask was cooled to -78 °C in a dry ice/acetone bath and 3.6 mL (6.8 mmol) of a 1.9 M solution of butyl lithium in hexanes was added dropwise *via* syringe while stirring. The reaction was stirred for 2 hours, after which 2.2 g (6.75 mmol) chlorodigermane **48** was added dropwise *via* syringe. After stirring overnight, the reaction was quenched with 100 mL saturated aqueous ammonium chloride. The aqueous layer was extracted with diethyl ether, which was then combined with the original THF layer. The combined ethereal fraction was washed with water and saturated aqueous sodium chloride and dried over anhydrous magnesium sulfate. The crude product, after filtration and removal of the solvent *in vacuo*, was purified by column chromatography (silica gel, hexanes) and crystallization, to yield 1.44 g (46% yield) clear colorless liquid **50**. **^{1}H NMR** (400 MHz, CD_2Cl_2): δ 0.90-1.53 (m, 25 H, Ge-$C_2\underline{H}_5$), 7.29-7.59 (m, 9 H, aromatic); **^{13}C NMR** (100 MHz, CD_2Cl_2): δ 5.99 (Ge-$\underline{C}H_2$-CH_3), 6.75 (Ge-$\underline{C}H_2$-CH_3), 10.22 (Ge-CH_2-$\underline{C}H_3$), 10.33 (Ge-CH_2-$\underline{C}H_3$), 91.10 ($\underline{C}$≡C), 92.12 (C≡$\underline{C}$), 124.24, 128.07, 128.23, 128.79, 129.02, 129.50, 131.88, 133.53, 135.39, 144.26; **GC-MS (EI)**: *m/z* (% relative intensity) 439 (M^+-Et, 66), 411 (6), 383 (5), 355 (6), 327 (18), 309 (27), 281 (29), 251 (54), 225 (11), 191 (15), 178 (100), 175 (26), 151 (21), 133 (38), 119 (6), 103 (47), 96 (13), 89 (6), 73 (19); **UV-vis** (hexanes): λ_{max} (nm) 204, 220, 244, 284, 302.

Photolysis of 50 in hexanes. A solution of 90 mg (0.19 mmol) of **50** in 25 mL HPLC-grade hexanes was irradiated at 254 nm for 1.5 hours. A single isomeric product, 2-phenyl-3-triethylgermyl-1,1-diethyl-1-germaindene (**51**), was formed in 96% yield. **^{1}H NMR** (400

MHz, CD_2Cl_2): δ 0.76 (q, J = 8 Hz, 6 H, vinyl Ge-C<u>H</u>$_2$-CH$_3$), 0.93 (t, J = 8 Hz, 9 H, vinyl Ge-CH$_2$-C<u>H</u>$_3$), 1.01-1.13 (m, 10 H, cyclic Ge-C$_2$<u>H</u>$_5$), 7.09-7.58 (m, 9 H, aromatic); **^{13}C NMR** (100 MHz, CD_2Cl_2): δ 6.27 (Ge-<u>C</u>$_2$H$_5$), 6.84 (Ge-<u>C</u>$_2$H$_5$), 9.33 (Ge-<u>C</u>$_2$H$_5$), 9.56 (Ge-<u>C</u>$_2$H$_5$), 126.09, 126.27, 126.32, 127.32, 128.44, 129.29, 132.71, 133.02, 139.55, 145.36, 153.75, 162.16; **GC-MS (EI)**: *m/z* (% relative intensity) 468 (M^+, 1), 437 (16), 381 (1), 353 (2), 325 (7), 309 (9), 279 (14), 263 (3), 251 (59), 225 (14), 205 (11), 191 (10), 178 (100), 165 (14), 161 (6), 151 (21), 133 (21), 103 (34), 89 (2), 75 (7); **HRMS**: *m/z* 469.11150 (calc. for $C_{19}H_{34}Ge_2$ 469.11069).

Photolysis of 50 in methanol. The photolysis was performed as above, except with HPLC-grade methanol as the solvent. As **50** is insoluble in methanol, 20 drops of ethyl acetate were added as a solubilizing agent. The reaction was monitored by GC-MS. After 7.5 hours, no products were formed; the starting material remained unchanged. A photolysis using diethyl ether in place of ethyl acetate did result in formation of the photoisomer, germaindene **51**, but the rate of formation was significantly retarded (see following photolysis).

Photolysis of 50 in hexanes and in methanol. Parallel photolyses, one in methanol/diethyl ether and one in hexanes, were performed as above and monitored by GC-MS. In both reactions, only one product was formed: photoisomer **51**. However, after 75 minutes of irradiation, the hexanes solution had undergone 79% conversion while the methanol/diethyl ether solution had undergone only 6% conversion.

Flow pyrolysis of 50. Flow pyrolysis was carried out at temperatures of 456, 530, 582, 626, and 657 °C on 130 mg (0.28 mmol) of **50** in 10 mL HPLC-grade hexanes. In the pyrolyses at the lower three temperatures, only starting material was detected by GC-MS. The pyrolyses at the higher two temperatures resulted in the complete disappearance of the starting material with no products detected by GC-MS.

Catalytic reaction of 50. To a 100 mL round bottom flask fitted with a magnetic stirrer and West condenser was added 530 mg (1.10 mmol) of **50** in 50 mL HPLC-grade hexanes.

Palladium(II) acetate (50 mg, 0.2 mmol) and 50 mg (0.36 mmol) 1,1,3,3-tetramethylbutyl isocyanide then were added. The reaction was heated to reflux and stirred overnight. The progress of the reaction was monitored by GC-MS. The reaction resulted in 98% conversion of the starting material to the photoisomer, germaindene **51**.

Synthesis of chloropentamethyldisilane.[33] The chlorodisilane was prepared in 80% yield by chlorination of pentamethyldisilane with carbon tetrachloride and catalytic benzoyl peroxide.[34]

Synthesis of 1,1,2,2,2-pentamethyl-1-(2-phenylethynyl)phenyldisilane (54). Bromotolane (3.02 g, 11.7 mmol) was dissolved in 200 mL dry tetrahydrofuran in a 500 mL 2-neck round bottom flask fitted with a Friedrichs condenser, magnetic stir bar, and rubber septum. The flask was cooled to -78 °C and 5.0 mL (11.5 mmol) of a 2.3 M solution of butyl lithium in hexanes was added dropwise *via* syringe. The reaction was stirred for 1½ hours and then 1.93 g (11.6 mmol) chloropentamethyldisilane were added *via* syringe. The reaction was stirred overnight while allowing it to warm to room temperature. The reaction mixture then was transferred to a 500 mL separatory funnel and 150 mL diethyl ether were added, followed by 150 mL saturated aqueous ammonium chloride. The ethereal layer then was washed sequentially with water and saturated aqueous sodium chloride (150 mL of each) and then dried over anhydrous magnesium sulfate. After filtration, removal of the solvent in vacuo, and column chromatography (silica gel, hexanes), the title compound was isolated as a clear colorless liquid in 88% yield. **^{1}H NMR** (400 MHz, CD_2Cl_2): δ 0.12 (s, 9 H, Si-($C\underline{H}_3$)$_3$), 0.55 (s, 6 H, Si-($C\underline{H}_3$)$_2$), 7.34-7.61 (m, 9 H, aromatic); **^{13}C NMR** (100 MHz, CD_2Cl_2): δ -2.68 (Si-$\underline{C}H_3$), -1.19 (Si-$\underline{C}H_3$), 92.32 ($\underline{C}$≡C), 92.51 (C≡$\underline{C}$), 124.13, 128.08, 128.87, 128.92, 129.04, 129.30, 131.88, 133.36, 134.92, 142.64; **GC-MS (EI)**: *m/z* (% relative intensity) 308 (M^+, 28), 293 (M^+-Me, 56), 277 (19), 235 (100), 219 (15), 205 (8), 191 (6), 177 (4), 165 (5), 159 (5), 135 (8), 131 (10), 115 (3), 105 (10), 73 (23), 53 (5); **HRMS**: *m/z* 308.16220 (calc. for $C_{19}H_{24}Si_2$ 308.14166).

Photolysis of 54. A solution of 520 mg (1.70 mmol) of **54** in 25 mL HPLC-grade hexanes was irradiated at 254 nm for 3½ hours. A single isomeric product, 2-phenyl-3-trimethylsilyl-1,1-dimethyl-1-silaindene (**55**), was formed in 78% yield. **^{1}H NMR** (400 MHz, CD_2Cl_2): δ 0.05 (s, 9 H, vinyl Si-C$\underline{H}_3$), 0.28 (s, 6 H, cyclic Si-C$\underline{H}_3$), 7.09-7.60 (m, 9 H, aromatic); **^{13}C NMR** (100 MHz, CD_2Cl_2): δ -4.24 (Si-$\underline{C}H_3$), 1.63 (Si-$\underline{C}H_3$), 126.18, 126.22, 126.27, 127.43, 128.46, 130.10, 132.06, 132.39, 139.08, 144.11, 155.95, 163.93; **GC-MS (EI)**: *m/z* (% relative intensity) 308 (M^+, 94), 293 (M^+-Me, 100), 277 (29), 234 (17), 219 (11), 205 (22), 191 (17), 177 (6), 165 (9), 159 (5), 135 (10), 131 (17), 115 (6), 105 (8), 73 (24), 53 (4).

Flow pyrolysis of 54. Flow pyrolysis was carried out at 577 °C on 0.52 g (0.17 mmol) of **54** in 20 mL HPLC-grade hexanes. The same isomeric product (silaindene **55**) obtained in the preceding photolysis was formed in 38% conversion.

Synthesis of 1,1,4,4-tetraphenyl-2-butyn-1,4-diol (57). The title compound was prepared from dilithioacetylene[28] and benzophenone according to Lin's method.[35] The diol was isolated as a cream-colored powder in 63% yield. **^{1}H NMR** (400 MHz, CD_2Cl_2): δ 3.03 (s, 2 H), 7.28-7.62 (m, 20 H); **m.p.** 191 °C (lit.[35] 197 °C).

Synthesis of 5,5,6,6-tetraethyl-3,3,8,8-tetraphenyl-4,7-dioxa-5,6-digermacyloöctyne (58). Diol **57** (3.82 g, 9.78 mmol) was dissolved in 250 mL dry THF in a 500 mL 2-neck round bottom flask fitted with a magnetic stir bar, Friedrichs condenser, and rubber septum. The flask was cooled to -78 °C and a 1.95 M solution of butyl lithium (10.0 mL, 19.5 mmol) in hexanes was added dropwise *via* syringe while stirring. After the addition, the reaction was stirred for 2 hours while allowing it to warm to room temperature. The flask then was cooled back down to -78 °C and 3.25 g (9.78 mmol) dichlorodigermane **43** was added dropwise *via* syringe. The reaction was stirred overnight, during which it was allowed to warm to room temperature. The solvent was removed *in vacuo* and crystallization in hexanes yielded 0.85 g (13% yield) colorless crystals of **58**. **^{1}H NMR** (400 MHz, CD_2Cl_2): δ 0.99 (s, 20 H, Ge-$C_2\underline{H}_5$), 7.19-7.68 (m, 16 H, aromatic); **^{13}C NMR** (100 MHz, CD_2Cl_2): δ 8.86 (Ge-$\underline{C}_2H_5$),

12.03 (Ge-$\underline{C}_2H_5$), 77.72 (Ph_2-$\underline{C}$-O), 95.35 ($\underline{C}\equiv\underline{C}$), 126.16, 127.58, 128.91, 147.90; **FTIR**: $\bar{\nu}$ (cm^{-1}) 3083 (m), 3027 (m), 2954 (s), 2929 (m), 1949 (w), 1804 (w), 1595 (m), 1487 (s), 1449 (s), 1190 (s), 1045 (s), 749 (s), 586 (m); **MS (EI)**: *m/z* (% relative intensity) 621 (M^+-Et, 22), 572 (18), 467 (37), 441 (16), 411 (20), 356 (100), 321 (16), 278 (33), 263 (21), 177 (25), 105 (13), 77 (10); **HRMS**: *m/z* 650.15073 (calc. for $C_{36}H_{40}O_2Ge_2$ 650.14976); **m.p.** 144-146 °C.

Photolysis of 58. Irradiation at 254 nm of a solution of 0.125 g (0.192 mmol) of **58** in 60 mL HPLC-grade hexanes for 7 hours resulted in 81% conversion of the starting material. A single isomeric product, 1-(3',3'-diphenylallenyl)-2,2-diphenyl-4,4,6,6-tetraethyl-4,6-digerma-3,5-dioxacyclohexene (**59**) was identified. **^{1}H NMR** (400 MHz, CD_2Cl_2): δ 0.92-1.17 (m, 20 H, Ge-$C_2\underline{H}_5$), 6.98-7.50 (m, 20 H, aromatic); **^{13}C NMR** (100 MHz, CD_2Cl_2): δ 7.65 (Ge-$\underline{C}_2H_5$), 7.92 (Ge-$\underline{C}_2H_5$), 11.38 (Ge-$\underline{C}_2H_5$), 12.12 (Ge-$\underline{C}_2H_5$), 84.95, 89.95, 107.94, 108.01, 127.20, 127.35, 127.47, 127.98, 128.50, 128.77, 137.29, 148.97, 203.29 (C=$\underline{C}$=C); **HRMS**: *m/z* 650.15061 (calc. for $C_{36}H_{40}O_2Ge_2$ 650.14976);

Flow pyrolysis of 58. A solution of 1.02 g (1.57 mmol) of **58** in 60 mL HPLC-grade hexanes was pyrolyzed at 531 °C. No starting material was detected, but 0.21 g (0.73 molar equivalents) of benzophenone (**60**) were isolated from the pyrolysate by column chromatography (silica gel, 4:1 hexanes:ethyl acetate) and identified by comparison to authentic samples. A separate flow pyrolysis at a lower temperature (507 °C) did result in leftover starting material, in addition to the previously observed benzophenone. For benzophenone: **^{13}C NMR** (100 MHz, CD_2Cl_2): δ 128.44, 128.83, 130.52, 132.93, 138.21, 196.89; **GC-MS (EI)**: *m/z* (% relative intensity) 182 (M^+, 35), 152 (2), 105 (100), 77 (56), 51, (21).

Sealed tube pyrolysis of 58. The starting material (40 mg, 0.062 mmol) was dissolved in 1 mL dodecane and sealed as described above in the pyrolysis tube. The tube then was heated to 194 °C for 14 hours. After cooling, the tube was opened and the dodecane was removed by vacuum distillation. No benzophenone or germanium-containing products, including starting material, were detected by GC-MS.

Catalytic reaction of 58. To a 100 mL round bottom flask fitted with a magnetic stirrer and West condenser was added 125 mg (0.192 mmol) of **58** in 50 mL HPLC-grade hexanes. Palladium(II) acetate (50 mg, 0.22 mmol) and 50 mg (0.36 mmol) 1,1,3,3-tetramethylbutyl isocyanide then were added and the reaction was heated to reflux. Periodic analysis by GC-MS revealed only starting material present. The reaction was stopped after 81½ hours. No products were detected.

Synthesis of 5,5,6,6,6-pentaethyl-3,3-dimethyl-1-phenyl-5,6-digerma-4-oxa-1-hexyne (62). This procedure was based on the synthesis of the silicon analogue by Ma.[15] Prior to use, the 3,3-dimethyl-1-phenyl-propyn-3-ol (**61**) was sublimed under reduced pressure (0.1 torr). The alcohol (2.47 g, 15.4 mmol) then was dissolved in 125 mL dry THF in a 250 mL 2-neck round bottom flask fitted with a Friedrichs condenser, magnetic stir bar, and a rubber septum. The flask was cooled to -78 °C and 8.1 mL (15.4 mmol) of a 1.9 M solution of butyl lithium was added dropwise *via* syringe. The reaction was stirred for 2 hours, during which it was allowed to warm to room temperature. After cooling the flask back down to -78 °C, 5.06 g (15.5 mmol) chlorodigermane **48** was added all at once. The reaction was allowed to warm to room temperature while stirring overnight. After removal of the solvent by distillation, the crude product was decanted from the residual salts as a clear colorless liquid. All attempted routine purification techniques, including column chromatography, resulted in complete loss of product. Product isolation was achieved only by preparative gas chromatography. **^{1}H NMR** (300 MHz, $CDCl_3$): δ 0.87-1.26 (m, 25 H, Ge-$C_2\underline{H}_5$), 1.56 (s, 6 H, OC-C$\underline{H}_3$), 7.27-7.43 (m, 5 H, aromatic); **^{13}C NMR** (75 MHz, $CDCl_3$): δ 5.66 (Ge-$\underline{C}_2H_5$), 8.89 (Ge-$\underline{C}_2H_5$), 10.14 (Ge-$\underline{C}_2H_5$), 12.25 (Ge-$\underline{C}_2H_5$), 33.93 (OC-$\underline{C}H_3$), 67.52 (O-$\underline{C}$-CH_3), 82.17 ($\underline{C}$≡C), 97.01 (C≡$\underline{C}$), 123.87, 128.01, 128.40, 131.71; **GC-MS (EI)**: *m/z* (% relative intensity) 421 (M^+-Et, 1), 363 (21), 335 (21), 307 (100), 279 (38), 249 (31), 233 (24), 219 (3), 207 (33), 191 (4), 175 (30), 161 (30), 149 (8), 143 (6), 133 (58), 129 (54), 119 (4), 115 (16), 103 (59), 91 (14), 77 (15), 65 (4).

Photolysis of 62 in hexanes. Irradiation at 254 nm of 90 mg (0.20 mmol) of **62** in 25 mL HPLC-grade hexanes yielded a single product after 7½ hours; no starting material remained.

All attempts at isolating the product through standard techniques (*e.g.*, column chromatography) resulted in loss of all material, presumably due to decomposition. However, a spectroscopically pure sample was obtained *via* preparative gas chromatography and identified as 5,5-diethyl-3,3-dimethyl-1-phenyl-5-germa-4-oxacyclopentene (**63**). **^{1}H NMR** (400 MHz, $CDCl_3$): δ 0.85-1.20 (m, 10 H, Ge-$C_2\underline{H}_5$), 1.34 (s, 6 H, ring $C\underline{H}_3$), 6.94 (s, 1 H, vinyl), 7.20-7.34 (m, 5 H, aromatic); **^{13}C NMR** (100 MHz, $CDCl_3$): δ 8.47 (Ge-$\underline{C}H_2$-CH_3), 11.04 (Ge-CH_2-$\underline{C}H_3$), 30.99 (Me_2-$\underline{C}$-O), 82.79 (vinyl $\underline{C}$-H), 127.33, 127.54, 129.24, 132.31, 138.76, 150.21; **FTIR**: $\bar{\nu}$ (cm^{-1}) 3410 (broad, m), 3020 (m), 2955 (s), 2870 (s), 2731 (m), 2152 (w), 1893; **GC-MS (EI)**: *m/z* (% relative intensity) 292 (M^+, 10), 277 (M^+-Me, 93), 263 (10), 219 (15), 188 (3), 175 (8), 151 (14), 145 (32), 129 (100), 117 (52), 102 (31), 91 (78), 77 (24), 63 (10), 57 (10), 51 (15).

Photolysis of 62 in hexanes and chlorobutane. The starting material (0.5 g, 1.1 mmol) was dissolved in 40 mL of a 50:50 (v:v) mixture of HPLC-grade hexanes and 1-chlorobutane. After 1½ hours (~40% conversion) of irradiation (254 nm), in addition to the photoproduct **63**, the formation of chlorotriethylgermane (**71**) was observed by GC-MS.

Flow pyrolysis of 62. Flow pyrolysis (531 °C, 95% decomposition) of 0.13 g (0.29 mmol) **62** in 10 mL HPLC-grade hexanes yielded hexaethyldigermoxane (**67**), 3-methyl-1-phenylbutyne (**68**), and 1,1-dimethyl-3-phenylpropadiene (**69**). Flow pyrolysis in toluene-d_8 also yielded the same results. All attempts at isolating the **67** through standard techniques (*e.g.*, column chromatography) either failed or resulted in loss of the digermoxane product. Column chromatography (silica gel, hexanes), however, successfully isolated the **68**/**69** mixture (35% combined yield) from the pyrolysate. The identity of **67** was confirmed by independent synthesis (*vide infra*). For **68** and **69**: **GC-MS (EI)**: *m/z* (% relative intensity) 144 (M^+, 32), 129 (M^+-Me, 100), 115 (18), 102 (6), 89 (5), 77 (6), 63 (11), 51 (12); **FTIR**: $\bar{\nu}$ (cm^{-1}) 3020 (m), 2927 (s), 2251 (s, C≡C), 1950 (w, C=C=C), 1605 (w), 1493 (m), 1453 (m), 1377 (m), 963 (m), 908 (s), 650 (m).

Synthesis of chlorotriethylgermane (71).[36] A 25 mL 2-neck round bottom flask was fitted with a septum, West condenser, and magnetic stir bar; the apparatus was flushed with argon and a positive pressure of argon kept thereafter. Tetraethylgermane (3.5 g, 19 mmol) and anhydrous aluminum chloride (0.06 g, 0.4 mmol) were added to the flask and isopropyl chloride (1.8 mL, 19 mmol) added dropwise *via* syringe. The reaction was heated to 95 °C in an oil bath for one hour. Distillation yielded 1.86 g (9.53 mmol, 50% yield) chlorotriethylgermane. **^{1}H NMR** (300 MHz, chloroform-*d*): δ 1.14 (s, 15 H); **^{13}C NMR** (75 MHz, chloroform-*d*): δ 8.02, 10.42; **b.p.** 175-178 °C (lit.[36] 173-177 °C).

Synthesis of hexaethyldigermoxane (67). The synthesis was carried out using a modification of Sohrin's method.[37] Chlorotriethylgermane (0.11 g, 0.56 mmol) was dissolved in 5 mL carbon tetrachloride in a 10 mL round bottom flask. To this solution was added 5.5 mL (.55 mmol) of a 0.1 M aqueous solution of sodium hydroxide. The reaction was stirred overnight with a magnetic stir bar. Hexaethyldigermoxane was formed in 75% yield. **GC-MS (EI)**: *m/z* (% relative intensity) 307 (M^+-Et, 100), 279 (61), 251 (41), 221 (15), 191 (8), 161 (52), 139 (13), 133 (93), 125 (11), 119 (4), 105 (86), 89 (10), 75 (15).[38]

Sealed tube pyrolysis of 62 in nonane. The starting material (40 mg, 0.089 mmol) was dissolved in 1 mL nonane and sealed as described above in the pyrolysis tube. The tube then was heated to 200 °C for 20 hours. The sole product formed was identified as 5,5,5-triethyl-3,3-dimethyl-1-phenyl-5-germa-4-oxa-1-pentyne (**73**) by independent synthesis (*vide infra*).

Sealed tube pyrolysis of 62 in toluene-d_8. The pyrolysis was performed as above, except deuterated toluene was used in place of nonane; the same results were obtained. No deuterium incorporation was observed (by NMR or GC-MS) in the product.

Catalytic reaction of 62. To a 100 mL round bottom flask fitted with a magnetic stirrer and West condenser was added 570 mg (1.30 mmol) of **62** in 50 mL HPLC-grade hexanes. Palladium(II) acetate (50 mg, 0.22 mmol) and 50 mg (0.36 mmol) 1,1,3,3-tetramethylbutyl isocyanide then were added and the reaction was heated to reflux overnight. After 14 hours,

GC-MS analysis indicated that all of the starting material was gone and an isomeric product had been formed. All attempts at isolating the product, including column chromatography, resulted in loss of all material, presumably due to decomposition. **GC-MS (EI)**: *m/z* (% relative intensity) 435 (M^+-Me, 2), 421 (M^+-Et, 4), 392 (59), 363 (86), 335 (46), 307 (34), 277 (8), 249 (28), 233 (28), 205 (24), 189 (5), 175 (100), 161 (56), 149 (29), 133 (93), 103 (100), 91 (27), 75 (22).

Synthesis of 5,5,5-triethyl-3,3-dimethyl-1-phenyl-5-germa-4-oxa-1-pentyne (73). Prior to use, the 3,3-dimethyl-1-phenyl-propyn-3-ol (**61**) was sublimed under reduced pressure (0.1 torr). The alcohol (1.35 g, 8.43 mmol) then was dissolved in 50 mL dry THF in a 100 mL 3-neck round bottom flask fitted with a West condenser, magnetic stir bar, and a rubber septum. The flask was cooled to -78 °C and 4.5 mL (8.55 mmol) of a 1.9 M solution of butyl lithium was added dropwise *via* syringe. The reaction was stirred for 2 hours, during which it was allowed to warm to room temperature. After cooling the flask back down to -78 °C, 1.63 g (8.35 mmol) chlorotriethylgermane (**71**) was added dropwise *via* syringe. The reaction was allowed to warm to room temperature while stirring overnight, after which 25 mL diethyl ether was added and the reaction was quenched with 25 mL saturated aqueous sodium chloride. The organic layer was washed thrice with 50 mL portions of water and then dried over anhydrous sodium sulfate. Filtration and removal of the solvent *in vacuo* yielded 2.05 g (77% yield) clear colorless liquid **73**. **^{1}H NMR** (400 MHz, CD_2Cl_2): δ 0.82-1.10 (m, 15 H, Ge-$C_2\underline{H}_5$), 1.54 (s, 6 H, OC-$C\underline{H}_3$), 7.31-7.43 (m, 5 H, aromatic); **^{13}C NMR** (100 MHz, CD_2Cl_2): δ 8.45 (Ge-$\underline{C}_2H_5$), 9.40 (Ge-$\underline{C}_2H_5$), 33.98 (OC-$\underline{C}H_3$), 67.51 (O-$\underline{C}$-Me_2), 82.53 ($\underline{C}$≡C), 96.84 (C≡$\underline{C}$), 124.02, 128.49, 128.75, 132.05; **GC-MS (EI)**: *m/z* (% relative intensity) 305 (M^+-Me, 14), 291 (M^+-Et, 35), 233 (100), 205 (29), 175 (28), 161 (27), 143 (27), 133 (29), 129 (42), 103 (30), 91 (26), 77 (14), 63 (4), 51 (6); **HRMS**: *m/z* 320.11999 (calc. for $C_{17}H_{26}OGe$ 320.11985).

Flow pyrolysis of 73. Flow pyrolysis was carried out at 507 °C on 70 mg (0.22 mmol) of **73** in 10 mL HPLC-grade hexanes. GC-MS analysis of the pyrolysate revealed only the presence of starting material; no decomposition was apparent.

Synthesis of 5,5,5-trimethyl-1-phenyl-5-sila-4-oxa-1-pentyne (78). The 3,3-dimethyl-1-phenyl-propyn-3-ol (**61**) was sublimed under reduced pressure (0.1 torr) prior to use. The alcohol (10.11 g, 63.10 mmol) then was dissolved in 150 mL dry THF in a 250 mL 2-neck round bottom flask fitted with a Friedrichs condenser, magnetic stir bar, and a rubber septum. Chlorotrimethylsilane (8.0 mL, 63 mmol) and imidazole (8.60 g, 126 mmol) were added and the reaction was stirred overnight. Diethyl ether (50 mL) was added to the reaction mixture, which then was quenched with 75 mL saturated aqueous sodium chloride. The aqueous layer was extracted with 50 mL diethyl ether. The organic layer was washed successively with water and saturated aqueous sodium chloride (100 mL each). The ether layers then were combined and dried over anhydrous sodium sulfate. Filtration and removal of the solvent *in vacuo* yielded 13.0 g of the title compound (89% yield). **^{1}H NMR** (400 MHz, CD_2Cl_2): δ 0.26 (s, 9 H, Si-C$\underline{H}_3$), 1.60 (s, 6 H, OC-C$\underline{H}_3$), 7.33-7.45 (m, 5 H, aromatic); **^{13}C NMR** (100 MHz, CD_2Cl_2): δ 2.20 (Si-$\underline{C}H_3$), 33.47 (OC-$\underline{C}H_3$), 67.51 (O-$\underline{C}$-Me_2), 83.41 ($\underline{C}$≡C), 95.04 (C≡$\underline{C}$), 123.69, 128.76, 128.94, 131.91; **GC-MS (EI)**: *m/z* (% relative intensity) 232 (M^+, 3), 217 (M^+-Me, 100), 201 (2), 159 (31), 143 (10), 141 (12), 128 (12), 115 (15), 102 (4), 89 (2), 91 (2), 75 (25), 73 (28), 63 (2), 61 (2), 59 (2); **HRMS**: *m/z* 232.12852 (calc. for $C_{14}H_{20}OSi$ 232.12834).

Flow pyrolysis of 78. Flow pyrolysis was carried out at 607 °C on 40 mg (0.17 mmol) of **78** in 10 mL HPLC-grade hexanes. GC-MS analysis of the pyrolysate revealed only the presence of starting material; no decomposition was apparent.

Sealed tube pyrolysis of hexaethyldigermane (42) and tolane (80). Hexaethyldigermane (50 mg, 0.16 mmol) and tolane (30 mg, 0.16 mmol) were dissolved in 1 mL nonane and sealed as described above in the pyrolysis tube. The tube then was heated to 200 °C for 18 hours. No reaction was observed by GC-MS; the starting materials were unchanged.

E. References

(1) Woodward, R. B.; Hoffmann, R. *Angew. Chem. Intern. Ed. Engl.* **1969**, *8*, 781-932.

(2) Woodward, R. B.; Hoffmann, R. *The Conservation of Orbital Symmetry*; Verlag Chemie: Weinheim, 1971.

(3) Barton, T. J. *Organosilicon Chemistry.* Dow Corning Corporate Lecture Series, Midland, MI, 1988.

(4) Fehér, F.; Plichta, P.; Guillery, R. *Inorg. Chem.* **1971**, *10*, 606-608.

(5) Casher, D. L.; Tsuji, H.; Sano, A.; Katkevics, M.; Toshimitsu, A.; Tamao, K.; Kubota, M.; Kobayashi, T.; Ottosson, C. H.; David, D. E.; Michl, J. *J. Phys. Chem. A* **2003**, *107*, 3559-3566.

(6) Silverstein, R. M.; Bassler, G. C.; Morrill, T. C. *Spectrometric Identification of Organic Compounds*; 5th ed.; Wiley: New York, 1991.

(7) Sharma, H. K.; Pannell, K. H. *Chem. Rev.* **1995**, *95*, 1351-1374.

(8) Horn, K. A. *Chem. Rev.* **1995**, *95*, 1317-1350.

(9) Sakurai, H.; Kamiyama, Y.; Nakadaira, Y. *J. Am. Chem. Soc.* **1975**, *97*, 931-932.

(10) Hayashi, T.; Kobayashi, T.-a.; Kawamoto, A. M.; Yamashita, H.; Tanaka, M. *Organometallics* **1990**, *9*, 280-281.

(11) Murakami, M.; Suginome, M.; Fujimoto, K.; Nakamura, H.; Andersson, P. G.; Ito, Y. *J. Am. Chem. Soc.* **1993**, *115*, 6487-6498.

(12) Ito, Y.; Suginome, M.; Murakami, M. *J. Org. Chem.* **1991**, *56*, 1948-1951.

(13) Suginome, M.; Oike, H.; Park, S.-S.; Ito, Y. *Bull. Chem. Soc. Jpn.* **1996**, *69*, 289-299.

(14) Yoshida, H.; Ikadai, J.; Shudo, M.; Ohshita, J.; Kunai, A. *J. Am. Chem. Soc.* **2003**, *125*, 6638-6639.

(15) Ma, Z. *Study of Additions of Disilanes to Acetylenes and Their Applications in Organic and Polymer Synthesis.* Ph.D. dissertation, Iowa State University, Ames, IA, 1998.

(16) Chen, Y. *The Addition of Disilanes to Cumulenes.* M.S. thesis, Iowa State University, Ames, IA, 1997.

(17) Serby, M. *Synthesis and Chemistry of Silicon and Acetylene Containing Compounds.* M.S. thesis, Iowa State University, Ames, IA, 2001.

(18) Ando, W.; Nakayama, N.; Kabe, Y.; Shimizu, T. *Tetrahedron Lett.* **1990**, *31*, 3597-3598.

(19) Sakurai, H.; Nakadaira, Y.; Hosomi, A.; Eriyama, Y.; Kabuto, C. *J. Am. Chem. Soc.* **1983**, *105*, 3359-3360.

(20) Pang, Y.; Schneider, A.; Barton, T. J.; Gordon, M. S.; Carroll, M. T. *J. Am. Chem. Soc.* **1992**, *114*, 4920-4921.

(21) Steinmetz, M. *Chem. Rev.* **1995**, *95*, 1527-1588.

(22) Tsumuraya, T.; Ando, W. *Organometallics* **1989**, *8*, 2286-2288.

(23) Hayashi, T.; Yamashita, H.; Sakakura, T.; Uchimaru, Y.; Tanaka, M. *Chem. Lett.* **1991**, 245-248.

(24) Mochida, K.; Hodota, C.; Yamashita, H.; Tanaka, M. *Chem. Lett.* **1992**, 1635-1638.

(25) Bulten, E. J.; Drenth, W. *J. Organomet. Chem.* **1973**, *61*, 179-190.

(26) Turro, N. J. *Modern Molecular Photochemistry*; University Science Books: Sausalito, 1991.

(27) Tamaki, T. *J. Phys. Chem.* **1983**, *87*, 2383-2386.

(28) Ijadi-Maghsoodi, S.; Pang, Y.; Barton, T. J. *J. Polym. Sci., Part A: Polym. Chem.* **1990**, *28*, 955-965.

(29) Lesbre, M.; Mazerolles, P.; Satgé, J. *The Organic Compounds of Germanium*; Wiley: New York, 1971.

(30) Sashida, H.; Yasuike, S. *J. Heterocyclic Chem.* **1998**, *35*, 725-726.

(31) Eaton, D. F. "Luminescence Spectroscopy" in *CRC Handbook of Organic Chemistry*; Scaiano, J. C., Ed.; CRC Press, Inc.: Boca Raton, 1989; Vol. I, pp 231-240.

(32) Sashida, H.; Sadamori, K.; Tsuchiya, T. *Synth. Commun.* **1998**, *28*, 713-727.

(33) Sakurai, H.; Tominaga, K.; Watanabe, T.; Kumada, M. *Tetrahedron Lett.* **1966**, *7*, 5493-5497.

(34) Petrich, S. *Thermal Isomerization and Decomposition of Ethynyldisilanes.* Ph.D. dissertation, Iowa State University, Ames, IA, 1992.

(35) Lin, J. *Synthesis and Study of Novel Silicon-Based Unsaturated Polymers.* Ph. D. dissertation, Iowa State University, Ames, IA, 1995.

(36) Vyazankin, N. S.; Razuvaev, G. A.; D'yachkovskaya, O. S. *J. Gen. Chem.* **1963**, *33*, 607-610.

(37) Sohrin, Y. *Anal. Chem.* **1991**, *63*, 811-814.

(38) Glockling, F.; Light, J. R. C. *J. Chem. Soc., A* **1968**, 717-734.

GENERAL CONCLUSIONS

The experiments described in this dissertation were undertaken in an effort to gain a better understanding of two areas of organogermanium chemistry: germacyclobutane thermochemistry and photo- and thermochemical additions of digermanes to acetylenes. In both studies, the organogermanium compounds underwent analogous reactions to those of their organosilicon counterparts in some cases. For example, germacyclobutane thermally decomposed *via* an initial 1,2-H shift, rather than the initial ring-cleavage observed for dimethylgermetane. Also, the first examples of photo- and thermochemical additions of digermanes to acetylenes have been demonstrated, though the mechanisms of these reactions have yet to be definitively established. It is clear from the results of these data that organogermanium chemistry is no less intriguing or stimulating than its more well-established predecessor, organosilicon chemistry.

APPENDIX A. ARRHENIUS PLOTS FROM SFR KINETICS

1. 4-germaspiro[3.3]heptane (spirodigermetane)

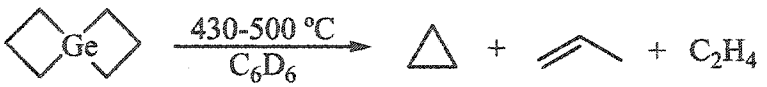

$E_a = 51.0 \pm 0.3$ kcal/mol
$\log A = 13.58 \pm 0.08$

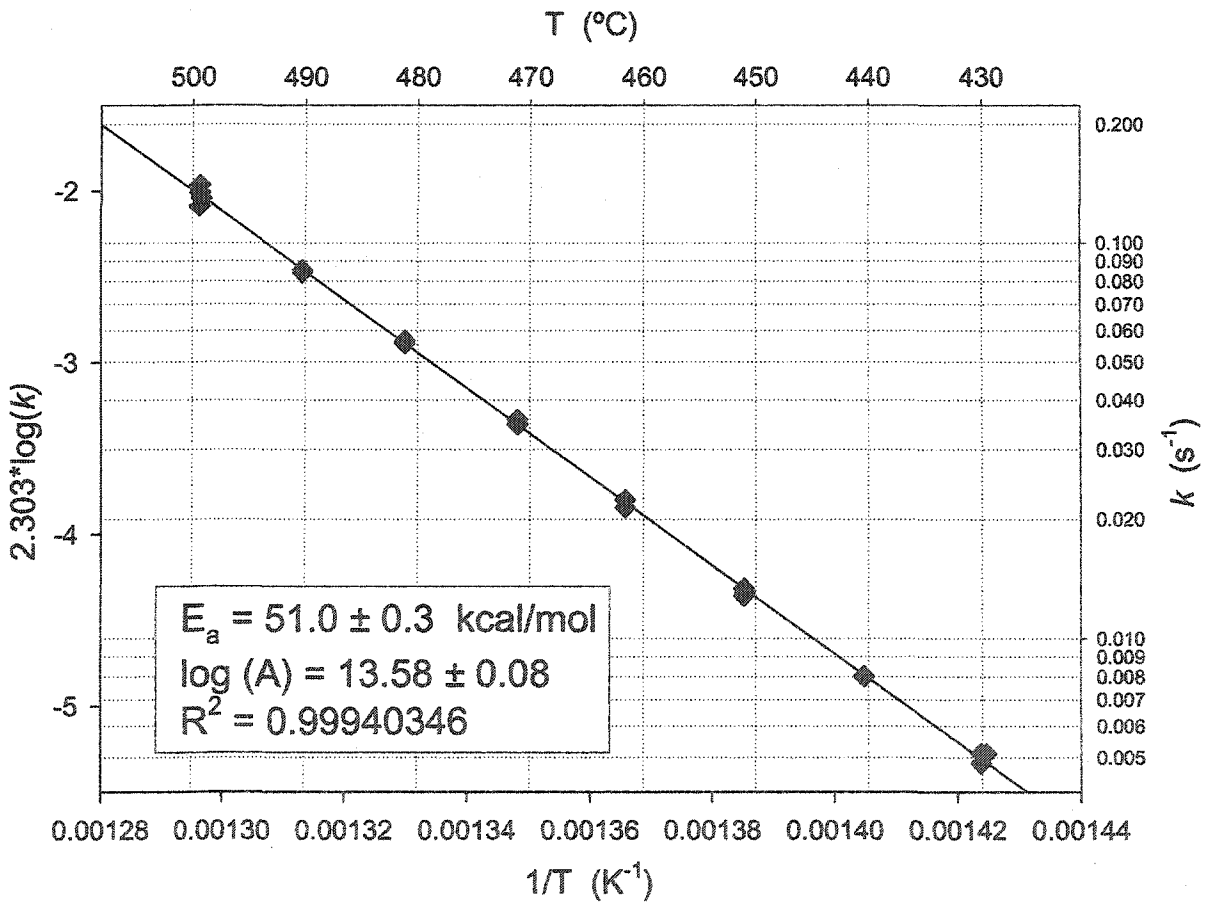

2. 1,1-dimethyl-1-germacyclobutane (dimethylgermetane)

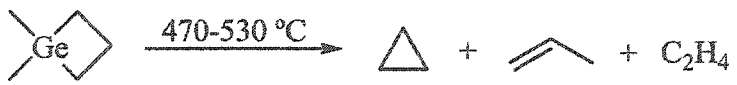

$E_a = 62.0 \pm 0.5$ kcal/mol
$\log A = 15.46 \pm 0.14$

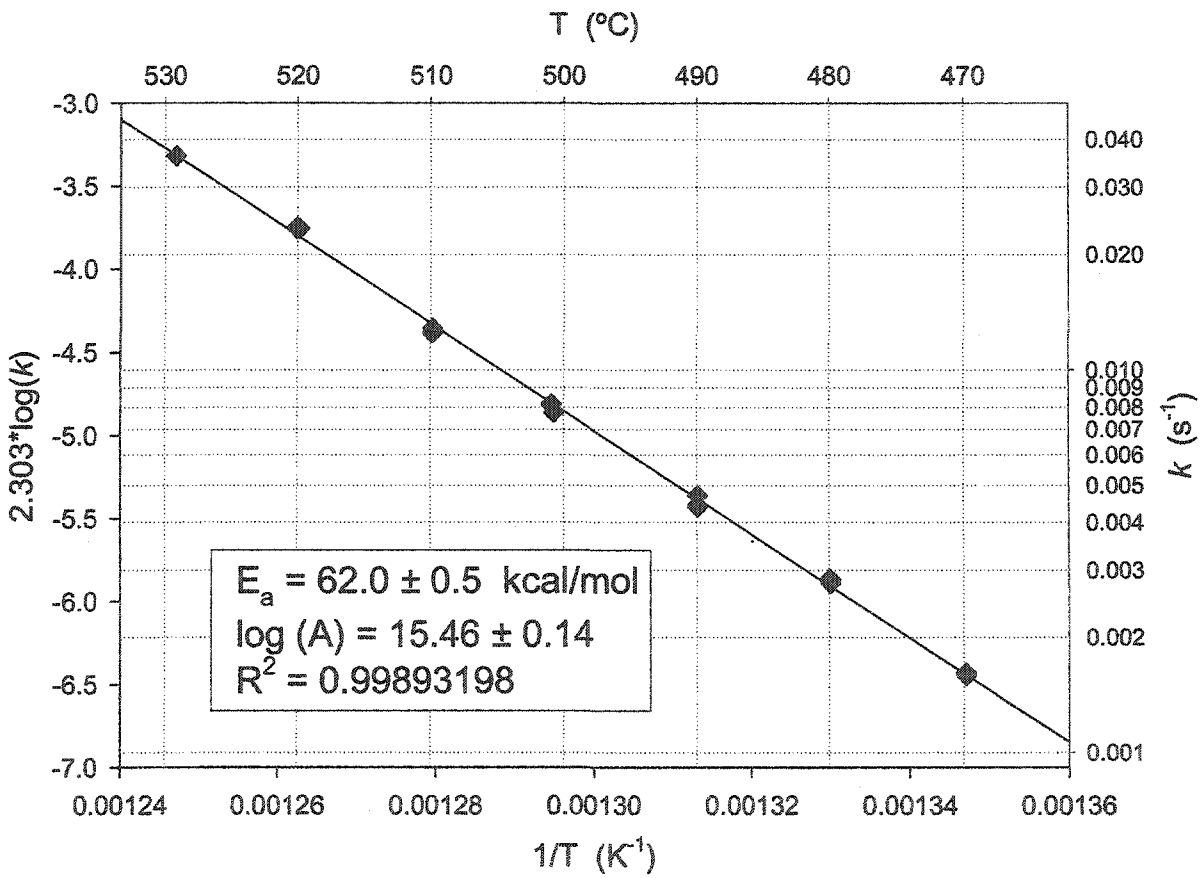

3. 1,1-diallyl-1-germacyclobutane (diallylgermetane)

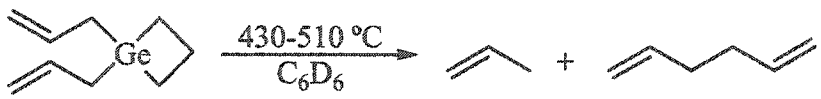

$E_a = 54.8 \pm 0.5$ kcal/mol
$\log A = 14.51 \pm 0.15$

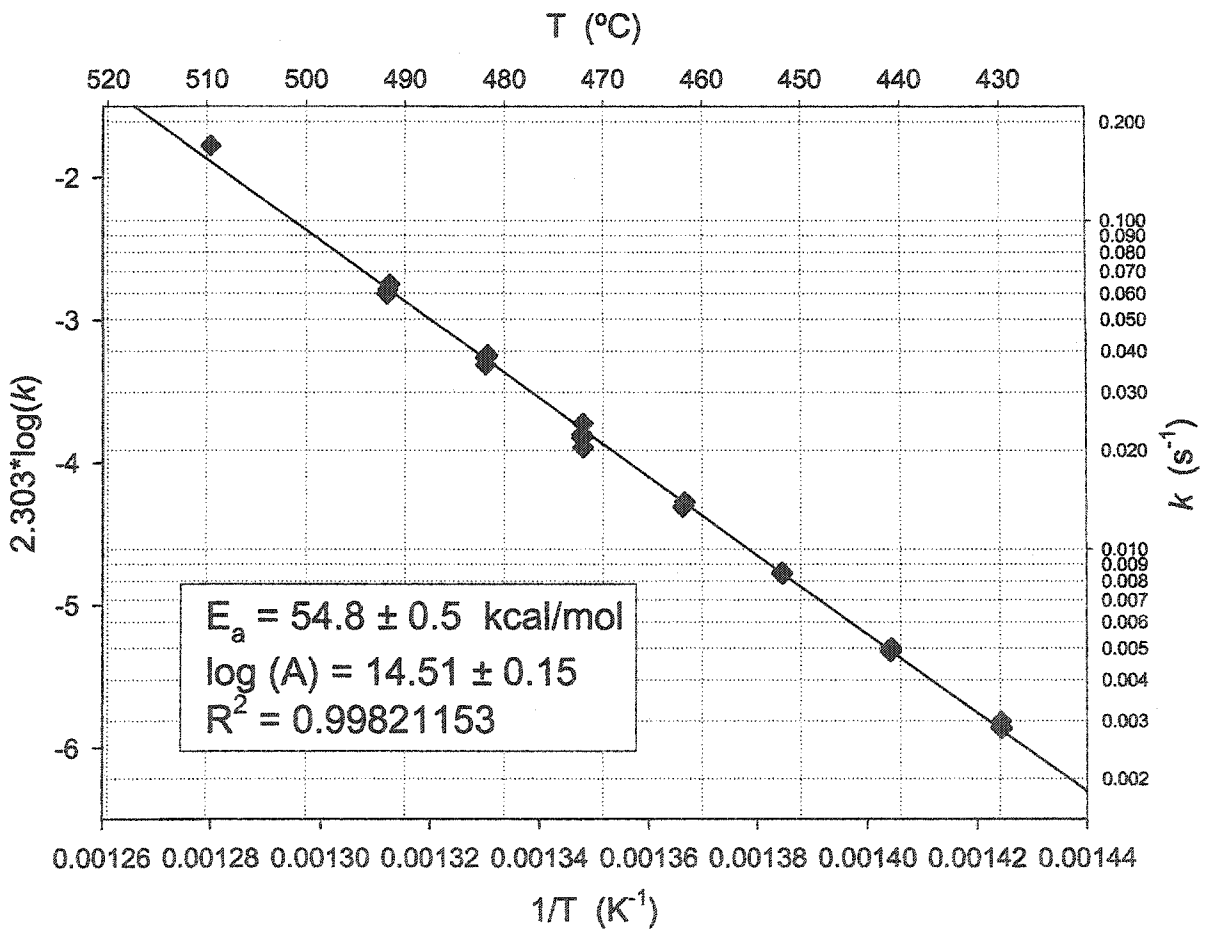

4. diallyldimethylgermane

$E_a = 52.7 \pm 1.4$ kcal/mol
$\log A = 13.8 \pm 0.4$

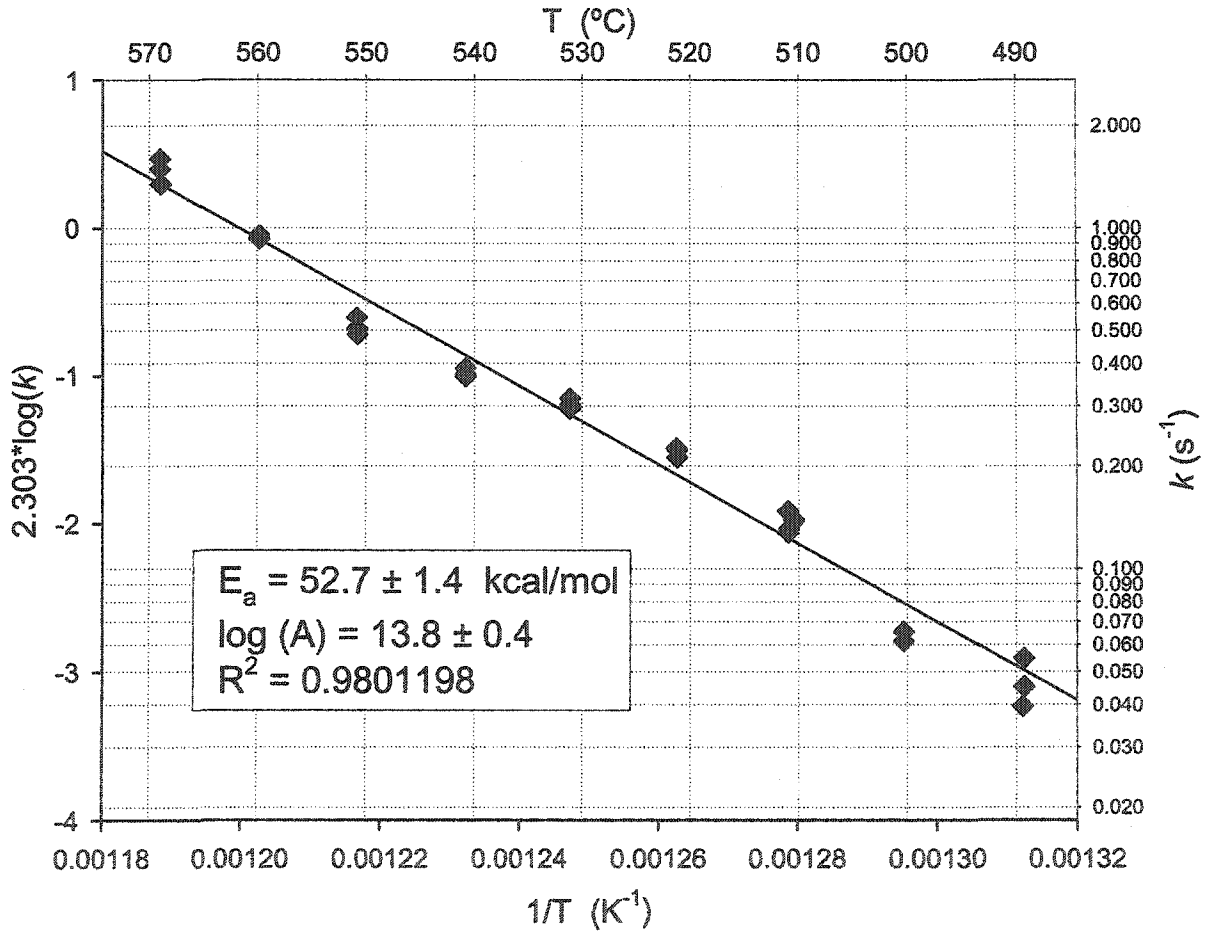

5. 1-germacyclobutane (germetane)

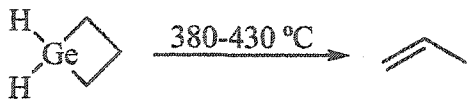

$E_a = 48.2 \pm 0.3$ kcal/mol
$\log A = 14.73 \pm 0.09$

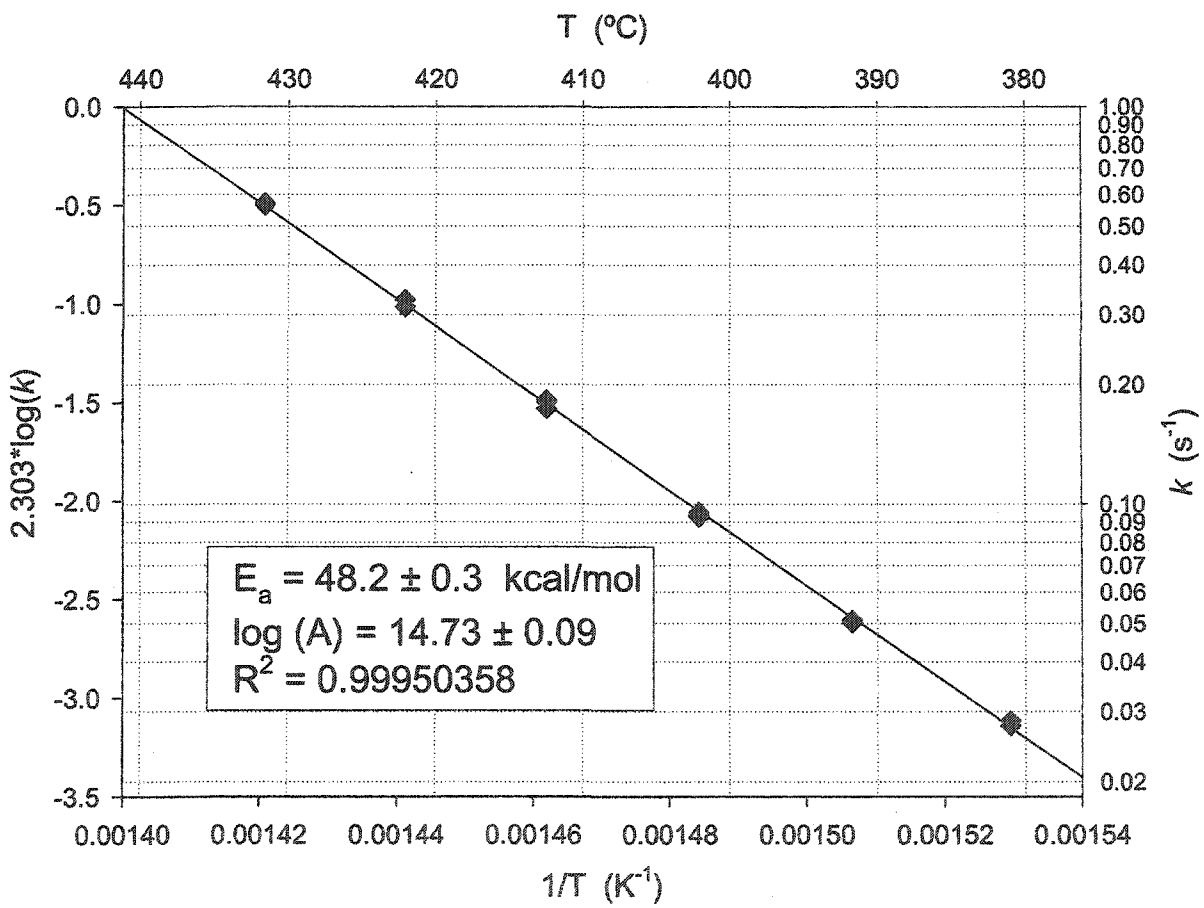

6. 1,1-dideuterio-1-germacyclobutane (germetane-*d*2)

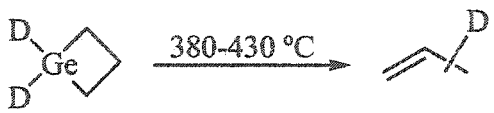

$E_a = 49.7 \pm 0.3$ kcal/mol
$\log A = 15.07 \pm 0.09$

$k_H/k_D = 1.57 \pm 0.04$ (at 410 °C)

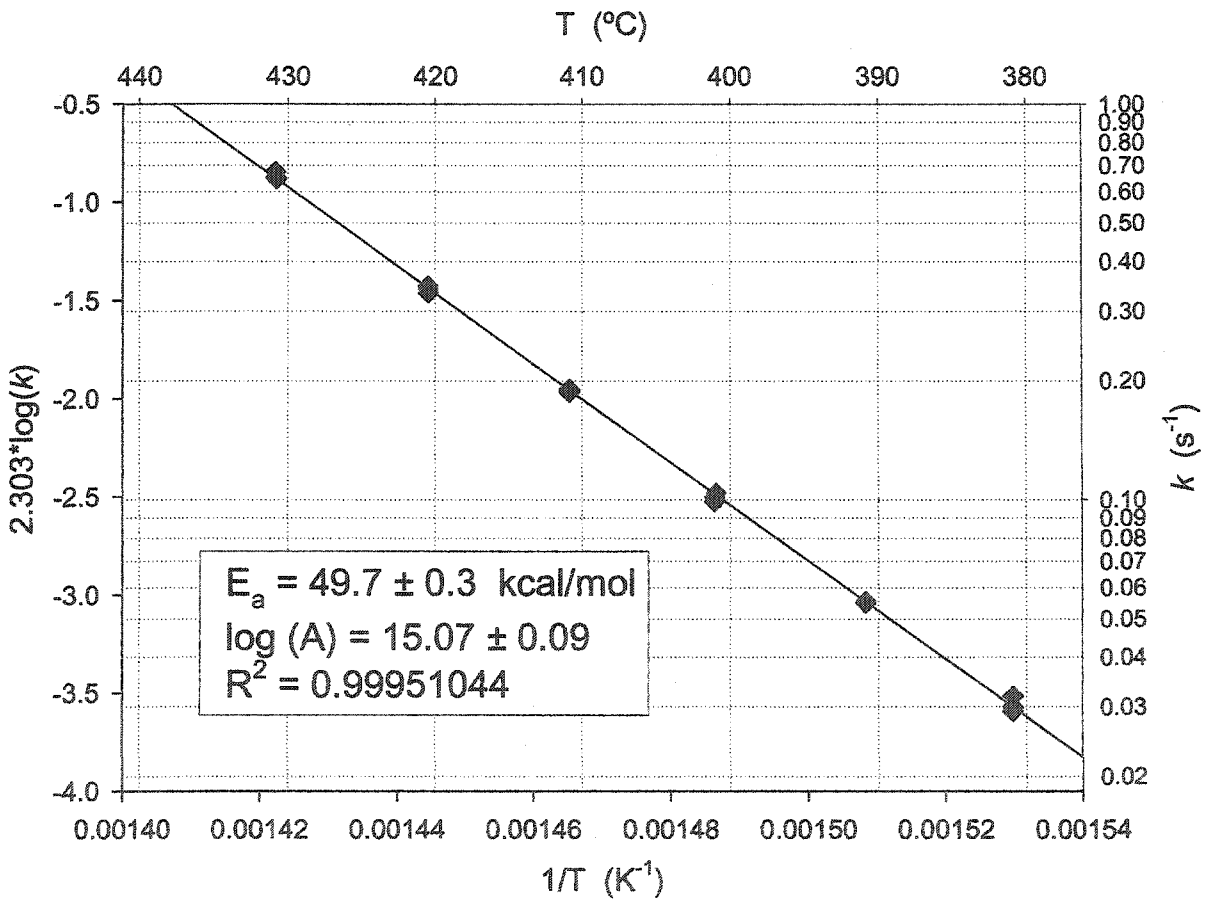

7. cyclopropane

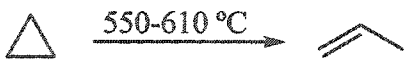

$E_a = 68.7 \pm 0.6$ kcal/mol
$\log A = 15.70 \pm 0.16$

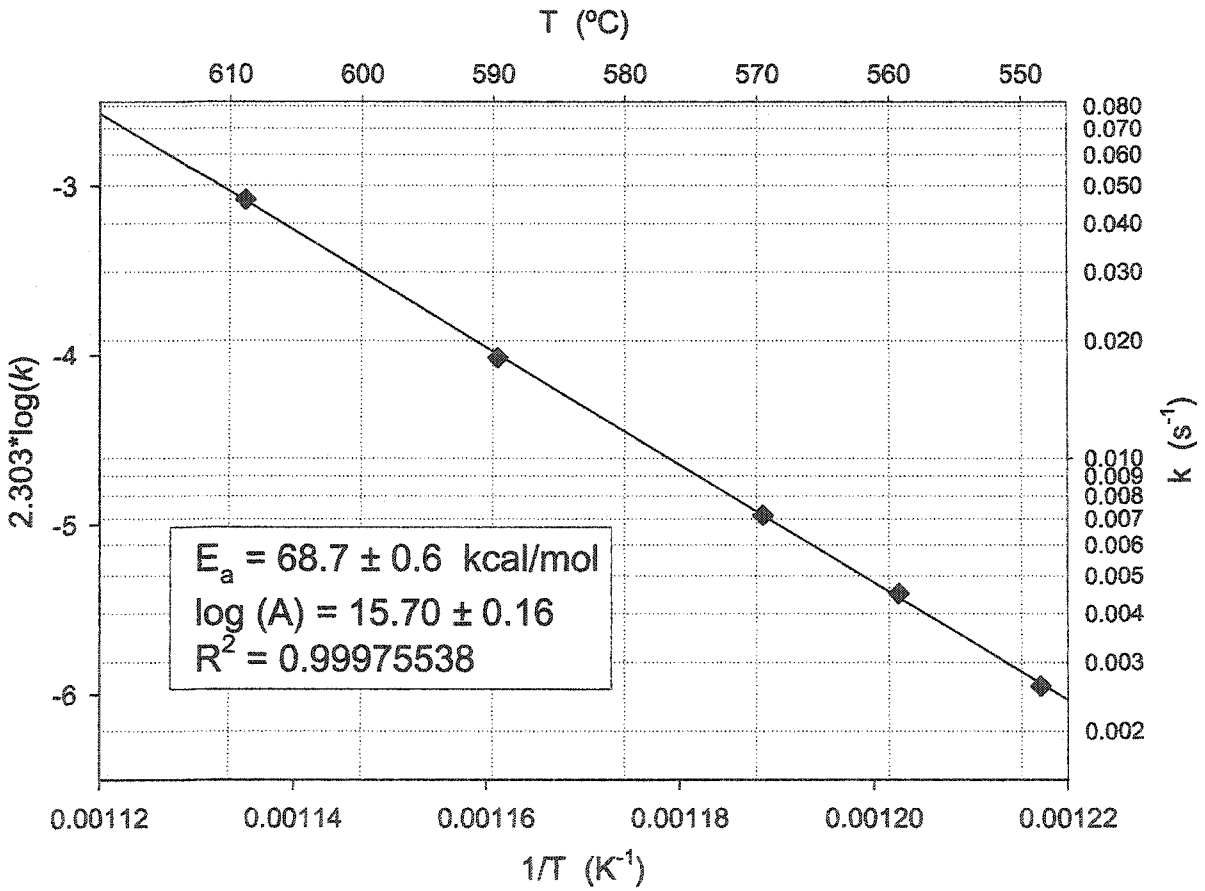

APPENDIX B. ISODESMIC REACTIONS

All calculations were carried out using the GAMESS program.[1] Geometry optimizations were performed at the Hartree-Fock (HF) level using the 6-31G* basis set. Single-point energies and zero-point energy (ZPE) corrections were calculated using second order Møller-Plesset perturbation theory (MP2) at the HF-optimized geometries (MP2//HF/6-31G*). Semiempirical calculations were performed with the HyperChem Release 4.5 for Windows program using the Austin Model 1 (AM1) method.[2-4] The results are summarized in Table 1. Balanced equations used in the determination of ring strain for each of the species follow the table.

Table 1. Results from *ab initio* and semiempirical calculations.

molecule	MP2 energy (hartrees/mol)	MP2 energy (kcal/mol)	ZPE (hartrees/mol)	ZPE (kcal/mol)	Final Energy (kcal/mol)
methane	-40.1951719022	-25222.8543	0.047772	29.977180	-25192.877116
ethane	-79.2287550012	-49716.80052	0.079758	50.048807	-49666.751716
germane	-2075.6179977988	-1302470.119	0.030757	19.300437	-1302450.818607
methylgermane	-2114.6684713873	-1326974.664	0.062912	39.477776	-1326935.186438
germetane	-2191.5493237228	-1375218.133	0.104121	65.336749	-1375152.796639
spirodigermetane	-2307.4850426452	-1447968.904	0.176349	110.660747	-1447858.243634
dimethylgermetane	-2269.6536291558	-1424229.331	0.166612	104.550938	-1424124.780129
methylgermetane	-2230.6019259129	-1399724.014	0.135659	85.127237	-1399638.887039

molecule	AM1 energy (kcal/mol)	HF E (hartrees/mol)	HF E (kcal/mol)
methane	-4225.4898901	-40.1951719022	-25222.8543
ethane	-7821.0053492	-79.2287550012	-49716.80052
germane	-3135.2451990	-2075.6179977988	-1302470.119
methylgermane	-6735.9796997	-2114.6684713873	-1326974.664
germetane	-13284.6640977	-2191.5493237226	-1375218.133
spirodigermetane	-23430.0884319	-2307.4850426446	-1447968.904
dimethylgermetane	-20484.5940995	-2269.6536291558	-1424229.331
methylgermetane	-16884.7042713	-2230.6019259129	-1399724.014

	Ring Strain	
	MP2//HF/6-31G* (kcal/mol)	AM1 (kcal/mol)
germetane	-21.63	-17.59
spirodigermetane	-39.79	-39.18
dimethylgermetane	-18.38	-19.13
methylgermetane	-19.91	-18.29

1. 1-germacyclobutane

2. 1-methyl-1-germacyclobutane

3. 1,1-dimethyl-1-germacyclobutane

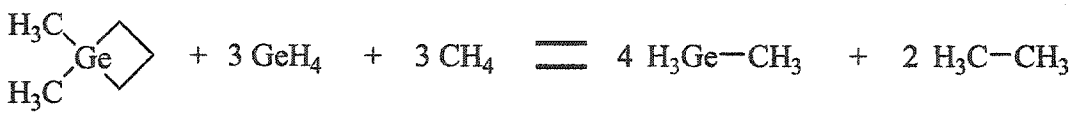

4. 4-germaspiro[3.3]heptane (spirodigermetane)

APPENDIX C. SPECIAL APPARATUS

1. allyl chloride Direct Process reactor

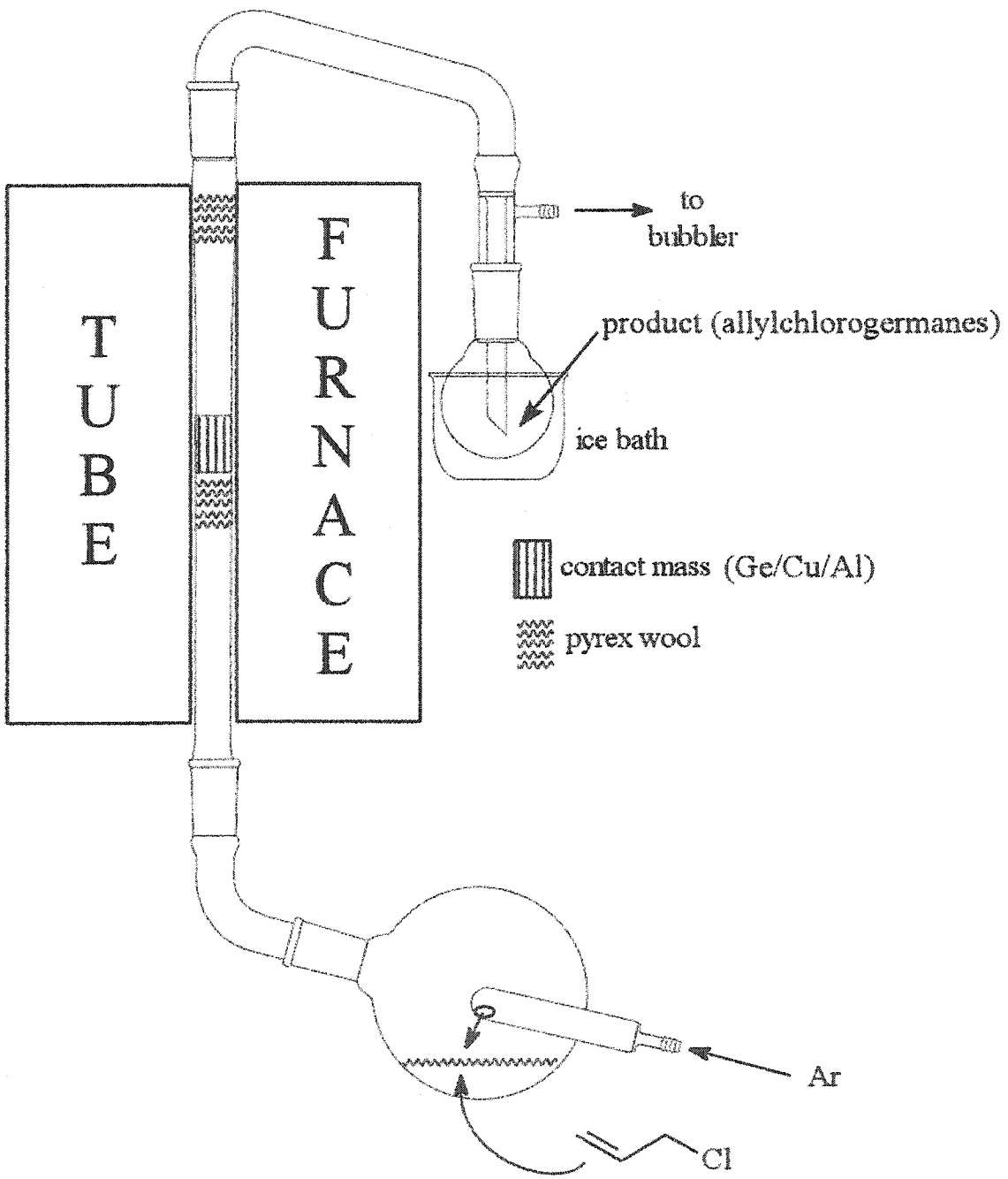

2. extraction apparatus for dichlorogermetane

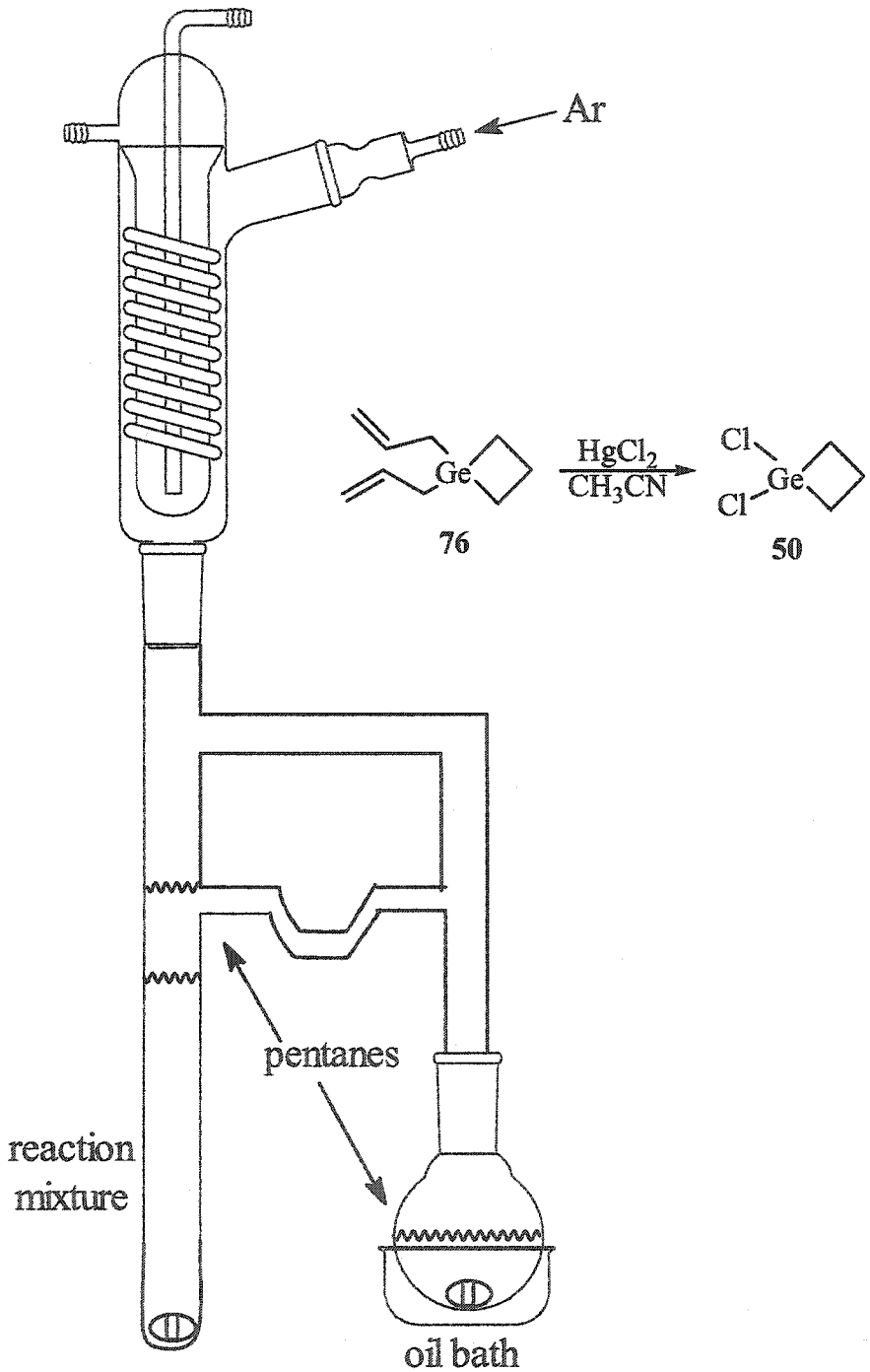

APPENDIX D. CRYSTAL STRUCTURE DATA

1. 5,5,6,6,13,13,14,14-octaethyl-5,6,13,14-tetragermatetrabenzo[c,g,k,o]-cyclohexadecyne (46). A colorless crystal with approximate dimensions 0.7 x 0.7 x 0.5 mm^3 was selected under ambient conditions. The crystal was mounted and centered in the X-ray beam by using a video camera. The crystal evaluation and data collection were performed at 293K on a Bruker CCD-1000 diffractometer with Mo K_α (λ = 0.71073 Å) radiation and the detector to crystal distance of 5.03 cm.

The initial cell constants were obtained from three series of ω scans at different starting angles. Each series consisted of 30 frames collected at intervals of 0.3° in a 10° range about ω with the exposure time of 15 seconds per frame. A total of 69 reflections were obtained. The reflections were successfully indexed by an automated indexing routine built in the SMART program. The final cell constants were calculated from a set of 1289 strong reflections from the actual data collection.

The data were collected using the hemi-sphere routine. A total of 12096 data were harvested by collecting four sets of frames with 0.3° scans in ω with an exposure time 15 sec per frame. This dataset was corrected for Lorentz and polarization effects. The absorption correction was based on fitting a function to the empirical transmission surface as sampled by multiple equivalent measurements[5] using SADABS software. All software and sources of the scattering factors are contained in the SHELXTL (version 5.1) program library (G. Sheldrick, Bruker Analytical X-Ray Systems, Madison, WI).

The systematic absences in the diffraction data were consistent for the space groups *C2/c* yielded chemically reasonable and computationally stable results of refinement. The positions of non-hydrogen atoms were found by direct methods. All non-hydrogen atoms were refined in full-matrix anisotropic approximation. All hydrogen atoms were placed in the structure factor calculation at idealized positions and were allowed to ride on the neighboring atoms with relative isotropic displacement coefficients. Final least-squares refinement of 218 parameter against 4390 independent reflections converged to R (based on F^2 for $I \geq 2\sigma$) and wR (based on F^2 for $I \geq 2\sigma$) of 0.040 and 0.102, respectively. The asymmetric unit of the

crystal cell contains a half of the centrosymmetrical molecule (Z=4). The ORTEP diagram with atom numbering was drawn at 50% probability level.

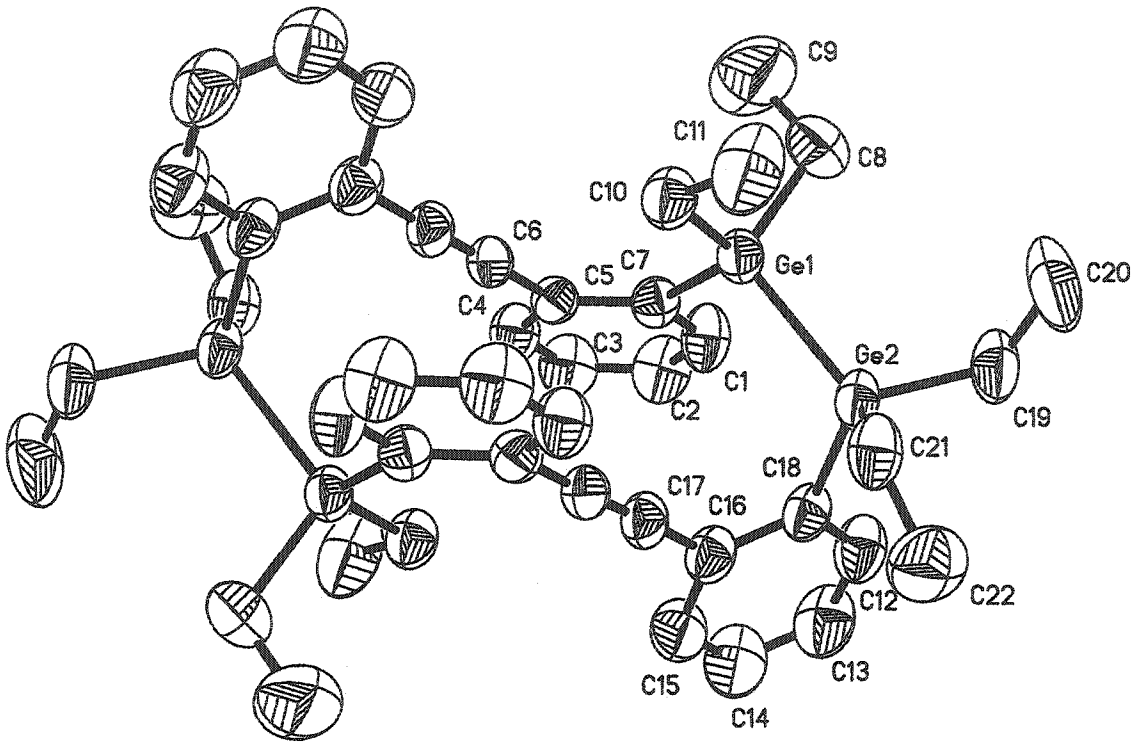

Figure 1. ORTEP of **46** (hydrogens omitted for clarity).

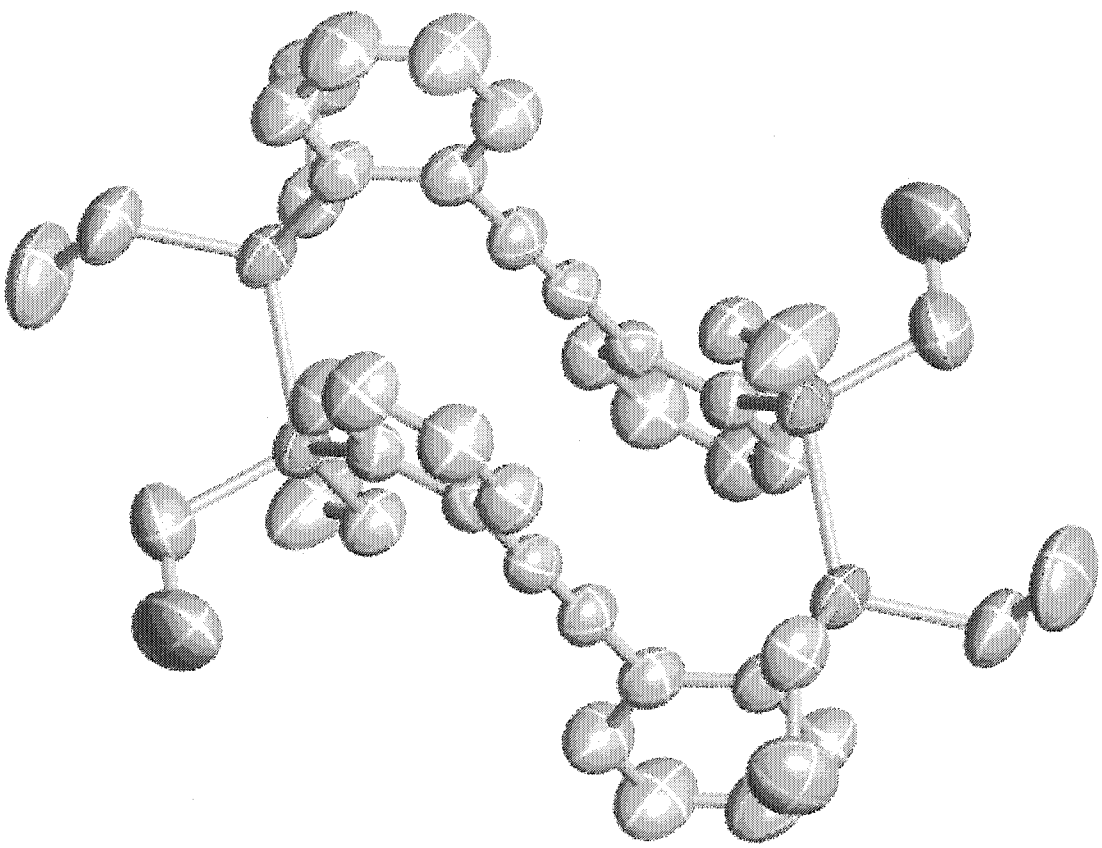

Figure 2. 3-D ORTEP of **46** (hydrogens omitted for clarity and Ge colored green).

Table 2. Crystal data and structure refinement for **46**.

Empirical formula	$C_{44}H_{56}Ge_4$	
Formula weight	875.25	
Temperature	298(2) K	
Wavelength	0.71073 Å	
Crystal system	Monoclinic	
Space group	C2/c	
Unit cell dimensions	a = 20.189(4) Å	α = 90°
	b = 13.424(3) Å	β = 106.054(4)°
	c = 16.566(3) Å	γ = 90°
Volume	4314.5(16) $Å^3$	
Z	4	
Density (calculated)	1.347 Mg/m^3	
Absorption coefficient	2.787 mm^{-1}	
F(000)	1792	
Crystal size	0.70 x 0.50 x 0.50 mm^3	
Theta range for data collection	1.84 to 26.34°.	
Index ranges	-20<=h<=25, -16<=k<=10, -20<=l<=20	
Reflections collected	12096	
Independent reflections	4390 [R(int) = 0.0392]	
Completeness to theta = 26.34°	99.6 %	
Absorption correction	Empirical	
Max. and min. transmission	0.38 and 0.30	
Refinement method	Full-matrix least-squares on F^2	
Data / restraints / parameters	4390 / 0 / 218	
Goodness-of-fit on F^2	0.986	
Final R indices [I>2sigma(I)]	R1 = 0.0399, wR2 = 0.1022	
R indices (all data)	R1 = 0.0627, wR2 = 0.1149	
Extinction coefficient	0.0074(3)	
Largest diff. peak and hole	0.650 and -0.805 $e.Å^{-3}$	

$R1 = \Sigma \, | \, |F_o| - |F_c| \, | \, / \, \Sigma \, |F_o|$ and $wR2 = \{ \, \Sigma \, [\, w(F_o^2 - F_c^2)^2 \,] \, / \, \Sigma \, [\, w(F_o^2)^2 \,] \, \}^{1/2}$

Table 3. Atomic coordinates (x 10^4) and equivalent isotropic displacement parameters ($Å^2$x 10^3) for **46**. U(eq) is defined as one third of the trace of the orthogonalized U_{ij} tensor.

Atom	X	Y	Z	U(eq)
Ge(1)	4067(1)	2980(1)	10275(1)	49(1)
Ge(2)	4186(1)	2123(1)	9019(1)	51(1)
C(1)	3481(2)	4658(3)	9271(2)	66(1)
C(2)	3041(2)	5422(3)	8927(3)	75(1)
C(3)	2468(2)	5583(3)	9197(3)	73(1)
C(4)	2335(2)	4982(3)	9799(2)	61(1)
C(5)	2772(2)	4195(2)	10151(2)	45(1)
C(6)	2602(2)	3588(3)	10790(2)	49(1)
C(7)	3361(2)	4020(2)	9881(2)	47(1)
C(8)	4914(2)	3740(4)	10791(3)	85(1)
C(9)	4812(4)	4525(6)	11392(4)	166(3)
C(10)	3925(2)	2064(3)	11136(2)	61(1)
C(11)	4466(3)	1250(4)	11325(3)	107(2)
C(12)	3582(2)	3161(3)	7423(2)	69(1)
C(13)	3058(2)	3528(4)	6762(3)	85(1)
C(14)	2384(3)	3356(4)	6736(3)	89(1)
C(15)	2228(2)	2824(3)	7363(3)	71(1)
C(16)	2750(2)	2446(3)	8040(2)	55(1)
C(17)	2567(2)	1882(3)	8684(2)	51(1)
C(18)	3450(2)	2612(3)	8071(2)	53(1)
C(19)	5074(2)	2448(4)	8813(3)	76(1)
C(20)	5692(2)	2009(4)	9438(4)	112(2)
C(21)	4126(2)	670(3)	8996(2)	66(1)
C(22)	3999(3)	263(4)	8110(3)	98(2)

Table 4. Bond lengths for **46**. Symmetry transformation #1: -x+1/2,-y+1/2,-z+2.

Bond	Length (Å)
Ge(1)-C(10)	1.963(4)
Ge(1)-C(8)	1.971(4)
Ge(1)-C(7)	1.974(3)
Ge(1)-Ge(2)	2.4466(6)
Ge(2)-C(18)	1.954(4)
Ge(2)-C(21)	1.954(4)
Ge(2)-C(19)	1.964(4)
C(1)-C(2)	1.372(5)
C(1)-C(7)	1.395(5)
C(2)-C(3)	1.369(5)
C(3)-C(4)	1.365(5)
C(4)-C(5)	1.397(5)
C(5)-C(7)	1.401(4)
C(5)-C(6)	1.450(5)
C(6)-C(17)#1	1.199(4)
C(8)-C(9)	1.502(7)
C(10)-C(11)	1.516(5)
C(12)-C(18)	1.387(5)
C(12)-C(13)	1.385(6)
C(13)-C(14)	1.369(6)
C(14)-C(15)	1.368(6)
C(15)-C(16)	1.404(5)
C(16)-C(18)	1.417(5)
C(16)-C(17)	1.438(5)
C(17)-C(6)#1	1.199(4)
C(19)-C(20)	1.504(6)
C(21)-C(22)	1.521(6)

Table 5. Bond angles for **46**. Symmetry transformation #1: -x+1/2,-y+1/2,-z+2.

Atoms	Bond Angle
C(10)-Ge(1)-C(8)	107.02(19)
C(10)-Ge(1)-C(7)	116.48(14)
C(8)-Ge(1)-C(7)	103.73(17)
C(10)-Ge(1)-Ge(2)	113.09(11)
C(8)-Ge(1)-Ge(2)	109.57(14)
C(7)-Ge(1)-Ge(2)	106.44(9)
C(18)-Ge(2)-C(21)	106.92(17)
C(18)-Ge(2)-C(19)	108.30(17)
C(21)-Ge(2)-C(19)	105.87(18)
C(18)-Ge(2)-Ge(1)	107.10(10)
C(21)-Ge(2)-Ge(1)	117.72(11)
C(19)-Ge(2)-Ge(1)	110.59(15)
C(2)-C(1)-C(7)	122.6(3)
C(3)-C(2)-C(1)	119.3(4)
C(2)-C(3)-C(4)	120.0(4)
C(3)-C(4)-C(5)	121.5(3)
C(4)-C(5)-C(7)	119.1(3)
C(4)-C(5)-C(6)	118.7(3)
C(7)-C(5)-C(6)	122.2(3)
C(17)#1-C(6)-C(5)	176.6(3)
C(1)-C(7)-C(5)	117.4(3)
C(1)-C(7)-Ge(1)	114.8(2)
C(5)-C(7)-Ge(1)	127.7(2)
C(9)-C(8)-Ge(1)	112.9(3)
C(11)-C(10)-Ge(1)	111.1(3)
C(18)-C(12)-C(13)	122.2(4)
C(14)-C(13)-C(12)	120.0(4)
C(15)-C(14)-C(13)	120.0(4)
C(14)-C(15)-C(16)	121.0(4)
C(15)-C(16)-C(18)	119.5(3)
C(15)-C(16)-C(17)	119.5(3)
C(18)-C(16)-C(17)	121.0(3)

Table 5. Bond angles for **46.** (continued)

Atoms	Bond Angle
C(6)#1-C(17)-C(16)	178.5(4)
C(12)-C(18)-C(16)	117.3(3)
C(12)-C(18)-Ge(2)	122.3(3)
C(16)-C(18)-Ge(2)	120.4(2)
C(20)-C(19)-Ge(2)	114.6(3)
C(22)-C(21)-Ge(2)	111.7(3)

Table 6. Anisotropic displacement parameters ($Å^2 x\ 10^3$) for **46.** The anisotropic displacement factor exponent takes the form: $-2\pi^2[h^2\ a^{*2}U_{11} + ... + 2\ h\ k\ a^*\ b^*\ U_{12}]$.

Atom	U_{11}	U_{22}	U_{33}	U_{23}	U_{13}	U_{12}
Ge(1)	42(1)	57(1)	51(1)	3(1)	16(1)	6(1)
Ge(2)	47(1)	60(1)	53(1)	8(1)	24(1)	14(1)
C(1)	69(2)	59(2)	81(3)	15(2)	41(2)	7(2)
C(2)	91(3)	57(2)	85(3)	18(2)	36(2)	8(2)
C(3)	79(3)	58(2)	81(3)	15(2)	23(2)	17(2)
C(4)	58(2)	58(2)	70(2)	3(2)	24(2)	12(2)
C(5)	45(2)	45(2)	46(2)	-5(1)	13(1)	2(1)
C(6)	41(2)	55(2)	51(2)	-6(2)	14(2)	8(2)
C(7)	49(2)	40(2)	54(2)	-5(1)	17(2)	-1(1)
C(8)	56(2)	107(4)	85(3)	-4(3)	11(2)	-13(2)
C(9)	163(6)	215(8)	134(5)	-85(6)	64(5)	-101(6)
C(10)	59(2)	68(2)	58(2)	9(2)	21(2)	13(2)
C(11)	117(4)	131(5)	84(3)	53(3)	46(3)	64(4)
C(12)	72(3)	76(3)	66(2)	18(2)	34(2)	16(2)
C(13)	93(3)	103(4)	68(3)	33(2)	35(2)	24(3)
C(14)	87(3)	109(4)	69(3)	36(3)	21(2)	36(3)
C(15)	61(2)	90(3)	62(2)	14(2)	16(2)	19(2)
C(16)	57(2)	60(2)	50(2)	4(2)	19(2)	15(2)
C(17)	44(2)	60(2)	52(2)	3(2)	18(2)	12(2)
C(18)	59(2)	54(2)	51(2)	6(2)	24(2)	15(2)

Table 6. Anisotropic displacement parameters **46.** (continued)

Atom	U_{11}	U_{22}	U_{33}	U_{23}	U_{13}	U_{12}
C(19)	62(3)	95(3)	86(3)	10(3)	43(2)	10(2)
C(20)	54(3)	153(6)	136(5)	29(4)	38(3)	27(3)
C(21)	63(2)	59(2)	85(3)	7(2)	33(2)	21(2)
C(22)	109(4)	82(3)	98(3)	-14(3)	21(3)	21(3)

Table 7. Hydrogen coordinates (x 10^4) and isotropic displacement parameters ($Å^2$x 10^3) for **46.**

Atom	X	Y	Z	U(eq)
H(1)	3873	4561	9090	79
H(2)	3132	5826	8514	90
H(3)	2169	6102	8971	87
H(4)	1944	5100	9978	73
H(8A)	5271	3283	11088	102
H(8B)	5072	4055	10351	102
H(9A)	5238	4870	11625	249
H(9B)	4665	4216	11836	249
H(9C)	4467	4989	11099	249
H(10A)	3947	2433	11646	73
H(10B)	3471	1766	10942	73
H(11A)	4386	815	11749	160
H(11B)	4915	1544	11523	160
H(11C)	4439	875	10823	160
H(12)	4037	3286	7432	82
H(13)	3164	3891	6336	102
H(14)	2032	3600	6291	107
H(15)	1769	2711	7342	86
H(19A)	5067	2215	8257	92
H(19B)	5125	3167	8818	92
H(20A)	6103	2197	9292	168
H(20B)	5653	1296	9432	168

Table 7. Hydrogen coordinates and isotropic displacement parameters for **46**. (continued)

Atom	X	Y	Z	U(eq)
H(20C)	5714	2253	9990	168
H(21A)	4552	394	9350	80
H(21B)	3754	462	9224	80
H(22A)	3973	-450	8122	147
H(22B)	4371	458	7887	147
H(22C)	3574	526	7761	147

2. 3,3,3',3'-tetraethyl-3,3'-digermaindeno[2,1-*a*]indene (47). A large colorless prism crystal with approximate dimensions 0.48 x 0.42 x 0.22 mm^3 was selected under ambient conditions. The crystal was mounted and centered in the X-ray beam by using a video camera. The rotation photo at room temperature was obtained and cell dimensions were found. Crystal was cooled to –20C, however rotation photo shown the decomposition of the crystal, therefore the crystal evaluation and data collection were performed at 298 K on a Bruker CCD-1000 diffractometer with Mo K_α (λ = 0.71073 Å) radiation and the detector to crystal distance of 5.03 cm.

The initial cell constants were obtained from three series of ω scans at different starting angles. Each series consisted of 30 frames collected at intervals of 0.3° in a 10° range about ω with the exposure time of 10 seconds per frame. A total of 41 reflections was obtained. The reflections were successfully indexed by an automated indexing routine built in the SMART program. The final cell constants were calculated from a set of 850 strong reflections from the actual data collection.

The data were collected using the hemi-sphere routine. A total of 3636 data were harvested by collecting four sets of frames with 0.3° scans in ω with an exposure time 10 sec per frame. This dataset was corrected for Lorentz and polarization effects. The absorption correction was based on fitting a function to the empirical transmission surface as sampled by multiple equivalent measurements[5] using SADABS software.[6]

The systematic absences in the diffraction data were consistent for the space groups *P*21/c [2] yielded chemically reasonable and computationally stable results of refinement.

The positions of almost all non-hydrogen atoms were found by the direct methods. The remaining atoms were located in an alternating series of least-squares cycles and difference Fourier maps. All non-hydrogen atoms were refined in full-matrix anisotropic approximation including disordered by two equivalent positions C11 atom. All hydrogen atoms were placed in the structure factor calculation at idealized positions and were allowed to ride on the neighboring atoms with relative isotropic displacement coefficients. Final least-squares refinement of 119 parameters against 1462 independent reflections converged to R (based on F^2 for $I \geq 2\sigma$) and wR (based on F^2 for $I \geq 2\sigma$) of 0.068 and 0.18, respectively.

The ORTEP diagram was drawn at 50% probability level. Hydrogen atoms and one of two disordered positions for C11 atom have been omitted for clarity.

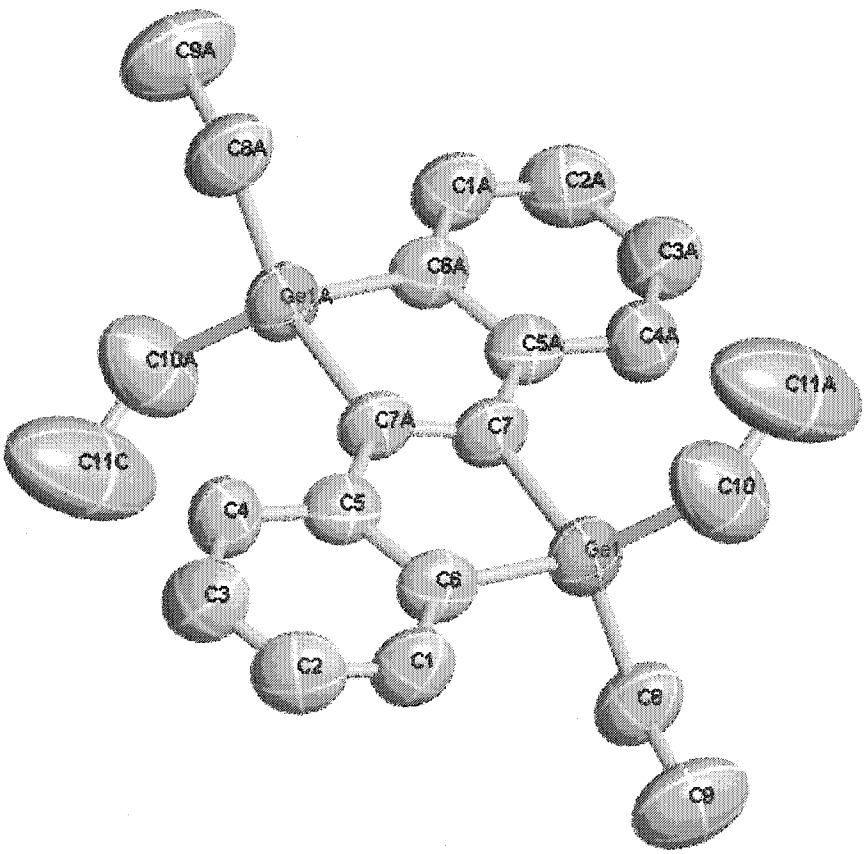

Figure 3. 3-D ORTEP of **47** (hydrogens omitted for clarity).

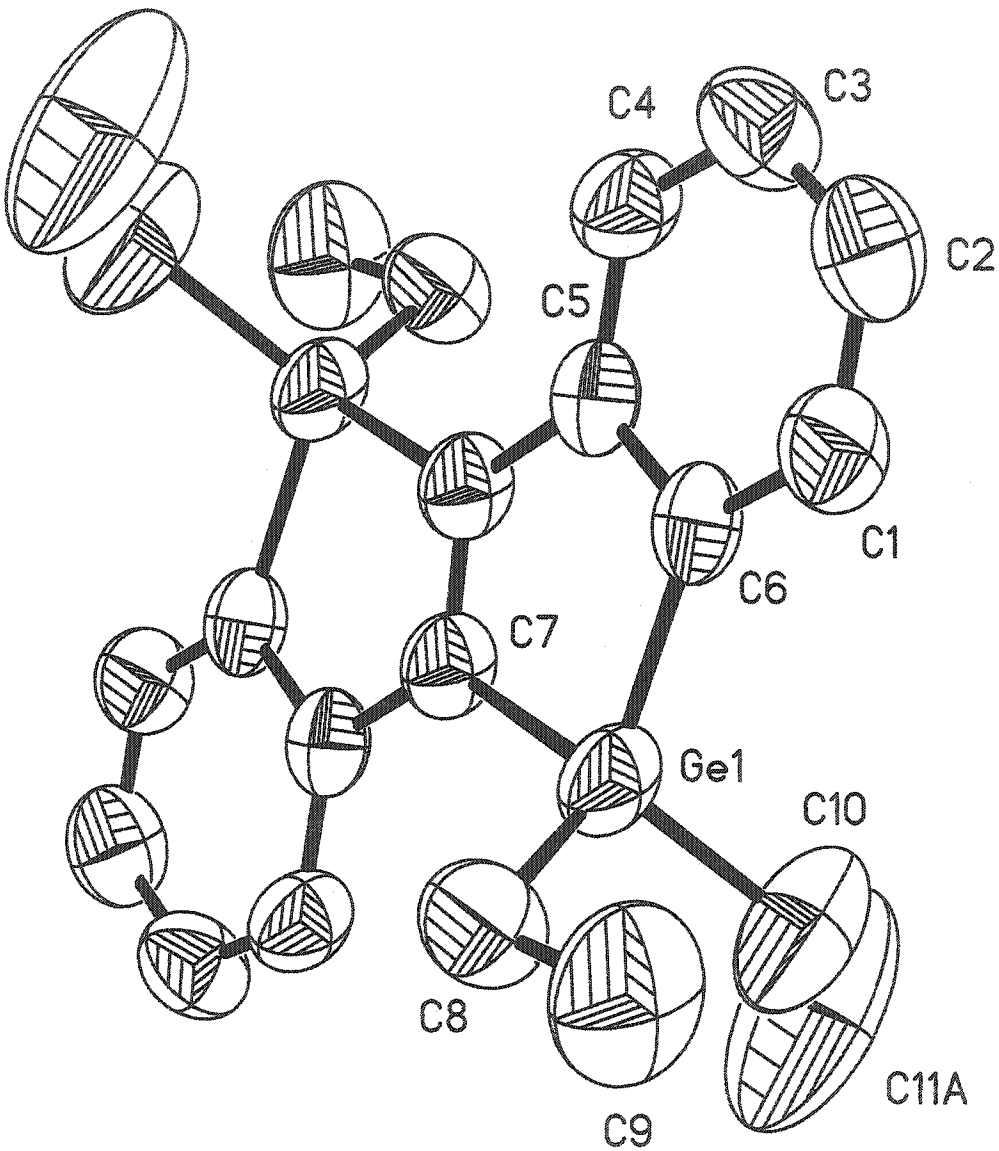

Figure 4. ORTEP of **47** (hydrogens omitted for clarity).

Table 8. Crystal data and structure refinement for 47.

Empirical formula	$C_{22}H_{28}Ge_2$	
Formula weight	437.62	
Temperature	298(2) K	
Wavelength	0.71073 Å	
Crystal system	Monoclinic	
Space group	P2(1)/c	
Unit cell dimensions	a = 10.323(4) Å	α = 90°
	b = 7.502(3) Å	β = 108.886(6)°
	c = 14.564(5) Å	γ = 90°
Volume	1067.1(7) $Å^3$	
Z	2	
Density (calculated)	1.362 Mg/m^3	
Absorption coefficient	2.817 mm^{-1}	
F(000)	448	
Crystal size	0.48 x 0.42 x 0.28 mm^3	
Theta range for data collection	2.09 to 23.26°.	
Index ranges	-11<=h<=11, -7<=k<=8, -16<=l<=16	
Reflections collected	3636	
Independent reflections	1462 [R(int) = 0.0519]	
Completeness to theta = 26.34°	95.2 %	
Absorption correction	Empirical	
Max. and min. transmission	0.60 and 0.35	
Refinement method	Full-matrix least-squares on F^2	
Data / restraints / parameters	1462 / 0 / 119	
Goodness-of-fit on F^2	1.075	
Final R indices [I>2sigma(I)]	R1 = 0.0680, wR2 = 0.1803	
R indices (all data)	R1 = 0.0807, wR2 = 0.1913	
Largest diff. peak and hole	0.827 and -0.899 $e.Å^{-3}$	

$R1 = \Sigma \, | \, |F_O| - |F_c| \, | \, / \, \Sigma \, |F_o|$ and $wR2 = \{ \, \Sigma \, [\, w(F_o^2 - F_c^2)^2 \,] \, / \, \Sigma \, [\, w(F_o^2)^2 \,] \, \}^{1/2}$

Table 9. Atomic coordinates (x 10^4) and equivalent isotropic displacement parameters ($Å^2$x 10^3) for **47**. U(eq) is defined as one third of the trace of the orthogonalized U_{ij} tensor.

Atom	X	Y	Z	U(eq)
Ge(1)	1894(1)	1748(1)	341(1)	64(1)
C(1)	2639(7)	189(9)	-1362(5)	69(2)
C(2)	2336(8)	-938(11)	-2140(6)	80(2)
C(3)	1172(9)	-1952(9)	-2381(6)	77(2)
C(4)	305(8)	-1914(8)	-1826(5)	68(2)
C(5)	625(6)	-789(8)	-1016(5)	57(2)
C(6)	1813(6)	282(8)	-786(5)	59(2)
C(7)	210(6)	589(7)	362(5)	57(2)
C(8)	1792(8)	4323(10)	55(7)	78(2)
C(9)	4812(4)	4525(6)	11392(4)	166(3)
C(10)	3925(2)	2064(3)	11136(2)	61(1)
C(11A)	4466(3)	1250(4)	11325(3)	107(2)
C(11B)	3688(18)	-480(30)	1685(18)	93(6)

Atom C11 disordered by two positions (C11A and C11B) with Occupancy factors 0.5.

Table 10. Bond lengths for **47**. Symmetry transformation #1: -x,-y,-z.

Bond	Length (Å)
Ge(1)-C(10)	1.918(11)
Ge(1)-C(7)	1.953(6)
Ge(1)-C(6)	1.955(6)
Ge(1)-C(8)	1.972(8)
C(1)-C(2)	1.366(10)
C(1)-C(6)	1.377(8)
C(2)-C(3)	1.368(11)
C(3)-C(4)	1.387(10)
C(4)-C(5)	1.400(9)
C(5)-C(6)	1.413(9)
C(5)-C(7)#1	1.484(8)

Table 10. Bond lengths for **47**. (continued)

Bond	Length (Å)
C(7)-C(7)#1	1.336(12)
C(8)-C(9)	1.488(9)
C(10)-C(11A)	1.32(3)
C(10)-C(11B)	1.34(2)

Atom C11 disordered by two positions (C11A and C11B) with Occupancy factors 0.5.

Table 11. Bond angles for **47**. Symmetry transformation #1: -x,-y,-z.

Atoms	Bond Angle
C(10)-Ge(1)-C(7)	114.8(4)
C(10)-Ge(1)-C(6)	112.8(5)
C(7)-Ge(1)-C(6)	88.1(2)
C(10)-Ge(1)-C(8)	109.9(5)
C(7)-Ge(1)-C(8)	116.9(3)
C(6)-Ge(1)-C(8)	112.9(3)
C(2)-C(1)-C(6)	121.0(7)
C(1)-C(2)-C(3)	120.2(7)
C(2)-C(3)-C(4)	121.1(7)
C(3)-C(4)-C(5)	118.9(7)
C(4)-C(5)-C(6)	119.4(6)
C(4)-C(5)-C(7)#1	125.0(6)
C(6)-C(5)-C(7)#1	115.5(6)
C(1)-C(6)-C(5)	119.2(6)
C(1)-C(6)-Ge(1)	132.3(5)
C(5)-C(6)-Ge(1)	108.4(4)
C(7)#1-C(7)-C(5)#1	117.7(7)
C(7)#1-C(7)-Ge(1)	110.2(5)
C(5)#1-C(7)-Ge(1)	132.1(5)
C(9)-C(8)-Ge(1)	113.5(6)
C(11A)-C(10)-C(11B)	61(2)

Table 11. Bond angles for **47.** (continued)

Atoms	Bond Angle
C(11A)-C(10)-Ge(1)	133.4(16)
C(11B)-C(10)-Ge(1)	115.5(12)

Atom C11 disordered by two positions (C11A and C11B) with Occupancy factors 0.5.

Table 12. Anisotropic displacement parameters ($Å^2 x\ 10^3$) for **47.** The anisotropic displacement factor exponent takes the form: $-2\pi^2[h^2\ a^{*2}U_{11} + ... + 2\ h\ k\ a^*\ b^*\ U_{12}]$.

Atom	U_{11}	U_{22}	U_{33}	U_{23}	U_{13}	U_{12}
Ge(1)	41(1)	86(1)	69(1)	-5(1)	22(1)	-14(1)
C(1)	56(4)	76(4)	84(5)	-3(4)	36(4)	-9(3)
C(2)	71(6)	93(5)	94(5)	4(5)	50(5)	4(4)
C(3)	84(6)	77(5)	83(5)	-11(4)	46(5)	-2(4)
C(4)	54(5)	85(5)	65(4)	-6(3)	20(4)	-12(3)
C(5)	44(4)	62(4)	66(4)	9(3)	22(3)	5(3)
C(6)	39(4)	71(4)	72(4)	6(3)	27(3)	0(3)
C(7)	44(4)	62(4)	68(4)	2(3)	25(3)	-9(3)
C(8)	76(6)	71(5)	102(5)	-11(4)	48(5)	-13(4)
C(9)	90(8)	112(7)	170(9)	17(7)	62(7)	-23(5)
C(10)	71(7)	196(12)	88(7)	24(7)	14(5)	-9(7)
C(11A)	110(20)	340(50)	170(30)	130(40)	20(20)	-10(30)
C(11B)	48(10)	116(17)	110(15)	41(12)	18(10)	-1(9)

Atom C11 disordered by two positions (C11A and C11B) with Occupancy factors 0.5.

Table 13. Hydrogen coordinates ($x\ 10^4$) and isotropic displacement parameters ($Å^2 x\ 10^3$) for **47.**

Atom	X	Y	Z	U(eq)
H(1A)	3414	905	-1219	83
H(2A)	2922	-1017	-2506	96
H(3A)	958	-2679	-2927	93
H(4A)	-475	-2623	-1989	81

Table 13. Hydrogen coordinates and isotropic displacement parameters for **47**. (continued)

Atom	X	Y	Z	U(eq)
H(8A)	1004	4548	-514	94
H(8B)	1652	4959	595	94
H(9A)	2921	6292	-255	179
H(9B)	3173	4434	-660	179
H(9C)	3818	4855	450	179
H(10A)	4059	550	1146	145
H(10B)	3934	2379	1588	145
H(11A)	4594	736	2707	324
H(11B)	3259	-417	2338	324
H(11C)	3174	1579	2632	324
H(11D)	4502	-593	2236	140
H(11E)	3796	-1131	1148	140
H(11F)	2919	-939	1843	140

Atoms H11A to H11F have occupancy factors 0.5

APPENDIX REFERENCES

(1) Schmidt, M. W.; Baldridge, K. K.; Boatz, J. A.; Elbert, S. T.; Gordon, M. S.; Jensen, J. J.; Koseki, S.; Matsunaga, N.; Nguyen, K. A.; Su, S.; Windus, T. L.; Dupuis, M.; Montgomery, J. A. *J. Comp. Chem.* **1993**, *14*, 1347-1363.

(2) Stewart, J. J. P. *J. Comp. Aided Mol. Design* **1990**, *4*, 1-105.

(3) Dewar, M. J. S.; Zoebisch, E. G.; Healy, E. F.; Stewart, J. J. P. *J. Am. Chem. Soc.* **1985**, *107*, 3902-3909.

(4) Dewar, M. J. S.; Dieter, K. M. *J. Am. Chem. Soc.* **1986**, *108*, 8075-8086.

(5) Blessing, R. H. *Acta Cryst.* **1995**, *A51*, 33-38.

(6) All software and sources of the scattering factors are contained in the SHELXTL (version 5.1) program library (G. Sheldrick, Bruker Analytical X-Ray Systems, Madison, WI).

ACKNOWLEDGEMENTS

I would like to begin by recognizing the mentors that have guided me throughout the years, partly through their advice, but mostly by example: the late Dr. Douglas Bashore, Mrs. Nancy Whitman, and Dr. Peter P. Gaspar. Their kindness, patience, and encouragement have proven invaluable and have continued to provide inspiration. I especially would like to thank the most recent addition to the list, Dr. Tom Barton, for his dedication and unflagging support and, most of all, for the example he has set as a mentor.

Thanks, too, to the members of the Barton group with whom I shared my graduate school career. I could not have gone without the advice and leadership of Dr. Sina Maghsoodi and I owe a debt of gratitude to Mrs. Kathie Hawbaker, who somehow managed to take care of the many little snags that arose. I also am grateful for the camaraderie of my fellow graduate students, particularly Nathan Classen and Michael Serby, who made graduate life that much more enjoyable and have provided me with a wealth of stories.

Lastly, I would like to express my sincerest and warmest thanks to my friends and family, especially my parents, grandparents, and brothers, Dr. Conrad Stoldt, Michael Dosmann, Dennis and Tijana Grove, and Viken Djerdjian. Without their support, faith, and love, none of this would be possible. Thank you.

The United States Government has assigned the DOE Report number IS-T 2570 to this thesis. This document has been authored by the Iowa State University of Science and Technology under Contract No. W-7405-ENG-82 with the U. S. Department of Energy. The U. S. Government retains a non-exclusive, paid-up, irrevocable, world-wide license to publish or reproduce the published form of this document, or allow others to do so, for U. S. Government purposes.